HEINRICH HEINE
UNIVERSITÄT DÜSSELDORF

Role of *miR-132-3p*

in the pathogenesis of Alzheimer's disease

Inaugural-Dissertation

zur Erlangung des Doktorgrades

der Mathematisch-Naturwissenschaftlichen Fakultät

der Heinrich-Heine-Universität Düsseldorf

vorgelegt von

Linda Thienpont

aus Maasbüll

Düsseldorf, April 2018

Aus dem Institut für Neuropathologie

der Heinrich-Heine-Universität Düsseldorf

(Direktor: Prof. Dr. Guido Reifenberger)

Gedruckt mit der Genehmigung der

Mathematisch-Naturwissenschaftlichen Fakultät der

Heinrich-Heine-Universität Düsseldorf

Referent: Prof. Dr. G. Reifenberger

Korreferent: Prof. Dr. D. Willbold

Tag der mündlichen Prüfung: 12.04.2018

Ich widme meine Dissertation allen Alzheimer-Patienten und ihren Angehörigen.

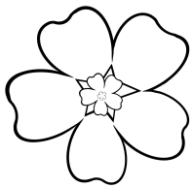

Contents

page

Abbreviations

AD	Alzheimer's disease
APS	ammonium persulfate
APP	amyloid precursor protein
APOE	apolipoprotein E
BACE1	beta-site APP cleaving enzyme 1
BSA	bovine serum albumine
bp	base pair
°C	degree Celsius
cDNA	complementary DNA
CHAPS	(3-[(3-Cholamidopropyl)-dimethylammonio]-propan- sulfonat)
CNS	central nervous system
CSF	cerebrospinal fluid
DEPC	diethyl pyrocarbonate
DPBS	Dulbecco's Phosphate-Buffered Saline
DMEM	Dulbecco's Modified Eagle Medium
DMSO	dimethyl sulfoxide
DNA	desoxyribonucleic acid
dNTP	desoxyribonucleoside-5'-triphosphate
DTT	dithiothreitol
EDTA	ethylenediaminetetraacetic acid
ELISA	enzyme linked immunosorbent assay
FCS	fetal calf serum
for	forward
GITC	guanidinium isothiocyanate
h	hour
IgG	immunoglobulin G

kb	kilobase
kDa	kilodalton
M	molar
mA	milliampere
min	minute
miRNA	micro ribonucleic acid
ml	milliliter
mRNA	messenger ribonucleic acid
non-AD	non Alzheimer´s disease control
µl	microliter
PAA	polyacrylamide
PBS	phosphate-buffered saline
PCR	polymerase chain reaction
PI	proteinase inhibitors
pmd	post mortem delay
pre	precursor
PSEN	presenilin
rev	reverse
RNA	ribonucleic acid
rpm	revolutions per minute
RT	room temperature
RT	reverse transcription
RT-PCR	reverse transcription - polymerase chain reaction
SD	standard deviation
sec	second
Taq	Thermus aquaticus
TBE	Tris-borate-EDTA
TBS-T	Tris-buffered saline with Tween 20

TE	Tris-EDTA
TEMED	N,N,N’,N’-Tetramethyl ethylenediamine
Tris	Tris(hydroxymethyl)aminomethane
U	unit
UTR	untranslated region
V	voltage
v/v	volume per volume
W	watt
wt	wild type
w/v	weight per volume

1 Introduction

Human life expectancy has nearly doubled over the past century in industrialized countries because of advanced medical treatment. However, this delay of mortality leads to an increase in age, which is the greatest risk factor for many neurodegenerative diseases. Worldwide, the number of people who suffer from Alzheimer's disease (AD) and other neurodegenerative diseases accompanied by cognitive decline is increasing rapidly. Therefore, to understand the biological mechanisms underlying aging and age-dependent neurodegenerative diseases is one of the most urgent topics in biomedical research.

1.1 Alzheimer´s disease

It was more than 100 years ago that the German psychiatrist and neuropathologist Alois Alzheimer published his findings about Auguste Deter, who became known as the first Alzheimer's disease patient (Alzheimer A 1907).

Alzheimer's disease (AD) is by far the most common and most studied form of dementia and the fourth leading cause of death in industrialized countries. The two main risk factors for the disease are age and a positive family history of AD (Rademarkers R 2003). Worldwide, more than 46 million people suffer from dementia, and in 50-75 % of these patients AD is the underlying cause (Cummings J 2016). The number of dementia patients is estimated to nearly double every 20 years (Kerantzoulis S 2011, Bettens K 2010). AD has been reported to affect more than 40 % of the population over 85 years of age (Lewczuk P 2015).

A definitive diagnosis of AD can only be obtained after an autopsy and a histopathological analysis of the brain. Nevertheless, in patients with clinical symptoms of cognitive decline, AD as the likely cause can be diagnosed with a high degree of accuracy through a combination of neuropsychological testing, brain imaging and biochemical tests. Three phases of AD have been proposed: 1. Preclinical phase, 2. Mild cognitive impairment (MCI), and 3. Symptomatic AD (Sperling R 2001). In the preclinical phase, the underlying disease process can only be defined by the study of biomarkers, specifically with positron emission tomography (PET) imaging of characteristic protein deposits in the brain. Most patients are completely asymptomatic at this stage of the disease, while a few show subtle cognitive decline (Jack C 2010). In the MCI stage, minor cognitive impairments are evident that do not substantially interfere with the activities of daily living (Peterson R 2004). The symptomatic phase of AD is characterized by episodic memory impairment, deficits in language and

executive functions, changes in personality and mood as well as psychiatric symptoms, and, in later stages of the disease, also motor symptoms (Salmon D 1999). Death in AD patients is usually caused by a secondary disease, frequently by infections leading to pneumonia. The average disease duration between diagnosis and death is 8-10 years, in very few instances up to 20 years (Förstl H 1999).

The major neuropathological hallmarks of AD are brain atrophy, widespread neuronal and synapse loss, extracellular amyloid-β (Aβ) plaques and intraneuronal neurofibrillary tangles consisting of aggregated tau protein (Braak H 1991). Additionally, neuroinflammation with activated astrocytes and microglia cells and activation of the complement system is always present and might contribute to the pathogenesis and neuronal cell death (Heneka MT 2015, Zhang B 2013).

1.2 Molecular pathology of Alzheimer's disease

1.2.1 The amyloid hypothesis

The ongoing development of novel AD therapies is mostly based on the amyloid hypothesis (Hardy J 2002). This hypothesis proposes that the neurodegeneration in AD is primarily caused by the accumulation and aggregation of Aβ peptides in the brain. The Aβ peptides can form smaller soluble aggregates (so called oligomers) or they can deposit in insoluble amyloid plaques in the brain parenchyma. Over the years, the hypothesis has been refined and it is now assumed that the smaller Aβ oligomers are the main drivers of synaptic loss and neurodegeneration, with a less important role for the insoluble amyloid plaques (Müller-Schiffmann A 2016). In contrast, neuroinflammation and the formation of intracellular tau aggregates are secondary events in the amyloid cascade that are dependent on the accumulation of Aβ in the brain. However, both of these pathologies likely also contribute to the death of neurons in the AD brain (Selkoe D 2016).

1.2.2 The amyloid precursor protein and Aβ generation

The amyloid precursor protein (APP) is a type-I integral membrane protein which is ubiquitously expressed. Its biological function in the central nervous system is only partially known and it has been implicated in synapse formation and function (Priller C 2006), as well as neural plasticity (Turner PR 2003). Aβ peptides are generated from APP by serial proteolysis. In the non-amyloidogenic pathway, α-secretase belonging to the ADAM (a disintegrin and metalloproteinase) family of proteases cleaves APP within the Aβ-domain preventing Aβ formation (Esch F 1990). In the amyloidogenic pathway, β- and γ-secretase cleave APP sequentially, which leads to the generation and secretion of Aβ with variable C-termini. Peptides with 40 amino acids (Aβ40) or with 42 amino acids (Aβ42) are predominantly produced (Klafki H 1996, Citron 1996) (Figure 1). Because of higher β-secretase expression, neurons have a higher tendency to use the amyloidogenic pathway compared to glial cell types or peripheral tissues (De Strooper B. 1995). The proteins presenilin 1 and presenilin 2 (PSEN 1 and PSEN 2) are ubiquitously expressed and form the catalytic subunit of the γ-secretase multiprotein protease complex (De Strooper B 1998).

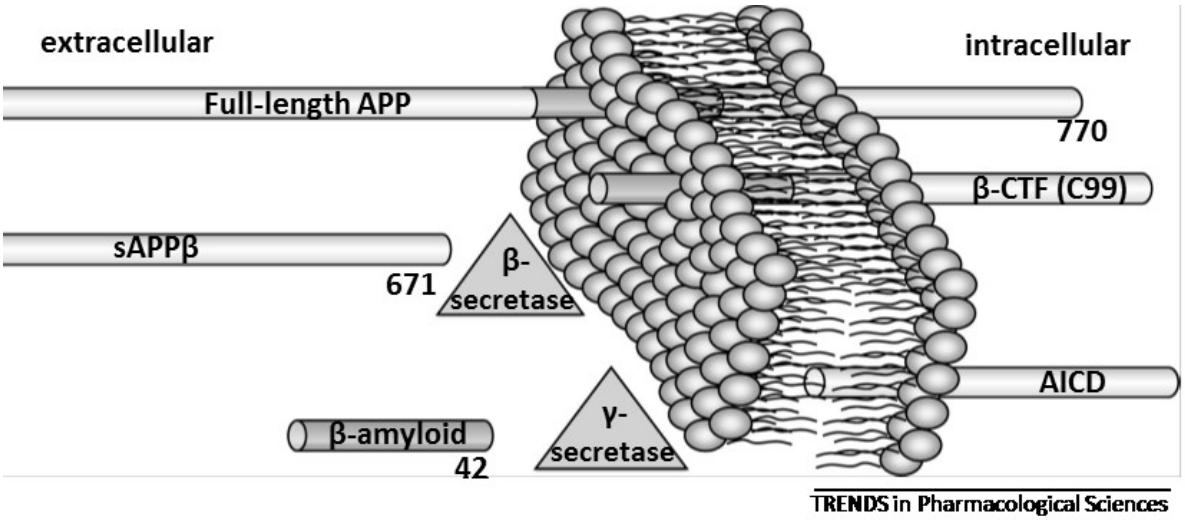

Figure 1: Schematic illustration of the amyloidogenic pathway generating Aβ peptides from the precursor APP (modified according to Blennow, 2015 (Blennow K 2015)).
In the amyloidogenic pathway, the full-length amyloid precursor protein (APP) is cleaved by β-secretase and γ-secretase releasing the soluble ectodomain APPβ (sAPPß) and neurotoxic Aβ peptides into the extracellular space. The AICD domain is released into the cytosol after γ-secretase cleavage and has potential signaling functions. AICD, amyloid precursor protein intracellular domain; β-CTF, β-C terminal fragment.

1.2.3 Tau biology and phosphorylation

Besides the extracellular amyloid-β plaques in AD brains, there are additional typical intracellular neurofibrillary tangles (NFT) consisting of hyperphosphorylated tau proteins in paired helical filaments (PHF) (Crowther 1991, Bakota L 2016). Tau is mainly present in neurons (Avila J 2004) and the most well-known function of tau is microtubule stabilization (Caceres A 1990, Medina M 2016). The interaction between microtubules and microtubule-associated proteins is necessary for intracellular transport processes as well as differentiation and polarization of the cell (Hochgräfe K 2013). The function of tau is primarily achieved through phosphorylation at many sites and an increase in tau phosphorylation by kinases has been correlated with increased tau aggregation (Noble W 2005). The most active tau kinases that phosphorylate tau at AD-specific epitopes are GSK3-α, GSK3-β and MAPK13 (Cavallini A 2013). Thus, an increase in tau phosphorylation reduces its affinity for microtubules, resulting in neuronal cytoskeleton instability (Medina M 2016). There are hints that hyperphosphorylation of tau seems to lead to toxicity (Avila J 2004) but the molecular mechanisms are still unclear (Medina M 2016).

The relationship between Aβ-proteins and tau hyperphosphorylation is not yet sufficiently understood and therefore subject of current research. A widely held theory suggests that generation of Aβ-proteins represents a trigger for AD and tau hyperphosphorylation is a downstream event which is required for Aβ dependent toxicity. Finally, tau aggregation disturbs the integrity of neuronal functions and leads to neuronal death (Hochgräfe K 2013).

1.2.4 Familial and sporadic Alzheimer's disease

AD patients can be divided into two groups: patients with early-onset familial Alzheimer's disease (FAD) and autosomal-dominant inheritance, and sporadic AD patients with a later disease onset. The large majority of FAD patients develop clinical symptoms before 60 years of age while most sporadic AD patients display a disease onset >65 years of age (Rademarkers R 2003). Only about 1-2 % of all AD cases are familial AD. Aside from the age of onset, the clinical symptoms, the disease duration and the neuropathology are largely identical between familial and sporadic AD (Bateman R J 2011).

Mutations in one of the following three genes have been identified in patients with familial AD: *APP, PSEN1* and *PSEN2* (Lander E 1995). The different mutations in these genes have been shown to either increase total Aβ levels or to increase the production of the longer, more aggregation-prone Aβ42 peptides over the Aβ40 peptides (Dimitrov M 2013). Both mechanisms promote Aβ aggregation and support the amyloid hypothesis (Cacace R 2016). So far, only one gene, the apolipoprotein E (*APOE*) gene, has been consistently associated with an increased risk for sporadic AD (Strittmatter W 1993). APOE is an apolipoprotein that transports cholesterol to neurons. The gene *APOE* is polymorphic with three different alleles: *APOEε2, APOEε3* and *APOEε4* (Corder E H 1993). Heterozygous *APOEε4* carriers have a three times higher risk while homozygous carriers have a 15 times higher risk for sporadic AD (Farrer L 1997). Approximately 7-20 % of all AD patients carry the risk allele *APOEε4* (Warwick D 2000). Genome-wide association studies have discovered additional genes, which are proposed as risk factors for sporadic AD with much smaller effect size compared to the *APOEε4* allele, including clusterin *(CLU),* complement receptor 1 *(CR1),* phosphatidylinositol-binding clathrin assembly protein *(PICALM)* (Bertram L 2004) and phospholipase D3 (*PLD3*) (Cruchaga 2014). Furthermore, chromosomes 6, 9, 10, 12 and 21 were repeatedly found by linkage scans in sporadic AD and affected sib-pairs (ASP) and are predicted to harbour susceptibility genes for AD. Although the contribution of the newly discovered risk alleles to AD remains largely unclear, some studies indicate that they might also promote Aβ accumulation and aggregation or inflammatory processes (Bertram L 2004).

1.3 Treatment strategies for Alzheimer's disease

1.3.1 Current state of Alzheimer's treatment

At present, the available therapies for AD can only delay the progress of clinical symptoms of the disease for a limited amount of time, but they do not modify the course of the disease (Folch J 2016). Five drugs have received Food and Drug Administration (FDA) approval for AD treatment. Four of these drugs (Donepezil, Rivastigmine, Tacrine and Galantamine) are acetylcholinesterase inhibitors. AD brains display reduced acetylcholine (ACh) levels because of the progressive loss of ACh producing nerve cells. ACh is an important neurotransmitter, which binds to nicotinic acetylcholine receptors and is linked with cognitive functions (Schneider LS 2014). The fifth drug is Memantine, an N-methyl-D-aspartate (NMDA) receptor antagonist. It is believed that excitotoxicity caused by excess amounts of the excitatory neurotransmitter glutamate contributes to the pathogenesis of AD. Too much glutamate strongly activates postsynaptic NMDA-receptors, which in turn can lead to a neurotoxic calcium influx (McShane R 2006). Memantine prevents an overstimulation of the NMDA-receptors and has been shown to stabilize cognitive functions in moderate and severe forms of AD (Reisberg B 2003).

1.3.2 Novel treatments in clinical development

The enzymes β-secretase (BACE1) and γ-secretase are promising drug targets in AD as inhibition of either enzyme has the potential to completely suppress the generation of Aβ peptides (Citron M 2010). However, clinical trials of γ-secretase inhibitors have failed because of unacceptable side-effects and clinical development has been stopped (Doody RS 2013, Coric V 2015). More recently, several new β-secretase inhibitors were shown to efficiently reduce the concentrations of both Aβ40 and Aβ42 peptides in the CSF of healthy volunteers and AD patients (Streffer J 2015, Kennedy ME 2016).

Anti-Aβ immunotherapy is also a promising therapeutic strategy to reduce the amyloid pathology in AD patients. Pre-clinical studies in various AD mouse models have shown beneficial effects by active immunization with Aβ peptides (Schenk D 1999) or passive immunization with anti-Aβ monoclonal antibodies (Bard F 2000). Unfortunately, the translation of these results from AD mouse models to patients has not been successful until now. Several antibodies have failed to provide cognitive benefits in Phase III clinical trials, presumably due to insufficient target engagement (Lannfelt L 2014). However, recently, a new antibody called aducanumab was able to remove amyloid plaques in AD patients as measured by *in vivo* PET imaging in a 12 months, double-blind, placebo-controlled study

(Sevigny J 2016). The observed effects were by far the strongest of all the anti-Aβ drugs evaluated in clinical trials up to now. Whether the removal of amyloid pathology will be accompanied by cognitive benefits is currently being evaluated in ongoing phase III clinical trials of aducanumab.

Finally, anti-tau therapy could also be promising, and many anti-tau antibodies and vaccines have been investigated in preclinical animal studies and found to be effective (Yanamandra K 2013). One tau-inhibitor, LMTM (Leuco-Methylthioninium Bis(Hydromethanesulphonate), showed little effect in a phase-3 clinical trial but only as monotherapy (Wilcock GK 2017).

1.4 MicroRNAs and their target genes

MicroRNAs (miRNAs) comprise a large family of small ~21-25 nucleotide (nt) long, non-coding RNA molecules that play an important role in posttranscriptional regulation of gene expression in a sequence-dependent manner. To date, more than 1870 human miRNAs are identified (www.mirbase.org), which are predicted to control more than 60 % of all protein-coding genes (Friedman R 2009). MiRNAs have the ability to fine-tune the activity of biological processes like development, cell proliferation, differentiation, apoptosis and metabolism, and they are aberrantly expressed in cancer and other diseases. Furthermore, there is an increasing indication that miRNAs play a crucial role in aging and neurodegenerative diseases like Alzheimer's disease (Bates D 2009). MiRNAs and epigenetic mechanisms have been shown to closely interact with each other and these reciprocal regulatory circuits appear to be disrupted in neuronal and glial cells affected by AD (Van den Hove 2014). Through the capability of one single miRNA to regulate a lot of different target mRNAs, which can bind many different miRNAs in turn, there is an amazing net of translational regulation (Krek A 2005).

The founding member of the miRNA family *lin-4* was identified in *C. elegans* (*Caenorhabditis elegans*) by a genetic screen (Chalfie M 1981, Ambros V 1989). The results showed mostly protein-coding genes but *lin-4* encoded a 22-nucleotide non-coding RNA molecule which is partially complementary to seven sites in the 3' untranslated region (UTR) of the *lin-14* gene (Lee R 1993). *Lin-14* encodes a nuclear protein which needs to be downregulated at the end of the first larval stage in *C. elegans* to initiate the transition to the second larval stage (Lee R 1993).

1.4.1 The biogenesis of miRNAs

MiRNA genes are encoded within the genome, except for the Y-chromosome, and most are transcribed by RNA Polymerase II, some by RNA Polymerase III (Cai X 2004). Approximately 50 % of mammalian miRNA-coding genes are located in intergenic spaces while ~ 40 % of miRNA genes are situated in introns and ~ 10 % in exons (Rodriguez A 2004, Smalheiser N 2008). Most mammalian miRNAs are processed by the canonical pathway while a few mammalian intronic miRNA genes and a lot of intronic miRNAs in *Drosophila* are generated by the non-canonical pathway (Berezikov 2007) (Figure 2).

The first two steps of the highly conserved miRNA biogenesis, the processing of primary miRNAs (pri-miRNAs), take place in the nucleus and the following steps, generating mature miRNAs, in the cytosol (Figure 2). Many miRNA genes are clustered which results in polycistronic transcription, while single miRNA genes are transcribed monocistronically (Lee

2002). In the canonical miRNA pathway, the pri-miRNAs are recognized by the nuclear microprocessor complex which contains the proteins Drosha and DGCR8 (DiGeorge syndrome critical region 8). First, DGCR8 binds the stem region of pri-miRNAs then the 60-70 nt long stem loop precursor miRNAs (pre-miRNAs) are cleaved and generated by the endonuclease Drosha (Denli A 2004, Han J 2004, Morlando M 2008). In the non-canonical pathway this step is independent of Drosha- and DGCR8-activity but the very short hairpin introns of mRNA coding genes are spliced and debranched to generate pre-miRNAs (Okamura K 2007, Ruby JG 2007). The nascent pre-miRNAs are exported in a GTP (guanosine-5'-triphosphate)-dependent manner to the cytosol by Exportin 5, a caryopherin protein (Bohnsack MT 2004). In the cytosol the RISC (RNA-induced silencing complex) loading complex (RLC) binds to pre-miRNA which is processed by the ribonuclease Dicer type III into a ~21-25 nt long miRNA/miRNA* duplex (Ketting RF 2001). This duplex becomes unwound and released as single-stranded mature ~21-25 nt long miRNA by proteins of the Argonaute (Ago) family (Kwak PB 2012). Besides the Argonaute proteins 1-4 and the ribonuclease Dicer, a double-stranded RNA-binding protein (TRBP) belongs to the RISC-loading complex and loads the mature miRNA to the RISC (Khvorova A 2003).

The bound mature miRNA in RISC binds the target mRNA which is followed by inhibition of translation or degradation and in very rare cases activation, depending on the degree of complementarity. The miRNA bases 2-7 are called “seed sequence” and must be perfectly complementary to the 3’ UTR region of the target mRNA sequence to define the target specificity (Doench 2004). In most instances, the miRNA binds in the 3’UTR region of the target mRNA, which leads to inhibition of translation with a range of 1.5-2-fold. But there are exceptions, for example it has been shown that some mRNAs have miRNA-binding sites in the 5’UTR or in the coding region, but with less robust regulation (Orom UA 2008, Easow G 2007). Interestingly, there are some instances which show an activation of the mRNA translation caused by miRNA binding in the 3’ or 5’ UTR region of the target mRNA (Orom 2008, Vasudeva 2007).

The presence of miRNAs involved in miRNA biogenesis and function in neuronal soma, dendrites and axons is an indication of their important role in translational regulation in these compartments. However, the transport mechanisms of miRNAs loaded to the RISC into the dendritic and axonal compartments are still unknown (O' Carrol D 2012).

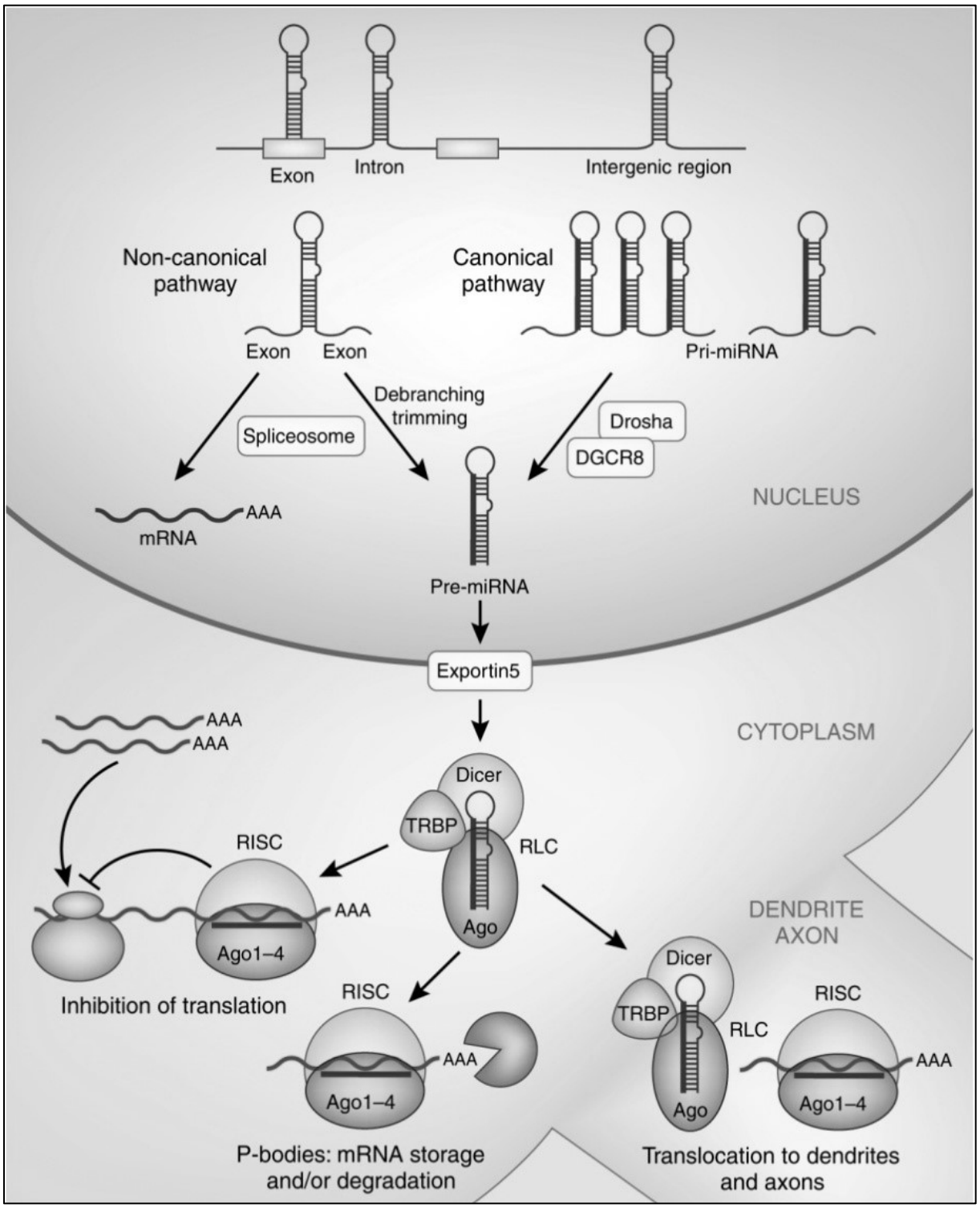

Figure 2: Schematic overview of canonical and non-canonical miRNA biogenesis (O' Carrol D 2012).In the canonical pathway, the pri-miRNAs encoded in exonic, intronic or intergenic regions are recognized by the nuclear microprocessor complex which contains the proteins Drosha and DGCR8 to generate the pre-miRNA. In the non-canonical pathway the hairpin introns of mRNA coding genes are spliced and debranched to generate pre-miRNAs. The pre-miRNAs are exported to the cytosol by Exportin 5. In the cytosol the RISC loading complex (RLC) binds to pre-miRNA which is processed by Dicer into miRNA/miRNA* duplex. The unwound single-stranded mature miRNA binds the target mRNA which is succeeded by inhibition of translation or degradation. The transport of the miRNAs loaded in the RISC into the dendritic and axonal compartments is still unknown. DGCR8, DiGeorge syndrome critical region 8; RISC, RNA-induced silencing complex; Ago, Argonaute.

The full complementarity between miRNA and its target mRNA leads to Ago-2 mediated endonucleolytic cleavage and degradation of the mRNA (Hammond SM 2001, Yekta S 2004). This mRNA decay is thought to occur in processing bodies (p-bodies) and stress granules (Sheth U 2003). The mechanism of miRNA-mediated mRNA degradation is described as deadenylation followed by decapping of the mRNA sequence (Figure 3). The deadenylation of the poly(A) tail occurs through the interaction between the miRNA inducing silencing complex (miRISC) and the CCR4-NOT1 (carbone catabolite repression 4 protein-negative on TATA-less) -deadenylase complex and the direct binding of the GW182 protein with the poly(A) binding protein (PABP). The decapping proteins 1 and 2 (DCP1/DCP2) are responsible for the decapping process of the 5' terminal cap followed by the subsequent mRNA decay (Franks TM 2008).

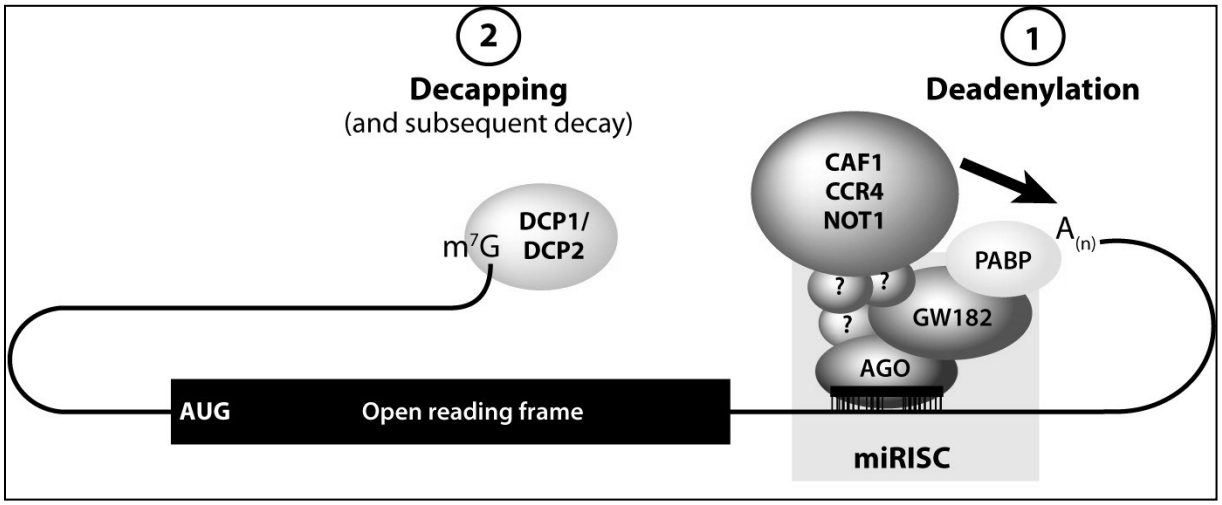

Figure 3: Schematic description of miRNA-mediated mRNA decay (Fabian MR 2010).
The deadenylation of the poly(A) tail occurs through the interaction between miRISC and the CCR4-NOT1-deadenylase complex and the direct binding of the GW182 protein with the poly(A) binding protein. The decapping proteins 1 and 2 are responsible for the decapping process of the 5' terminal cap followed by the subsequent mRNA decay. CCR4, carbone catabolite repression 4 protein; NOT1, negative on TATA-less; AGO, Argonaute; CAF1, CCR4-associated factor; PABP, poly(A)-binding protein; miRISC, miRNA inducing silencing complex.

Most animal miRNAs are partially complementary to their target mRNAs and build mismatches or bulges which prevent Ago-2 cleavage of the mRNA (Hutvagner G 2002). The translational repression is described in two different processes, the initiation block and the postinitiation block (Figure 4). In the initiation block, the miRNA inducing silencing complex (miRISC) represses the eIF4E (elongation initiation factor 4E) cap recognition and the binding of the ribosomal subunits 60S and 40S that both are necessary for translation initiation. In the postinitiation block, the miRNA bound in RISC inhibits ribosome elongation, induces ribosome drop-off, or facilitates proteolysis of nascent polypeptides that lack in-frame termination codons (Fabian MR 2010).

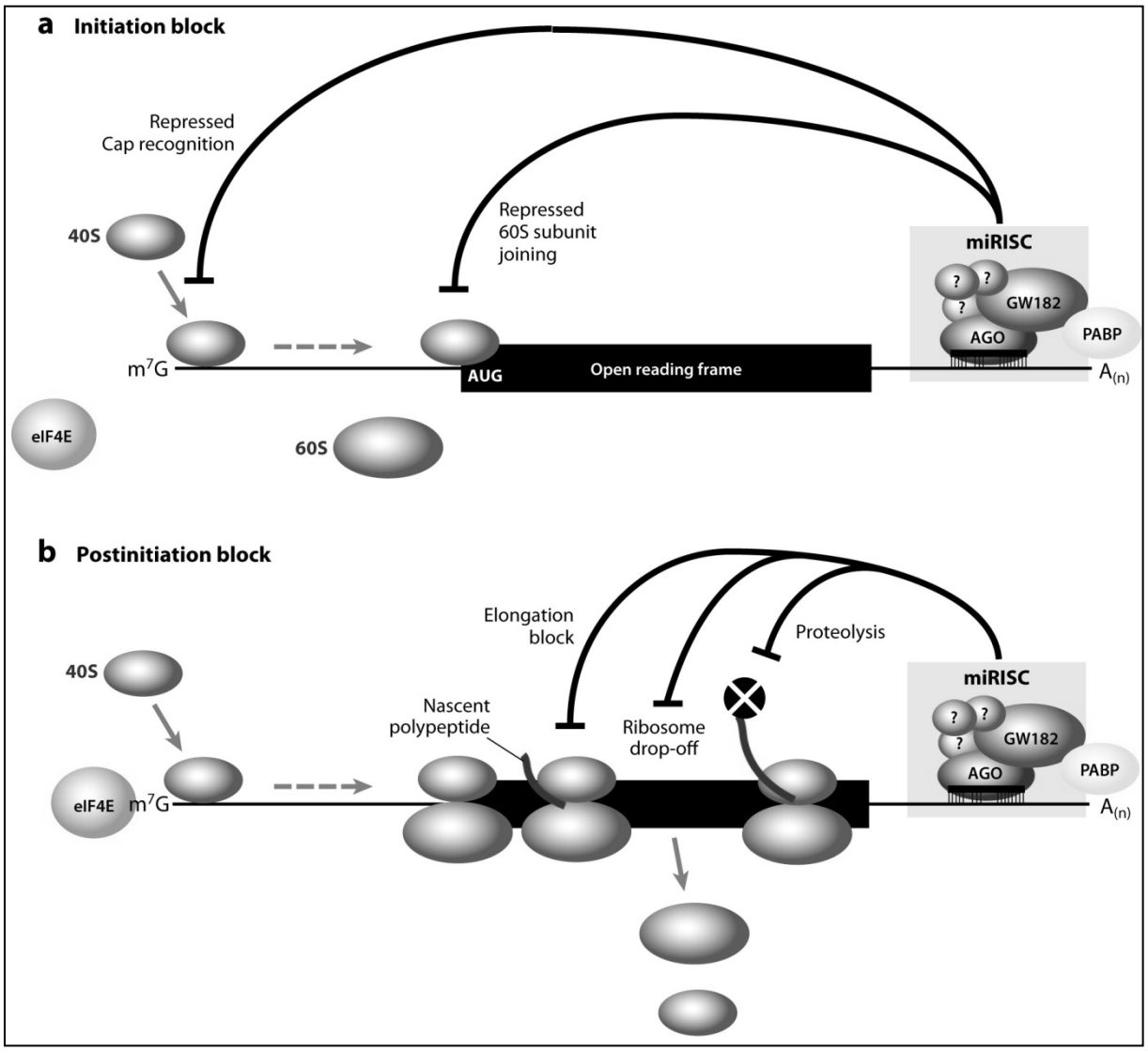

Figure 4: Schematic description of miRNA mediated translational mRNA inhibition (Fabian MR 2010)**.**
a) In the initiation block, miRISC represses the eIF4E-cap recognition and the binding of the ribosomal subunits 60S and 40S. b) In the postinitiation block, miRISC inhibits ribosome elongation, induces ribosome drop-off, or facilitates proteolysis of nascent polypeptides. eIF4E, elongation initiation factor 4E; AGO, Argonaute; PABP, poly(A)-binding protein; miRISC, miRNA inducing silencing complex.

1.4.2 The role of miRNAs in Alzheimer's disease

As indicated by a large amount of studies, miRNAs play a major role in development and aging of the brain as well as in neurodegenerative disorders like AD (Nowak JS 2013, Smith-Vikos T 2012, Femminella GD 2015). It has been proposed that about 70 % of all miRNAs are expressed in the human central nervous system (CNS), which demonstrates their important role in the structural organization and proper function of this organ (Nowak JS 2013). In the last couple of years, many studies have found differentially expressed miRNAs in human AD tissue and animal models of AD, and their targets have often been linked to AD pathology (Chunmei W 2014, Van den Hove DL 2014). MiRNAs, which are often mentioned

in the literature in relation to AD are *miR-9, miR-107, miR-146a, miR-29a/b-1, miR-34* and *miR-106* (Femminella GD 2015).

MiR-9, which was repeatedly reported to be differentially expressed in AD, is downregulated in AD patient sera and targets SIRT1 (Krichevsky AM 2003). *MiR-107* has been proposed to be downregulated at an early stage of AD in the temporal cortex (Nelson PT 2010). *MiR-107* targets CDK5 (cyclin-dependent kinase 5), which is known to be dysregulated in AD, as well as BACE1 and ADAM10, which are involved in Aβ production (Goodall EF 2013). *MiR-146a* was shown to be upregulated in the temporal cortex and hippocampus of AD patients and is a known regulator of inflammation-related mRNAs (Sethi P 2009). *MiR-29* is a miRNA family whose expression might play a role in brain aging and modulation of microglia activity (Femminella GD 2015). *MiR-29a* and *miR-29b-1* were found to be downregulated in human AD temporal cortex and their expression was shown to be inversely correlated to β-secretase (BACE1) expression (Hebert SS 2008). *MiR-34* is also a miRNA family and is known to regulate the expression of p53, which might have a role in tau phosphorylation (Hooper C 2007). *MiR-34c* was reported to be upregulated in the hippocampus of AD patients as well as in AD transgenic mouse models. *MiR-106a* and *miR-106b* target APP and were shown to be downregulated in the temporal cortex of AD patients (Kim J 2012).

Some miRNAs, including *miR-9*, *miR-181c*, *MiR-34c* and *miR-188-3p* were found to be dysregulated in both *APP*-transgenic mouse models and human AD brain tissue (Schonrock N 2012, Zovoilis A 2011, Zhang J 2014). In addition, it was possible to rescue some cognitive and synaptic deficits in AD mouse models through the downregulation (*miR-34c*) or upregulation (*miR-188-3p*) of miRNAs (Zovoilis A 2011, Zhang J 2014). This seems to indicate that, in principle, miRNAs could be a therapeutic target in AD.

MiRNAs might also have the potential to function as biomarkers in AD because they are altered in the CSF (Cogswell JP 2008) and blood sera (Geekiyanage H 2012) of AD patients. However, until now, it is not understood how deregulated miRNAs contribute to AD as their deregulation could be a cause or a consequence of the AD pathology. In addition, a single miRNA can regulate multiple mRNAs and also one mRNA can be regulated by many miRNAs. This mRNA-miRNA network could be a limitation for a therapeutic approach because of interference with too many biological processes (Femminella GD 2015).

1.5 Goals and experimental approach of this study

The aim of this project was the identification and functional characterization of miRNAs whose expression is altered in the brains of AD patients versus healthy control subjects. Specifically, this study set out to address the following questions:

(1) Which miRNAs are differentially expressed in brain tissue samples of AD patients vs. age matched non-AD brain tissue samples?

(2) Can a set of eight microRNAs previously be identified as being differentially expressed in the *APP*655sw/*PS1*deltaExon9 mouse model of AD be confirmed in brain samples from human AD patients?

(3) What are the relevant target genes regulated by differentially expressed miRNAs and are these target genes differentially expressed in AD brains?

(4) What is the functional significance of these target genes and the respective miRNA species in the pathogenesis of AD?

The project started with the analysis of eight microRNAs in AD brain tissue samples compared to non-AD brain tissue samples, which were known to be differentially expressed in brain tissue samples of the AD mouse model *APP*655sw/*PS1*deltaExon9. This analysis was done by real-time RT-PCR. In addition, an expression analysis of miRNAs by GeneChip® miRNA Arrays in human autopsy AD brain tissue samples and age-matched non-AD brain tissue samples was carried out. The miRNAs which showed significantly deregulated expression were then further investigated.

The next step was the identification of targets of the respective miRNAs with different target prediction programs. The expression of these putative targets was then investigated by real-time reverse transcription PCR in AD brain tissue samples compared to non-AD brain tissue samples. The aim was to identify putative targets whose expression was inversely correlated with the expression of the differentially expressed miRNAs in AD tissue samples. Afterwards, the putative targets were investigated by real-time RT-PCR based expression analyses in miRNA transfected cells to proof the expected interaction between corresponding miRNA and putative target. For the validation of the putative target genes, luciferase assays were carried out in T98G cells to validate the direct binding of the identified candidate miRNAs to their predicted mRNA targets. The protein expression level of these target mRNAs was also investigated in miRNA transfected Hek293sw(*APP*695sw) and SH-SY5Y cells by western blot analyses.

The validated miRNAs were then functionally characterized by assessing the effect of overexpression of the pre-miRNAs in the cell line Hek293sw(*APP*695sw) on the expression of different peptides and proteins that play an important role in the pathogenesis of AD. Therefore, the expression of Aβ40/Aβ42, APP and BACE1 was investigated by ELISA, Western-blot or real-time PCR analyses. The validated targets were functionally characterized through targeted inhibition by siRNA transfection in the cell line Hek293sw(*APP*695sw). Afterwards the expression of the proteins Aβ40/Aβ42 and APP was again investigated by ELISA or western-blot analyses. All these experiments aimed to provide further insights into the role of the identified candidate miRNAs and their targets in the pathogenesis of AD.

2 Materials

2.1 Human brain tissue samples

In total, 30 brain tissue samples from Alzheimer's disease patients and 30 brain tissue samples from age- and gender-matched non-AD patients (controls) were obtained from the Netherlands Brain Bank (NBB, www.brainbank.nl). The Braak stage of the Alzheimer's disease patients was between five and six while the Braak stage of the non-AD controls was between zero and two.

The first set of 20 brain tissue samples (screening samples) are listed in Table 1. The second set of 40 brain tissue samples are listed in Table 2.

Table 1: First set of brain tissue samples. F, female; m, male; Pmd, post mortem delay; AD, Alzheimer`s disease; Sample-ID, sample identification number. Age in years, Pmd in hours.

Sample-ID	Gender	Age	Braak stage	Pmd	Diagnosis	Brain region
S07/236	f	62	6	04:45	AD	medial frontal gyrus
S05/013	f	94	5	04:30	AD	medial frontal gyrus
S01/131	f	86	6	05:00	AD	medial frontal gyrus
S01/195	f	89	5	03:15	AD	medial frontal gyrus
S01/232	f	55	6	05:30	AD	medial frontal gyrus
S04/271	f	85	6	05:40	AD	medial frontal gyrus
S04/134	f	88	5	05:10	AD	medial frontal gyrus
S94/116	f	82	6	04:00	AD	medial frontal gyrus
S95/340	m	57	6	05:00	AD	medial frontal gyrus
S08/092	m	62	6	04:15	AD	medial frontal gyrus
S97/221	f	78	1	04:15	non-AD	medial frontal gyrus
S08/325	f	87	2	05:00	non-AD	medial frontal gyrus
S09/067	f	77	1	02:55	non-AD	medial frontal gyrus
S08/230	f	50	1	04:10	non-AD	medial frontal gyrus
S99/122	f	79	2	05:30	non-AD	medial frontal gyrus
S05/307	f	85	1	05:00	non-AD	medial frontal gyrus
90/205.3	m	88	n/a	04:30	non-AD	medial frontal gyrus
S09/009	m	82	1	05:10	non-AD	medial frontal gyrus
S09/001	m	88	2	04:43	non-AD	medial frontal gyrus
S07/030	m	84	1	05:35	non-AD	medial frontal gyrus

Table 2: Second set of brain tissue samples. F, female; m, male; Pmd, post mortem delay; AD, Alzheimer`s disease; Sample-ID, sample identification number. Age in years, Pmd in hours.

Sample-ID	Gender	Age	Braak stage	Pmd	Diagnosis	Brain region
S01/219	f	81	6	05:30	AD	superior frontal gyrus
S08/005	f	82	6	04:20	AD	superior frontal gyrus
S07/297	f	54	6	06:35	AD	superior frontal gyrus
S02/299	f	82	6	06:00	AD	superior frontal gyrus
S03/315	f	82	5	04:35	AD	superior frontal gyrus
S09/280	f	84	6	04:50	AD	superior frontal gyrus
S09/133	f	85	6	05:10	AD	superior frontal gyrus
S01/161	f	86	6	05:40	AD	superior frontal gyrus
S06/017	f	87	6	05:00	AD	superior frontal gyrus
S05/050	f	89	6	04:30	AD	superior frontal gyrus
S01/151	f	96	5	05:50	AD	superior frontal gyrus
S01/267	f	57	6	04:05	AD	superior frontal gyrus
S00/196	f	61	6	06:25	AD	superior frontal gyrus
S96/266	f	74	5	06:05	AD	superior frontal gyrus
S06/264	f	77	5	06:05	AD	superior frontal gyrus
S01/173	f	78	6	03:45	AD	superior frontal gyrus
S00/081	m	78	5	07:45	AD	superior frontal gyrus
S05/280	m	82	5	05:05	AD	superior frontal gyrus
S01/145	m	85	5	04:45	AD	superior frontal gyrus
S05/039	m	93	5	04:30	AD	superior frontal gyrus
S06/023	f	85	2	04:40	Non-AD	superior frontal gyrus
S10/023	f	85	2	05:19	Non-AD	superior frontal gyrus
S94/325	f	51	0	07:40	Non-AD	superior frontal gyrus
S97/145	f	55	0	05:35	Non-AD	superior frontal gyrus
S10/196	f	60	1	07:30	Non-AD	superior frontal gyrus
S10/035	f	73	1	07:45	Non-AD	superior frontal gyrus
S09/067	f	77	1	02:55	Non-AD	superior frontal gyrus
S96/249	f	78	2	07:30	Non-AD	superior frontal gyrus
S08/083	f	80	1	06:58	Non-AD	superior frontal gyrus
S07/275	f	82	2	05:10	Non-AD	superior frontal gyrus
S02/209	f	82	1	07:08	Non-AD	superior frontal gyrus
S04/038	f	82	1	07:00	Non-AD	superior frontal gyrus
S09/134	f	84	1	06:55	Non-AD	superior frontal gyrus
S04/196	f	88	n/a	06:15	Non-AD	superior frontal gyrus
S06/282	f	89	2	06:25	Non-AD	superior frontal gyrus
S10/181	f	94	1	05:50	Non-AD	superior frontal gyrus
S04/188	m	85	1	04:15	Non-AD	superior frontal gyrus

S04/053	m	96	1	05:23	Non-AD	superior frontal gyrus
S97/270	m	80	0	06:56	Non-AD	superior frontal gyrus
S07/308	m	81	2	07:55	Non-AD	superior frontal gyrus

2.2 Laboratory equipment

Table 3 summarizes the most important laboratory equipment that was used in this study.

Table 3: Laboratory equipment used in this study.

Equipment	Version	Manufacturer
Bioanalyzer	2100	Agilent Technologies Inc, Santa Clara, CA
Bunsen burner, fireboy plus		Integra biosciences, Wallisellen
Cell incubator	CB150	Binder GmbH, Tuttlingen
Centrifuge	5424	Eppendorf AG, Hamburg
Clean bench	4A	Gelaire, Sydney
DNA sequencer	ABI PRISM™ 377	Applied Biosystem, Foster City
ELISA reader, Paradigm TM		Beckmann Coulter, Brea, CA
GeneChip Fluidics Station	450	Affymetrix, Santa Clara, CA
GeneChip Hybridization	645	Affymetrix, Santa Clara, CA
Odyssey® CLx Western Blot Detection System		LI-COR, Bad Homburg
Oven GeneChip Scanner	3000 7G	Affymetrix, Santa Clara, CA
Gel chamber (agarose gels)	Sub-Cell	PeqLab GmbH, Erlangen
Gel chamber (protein)	Mini Protean	BioRad GmbH, München
Gel documentation system		Vilber, Eberhardzell
Imager	LAS-3000 mini	FUJIFILM, Düsseldorf
PCR thermocycler	T3000	Biometra GmbH, Göttingen
pH meter	pH 525	WTW, Weilheim
Photometer	Nanodrop ND1000	PeqLap GmbH, Erlangen
Potter homogenizer		Wheaton Science Products, Millville, USA
Power supply	PowerPAC 3000	BioRad GmbH, München
Real time PCR	StepOnePlus™	Applied Biosystem, Foster City, CA
Refrigerated centrifuge	Rotina 46R	Hettich GmbH, Tuttlingen
Centrifuge	EBA 12R	Hettich GmbH, Tuttlingen
Sequence detection system	ABI 7900HT	Applied Biosystem, Foster City, CA
Sonicator QSonica	S-4000	Misonix, Farmingdale, NY
Table centrifuge	UEC6	UniEquip, München

Thermobloc	RS232	PeqLab Biotechnologie GmbH, Erlangen
Ultracentrifuge	SW41	Beckman Coulter, Brea, CA
Ultra turrax	T25	IKA-Werke GmbH, Staufen
Vortexer	MS1	IKA-Works INC., Wilmington, NC
Water bath	1052	GFL GmbH, Burgwedel

2.3 Consumables

Table 4 provides an overview of the different types of consumables used in this study.

Table 4: Consumables used in this study.

Consumables	Manufacturer
Amicon ultra-0.5 (10k)	Merck Millipore, Billerica, MA
Cell dishes/flasks/well plates	Thermo Scientific, Waltham, MA
Cell scraper	Thermo Scientific, Rockford, IL
Conical tubes (15 ml; 50 ml)	Greiner AG, Kremsmünster
Cryo tubes	VWR, Langenfeld
Disposable pipet (1 ml, 5 ml, 10 ml, 25 ml)	Corning Inc., Corning, NY
Filter paper	Whatman GmbH, Dassel
Gene Chip miRNA Array, 2.0	Affymetrix, Santa Clara, CA
Gloves	Semperit GmbH, Vienna
Micro amp 96 well plates	Applied Biosystem, Foster City
Nitrocellulose membrane	VWR, Langenfeld
PCR tubes	Bio-Budget GmbH, Krefeld
Pipets	Gilson, Villiiers-Le-Bel, France
Pipet tips (normal, plugged)	StarLab GmbH, Ahrensburg
Pipettor	Labbay BV, Geldermalsen, NL
reaction tubes (2 ml; 1.5 ml; 0.5 ml)	Sarstedt AG, Nümbrecht
	Eppendorf AG, Hamburg
Reaction tubes (0.2 ml)	Biozym Scientific GmbH, Oldendorf
Tissues clou prestige	Wepa Professional GmbH, Arnsberg
Ultracentrifuge polyallomer tubes	Herolab GmbH, Wiesloch
Well plates (96, 24, 6)	Thermo Scientific, Rockford, IL

2.4 Chemicals

The various chemicals used in this study are listed in the following Table 5.

Table 5: Chemicals used in this study.

Chemicals	Manufacturer
Acetic acid	VWR, Langenfeld
Acrylamide/bisacrylamide (30 %; 37.5:1)	VWR, Langenfeld
Acrylamide/bisacrylamide (30 %; 29:1)	VWR, Langenfeld
Agar	Carl Roth GmbH, Karlsruhe
Agarose	Bio-Budget GmbH, Krefeld
Ammonium acetate	Carl Roth GmbH, Karlsruhe
Ampicillin	VWR, Langenfeld
Ammonium persulphate (APS)	Sigma-Aldrich GmbH, Steinheim
Biotinylated protein ladder	Cell Signaling, Danvers, MA
Blasticidin S	Invitrogen, Carlsbad, CA
Bromophenole blue	Sigma-Aldrich GmbH, Steinheim
Bovine serum albumin (BSA)	Carl Roth GmbH, Karlsruhe
Boracic acid	Sigma-Aldrich GmbH, Steinheim
BSA 100x	New England Biolabs Inc, Ipswich
Caesium chloride	Pharmacia AB, Uppsala
CHAPS	Sigma-Aldrich GmbH, Steinheim
Chloroform	VWR, Langenfeld
DEPC treated water	Carl Roth GmbH, Karlsruhe
Dextran blue	Sigma-Aldrich GmbH, Steinheim
DMEM	Invitrogen, Carlsbad, CA
DMSO	Sigma-Aldrich GmbH, Steinheim
DNA ladder (100 bp)	Bio-Budget GmbH, Krefeld
DNA ladder (1 kb)	Bio-Budget GmbH, Krefeld
dNTPs	Bio-Budget GmbH, Krefeld
Dithiothreitol (DTT)	Invitrogen, Carlsbad, CA
DPBS	Invitrogen, Carlsbad, CA
EDTA	Carl Roth GmbH, Karlsruhe
Ethanol	VWR, Langenfeld
Ethidium bromide	Sigma-Aldrich GmbH, Steinheim
Fetal calf serum	Invitrogen, Carlsbad, CA
Glycine	Carl Roth GmbH, Karlsruhe

Glycerol	VWR, Langenfeld
Fast AP TM thermosensitive alkaline phosphatase	Fermentas GmbH, St. Leon-Rot
Formamid	VWR, Langenfeld
Guanidinium isothiocyanate (GITC)	Carl Roth GmbH, Karlsruhe
Hepes	Merck KGaA, Darmstadt
Isopropanol	VWR, Langenfeld
Lipofectamine^{TM} 2000	Invitrogen, Carlsbad, CA
Magnesium chloride	Carl Roth GmbH, Karlsruhe
ß-Mercaptoethanol	Fluka Chemie AG, Buchs, CH
Midori green advance	Biozym Scientific GmbH, Oldendorf
Methanol	Carl Roth GmbH, Karlsruhe
Milk powder	Carl Roth GmbH, Karlsruhe
NEB-buffer 3	New England Biolabs Inc, Ipswich
Nonidet P-40	AppliChem, Darmstadt
OPTI-MEM reduced serum media	Invitrogen, Carlsbad, CA
pd$(N)_6$ random hexamer phosphorylated	GeneLink, Hawthorne, NY
Phenol	Carl Roth GmbH, Karlsruhe
Poly-L-Lysine	Sigma-Aldrich GmbH, Steinheim
Ponceau S	Sigma-Aldrich GmbH, Steinheim
Potassium acetate	VWR, Langenfeld
Prestained protein ladder	Fermentas GmbH, St. Leon-Rot
QuickStart Bradford 1 x Dye Reagent	BioRad Laboratories, Hercules, CA
SDS	Carl Roth GmbH, Karlsruhe
SOC-Medium	Invitrogen, Carlsbad, CA
Sodium acetate	VWR, Langenfeld
Sodium chloride	Carl Roth GmbH, Karlsruhe
Sodium citrate	VWR, Langenfeld
Sodium hydroxide	VWR, Langenfeld
Sucrose	VWR, Langenfeld
TEMED	Sigma-Aldrich GmbH, Steinheim
Tris	VWR, Langenfeld
TritonX-100	Carl Roth GmbH, Karlsruhe
Tween-20	Carl Roth GmbH, Karlsruhe
Urea	VWR, Langenfeld
Xylene cyanol	Sigma-Aldrich GmbH, Steinheim

2.5 Kits, reagents and assays

The following Table 6 provides a list of the different kits, reagents and assays that were employed in this study.

Table 6: Kits, reagents and assays used in this study.

Kits, reagents, assays	Order no.	Manufacturer
AlamarBlue®	DAL1025	Life technologies, Carlsbad, CA
BCA Protein Assay Reagent	23225	Thermo Scientific, Rockford, IL
BigDye® terminator v1.1 cycle Sequencing Kit	4337449	Applied Biosystem, Foster City, CA
Dual-Glo® Luciferase Assay System	E2940	Promega Corporation, Madison, WI
EZ DNA Methylation gold Kit™	ZRC169911	Zymo Research, Irvine, CA
EZ-Link™ Plus Activated Peroxidase kit	31489	Thermo Scientific, Rockford, IL
FlashTag™ Biotin HSR Labeling Kit	FT10AFYB	Genisphere, Hatfield, PA
JetQuick Gel extraction Kit	420250	Genomed GmbH, Löhne
miRCURY LNA Univ. RT miRNA PCR	20330	Exiqon, Vedbaek
miRNeasy Micro Kit	217084	Qiagen, Hilden
miRNeasy Mini Kit	217004	Qiagen, Hilden
MSB® Spin PCRapace	BP10-0040	Invitek, Berlin
PeqGold Plasmid Miniprep Kit 1	12-6942-02	Peqlab, Erlangen
Platinum® SYBR® Green	11733-046	Invitrogen, Carlsbad, CA
TRIzol®-reagent	15596-018	Invitrogen, Carlsbad, CA
RNeasy MinElute Clean up Kit	74204	Qiagen, Hilden
TaqMan® Universal PCR Master Mix	4326614	Applied Biosystem, Foster City, CA
TaqMan® MicroRNA Reverse Transkription Kit	4366596	Applied Biosystem, Foster City, CA
TMB ELISA ultrasubstrate	34029	Thermo Scientific, Rockford, IL
Ultra Vision LP Large Volume Detection System HRP Polymer (ready-to-use)	TL-125-HL	Thermo Scientific, Rockford, IL

2.6 Solutions, buffers, media and gels

The following Table 7 and Table 8 provide lists of the different solutions, buffers, media and gels that were used in this study.

Table 7: Solutions for DNA, RNA and protein extraction by ultracentrifugation used in this study.

Solutions	Content
GITC solution (4 M)	4 M Guanidinium isothiocyanate 25 mM sodium citrate 0.8 % v/v β-mercaptoethanol ad 1058 ml distilled water pH 7 with NaOH
RNAsin mix	90 µl RNAsin (40 U/µl) 3 mM DTT ad 7,2 ml DEPC-treated water
CsCl solution	6 M caesium chloride 25 mM sodium acetate, pH 5 ad 500 ml DEPC-treated water
Proteinase K buffer	0.01 M Tris/HCl 5 mM EDTA 0.5 % v/v SDS ad DEPC-treated water

Table 8: Additional solutions, buffers, media and gels used in this study.

Solutions	Content
6 x loading buffer for sequencing gels	76.2 % v/v formamid 19 % v/v 25 mM EDTA-solution, pH 8 4.8 µg dextran blue
6 x loading buffer for agarose gels	30 % v/v glycerol 0.25 % w/v xylene cyanol 0.25 % w/v bromphenol blue
50 x TAE-buffer	2 M tris(hydroxymethyl) aminomethane 1 M acetic acid 50 mM EDTA pH 8.0
1 x TBE buffer	0.89 M tris(hydroxymethyl) aminomethane 0.89 M boracic acid 20 mM EDTA pH 8.0
1 x TE buffer	10 mM tris(hydroxymethyl) aminomethane 1 mM EDTA pH 7.5
10 x TBS buffer	1.37 M NaCl 0.2 M tris(hydroxymethyl) aminomethane pH 7.6
LB media	1 % w/v bacto-trypton 0.5 % w/v yeast-extract 1 % w/v NaCl (15 % w/v agar) 100 µg/ml ampicillin
PAA-gel for sequencing (7 %; 29:1)	10 M urea 7.2 % v/v acrylamide/bisacrylamide (30 % v/v; 29:1) 0.02 % v/v TBE 0.1 % v/v APS 30 µl TEMED ad 35 ml H_20

10 x PBS	1370 mM NaCl 27 mM KCL 80 mM Na_2HPO_4 15 mM KH_2PO_4 pH 7.4
1 x PBS-Tween	1 x PBS (1:10 dilution of 10 x PBS) 0.05 % v/v Tween-20
Running buffer (10x) for SDS-PAGE	0.25 M Tris 2 M glycine 1 % v/v SDS
Transfer buffer (1x) for western blot assay	25 mM Tris 0.2 M glycine 20 % v/v methanol
Ponceau S (0,1% (w/v))	1 g ponceau S 50 ml acetic acid
1 x Nonidet P-40 buffer	50 mM Tris-HCl, pH 7,8 150 mM NaCl 1 % v/v Nonidet P-40 PI 1:25 Phos Stop 1 tablet ad 10 ml DEPC-treated water
ELISA-Assay buffer	1 x PBS (1:10 dilution of 10 x PBS) 0.05 % v/v Tween-20 1 % w/v BSA
2 M H_2SO_4	55.53 ml 96 % v/v H_2SO_4 ad 500 ml H_2O

2.7 Oligonucleotides, enzymes and antibodies

Primers used for real-time-PCR analysis and 3' UTR luciferase reporter gene assays are listed in Table 9. All primers were generated with the tool Primer3 (http://primer3.ut.ee) and ordered from Eurofins MWG GmbH (Ebersberg, Germany).

Table 9: Primers used in this study

Gene	Primer sequence	Fragment size [bp]
	Real-time-PCR	
ARF1	5´-GACCACGATCCTCTACAAGC-3´ (for)	
	5´-TCCACACAGTGAAGCTGATG-3´ (rev)	111
ATXN1	5´-AGCATCGTGCATCAAGTCAC-3´ (for)	
	5´-TGGTCTGCAGCAGCACTAAG-3´ (rev)	176
BACE1	5´-GGCACTGTTATGGGAGCTGT-3´ (for)	
	5´-GCCACAGTCTTCCATGTCCA-3´ (rev)	162
EPHB2	5´-TCCATCTGGGACTTTCAAGG-3´ (for)	
	5´-GCATGAGGGAGGTCTCATTG-3´ (rev)	209
EP300	5´-CAAGCGGCCTAAACTCTCAT-3´ (for)	
	5´-CACCACCATTGGTTAGTCCC-3´ (rev)	118
ERK1	5´-CCTGGAAGCCATGAGAGATG-3´ (for)	
	5´-TGTTGATGAGCAGGTTGGAG-3´ (rev)	194
ERK2	5´-GCGCTTCAGACATGAGAACA-3´ (for)	
	5´-GTTGGAAGGCTTGAGGTCAC-3´ (rev)	235
FMR1	5´-TCCTCACTTTAGCTAACCACCA-3´ (for)	
	5´-GGCAGCCTGATAGGCAGAT-3´ (rev)	150
NCL	5´-AAATGGCTCCTCCTCCAAAG-3´ (for)	
	5´-ACGACCACCTTCTTTGCTGA-3´ (rev)	151
NR4A2	5´-AACTGCACTTCGGCAGAGTT-3´ (for)	
	5´-AGCCGAGTTACAGGCGTTT-3´ (rev)	173
OLFM1	5´-CTCCTCAGCCTCCTCTTCCT-3´ (for)	
	5´-GAACACATGGTCTGCTGTGG-3´ (rev)	155
P21	5´-GGAAGACCATGTGGACCTGT-3´ (for)	
	5´-GGATTAGGGCTTCCTCTTGG-3´ (rev)	178
RB1	5´-GAGCTTGGTTAACTTGGGAGAA-3´ (for)	
	5´-CATCTAGGTCAACTGCTGCAA-3´ (rev)	117
SIRT1	5´-ATTTATGCTCGCCTTGCTGT-3´ (for)	

	5´-CCAGCGTGTCTATGTTCTGG-3´ (rev)	217
TIMM9	5´-CCACGTGTTCTTTCCCATCT-3´ (for)	
	5´-TTGTCCAACCTTTGCTTGAA-3´ (rev)	173
TMEM106B	5´-ATTTGCCTTTGCATTCAAGC-3´ (for)	
	5´-ATGGAATCAATGCCACCAGT-3´ (rev)	231
U6	5´-CTCGCTTCGGCAGCACA-3´ (for)	
	5´-AACGCTTCACGAATTTGCGT-3´ (rev)	94
WT1	5´-CCAGCTCAGTGAAATGGACA-3´ (for)	
	5´-GACACCGTGCGTGTGTATTC-3´ (rev)	116
Z30	5´-ATGCGATGATGAGTGAAGTAGAG-3´ (for)	
	5´-CAGCTCAGAGAGAAGATTAAGAG-3´ (rev)	97
	3’ UTR luciferase reporter gene assay	
FMR1-WT	5´-GGGTATCTCGAGTTGATGCAATCCTTACAAATGA-3´ (for)	
	5´-CCGATAGCGGCCGCCCTTGCTGAATACAGCCTTTG-3´ (rev)	275
ERK1-WT	5´-GGGTATCTCGAGCCCTAGCCCAGACAGACATC-3´ (for)	
	5´-CCGATAGCGGCCGCAGGCCTCAGCAAAGGAGAG-3´ (rev)	166
ERK1-del	5´-CTCCCGCCGAAAATGGACACTGTGCCCAGCCCGGA-3´ (for)	
	5´-CCATTTTCGGCGGGAGAGGGGCAGGCAGGA-3´ (rev)	157
ERK2-WT	5´-GGGTATCTCGAGTGACTTCCCCACTGCTCTCT-3´ (for)	
	5´-CCGATAGCGGCCGCTGGGAAGGAGCTCACAGTCT-3´ (rev)	1091
ERK2-del 1	5´-CCTCGCATCAGCTTTCTGTGCAGAGATGACTG-3´ (for)	
	5´-GAAAAGCTGATGCGAGGGTACAGTAATTAT-3´ (rev)	1083
ERK2-del 2	5´-AGAAATGTCCGGATAACACTGATTAGTCAG-3´ (for)	
	5´-TTATCCGGACATTTCTGTGTCCCGTCAATG-3´ (rev)	1083

MiRNAs, pre-miRNAs, siRNAs, inhibitors and scrambled oligonucleotides used in this study are listed in Table 10.

Table 10: MiRNAs, pre-miRNAs, siRNAs, inhibitors and scrambled oligonucleotides used in this study

miRNAs	**Manufacturer**
hsa-miR-132-3p	Exiqon, Vedbaek
LNA™ PCR primer set, UniRT	
ID: 204129	
hsa-miR-212-3p	Exiqon, Vedbaek
LNA™ PCR primer set, UniRT	

ID: 204170	
U6snRNA LNA PCR primer set, UniRT ID: 203907	Exiqon, Vedbaek

Pre-miRNAs/scrambled oligonucleotides	**Manufacturer**
hsa-miR-132-3p pre-miR miRNA precursor ID: PM10166	Ambion, Carlsbad, CA
pre-miR™ miRNA precursor negative control#1 pre-miR miRNA precursor molecules ID: AM17110	Ambion, Carlsbad, CA
pre-miR™ miRNA precursor negative control#2 pre-miR miRNA precursor molecules ID: AM17111	Ambion, Carlsbad, CA

siRNAs/scrambled oligonucleotides	**Manufacturer**
Signal Silence p44/42 (ERK1/2) siRNA ID: 6560	Cell Signaling, Danvers, MA
Mm/Hs MAPK1 control siRNA ID: 1022564	Qiagen, Hilden
Signal Silence Control siRNA ID: 6201	Cell Signaling, Danvers, MA

inhibitors/scrambled oligonucleotides	**Manufacturer**
InSolution™ ERK-Inhibitor II ID: FR180204	Merck Millipore, Billerica, MA
ERK-Inhibitor, Negative control ID: FR180209	Merck Millipore, Billerica, MA

The different enzymes used in this study are listed in the following Table 11.

Table 11: Enzymes used in this study.

Enzymes	Order no.	Manufacturer
Hot star Taq DNA polymerase, 5 U/µl	203205	Qiagen, Hilden
HotStar HiFidelity Taq DNA polymerase, 2.5 U/µl	202602	Qiagen, Hilden
NotI, 10,000 U/ml	R0189L	New England Biolabs Inc, Ipswich
Phos Stop	04906837001	Roche, Mannheim
Proteinase K, 600 mAU/ml	70633	Merck KGaA, Darmstadt
Protease inhibitor tablets	11836170001	Roche, Mannheim
RNAse A, 50 U/mg	1010914200	Roche, Mannheim
RNAsin (40 U/µl)	N2115	Promega Corporation, Madison
RiboLock™ RNase Inhibitor, 40 U/µl	EO0381	Fermentas GmbH, St. Leon-Rot
Superscript II Reverse transcriptase, 200 U/µl	100004925	Invitrogen, Carlsbad, CA
T4-DNA-Ligase, 1U/µl	15224-017	Invitrogen, Carlsbad, CA
Taq DNA polymerase, 5 U/µl	10342-020	Invitrogen, Carlsbad, CA
Trypsin-EDTA	L11-004	PAA GmbH, Pasching
XhoI, 20,000 U/ml	R01462	New England Biolabs Inc, Ipswich

The different antibodies used for western blot (WB), immunohistochemical (IHC) staining and Enzyme linked Immunosorbent Assay (ELISA) analyses are listed in the following table.

Table 12: Antibodies used in this study.

Antibodies	Dilution	Manufacturer
Primary antibodies		
Mouse α-total ERK1/2 (#9107)	WB 1:2000	Cell Signaling, Danvers, MA
Rabbit α-p-ERK1/2 (#4370)	WB 1:1000; IHC 1:400	Cell Signaling, Danvers, MA
Rabbit α-total APP CT15Z	WB 1:3500	Gift of Dr. Edward Koo, University of California, San Diego
Rabbit α-total sAPP IG7/5A3	WB 1:50	Gift of Dr. Edward Koo, University of California, San Diego (Leuchtenberger S 2009)
Mouse α-human sAPPβ-sw (6A1) (#10321)	WB 1:50	Immuno-Biological Lab. Hamburg

Rabbit α-tubulin (#2144)	WB 1:3000	Cell Signaling, Danvers, MA
Rabbit α-beta-actin (#ab8227)	WB 1:1000	Abcam, Cambridge, MA
Rabbit α-vinculin (#ab129002)	WB 1:2000	Abcam, Cambridge, MA
Mouse α-Aβ40-BAP24	ELISA 1:1000	Roche, Mannheim
Mouse α-Aβ42-BAP15	ELISA 1:500	Roche, Mannheim
Mouse α-Aβ-IC16	ELISA 1:250	Roche, Mannheim

Secondary antibodies

Goat α-rabbit IRDye 800CW (#926-32211)	1:10,000	LI-COR, Bad Homburg
Goat α-mouse IRDye 800CW (#926-32210)	1:10,000	LI-COR, Bad Homburg
Goat α-rabbit IRDye 680RD (#926-68071)	1:10,000	LI-COR, Bad Homburg
Goat α-mouse IRDye 680RD (#926-68070)	1:10,000	LI-COR, Bad Homburg

2.8 Commercially available DNAs, vectors, bacteria and cell lines

The commercially available DNAs listed in Table 13 were used for the generation of the wild type 3' UTR fragments. The 3' UTR fragments were cloned in the psiCHECK^{TM}-2 vector (Promega, Madison, WI) and the vector map is shown in Figure 5. The clonal production of these vectors was done in the bacteria *Escherichia coli* DH5-α competent cells (Life technologies, Carlsbad, CA). The glioblastoma cell line T98G (Table 14) was used for transient transfection of pre-miRNAs and vectors.

Table 13: Commercially available DNA used in this study.

Commercially available DNA	Source
Human fetal tissue brain	BioChain Institute, Hayward, CA
Human normal tissue brain	BioChain Institute, Hayward, CA
Human normal tissue brain occipital lobe	BioChain Institute, Hayward, CA

Commercially available vector used in this study:

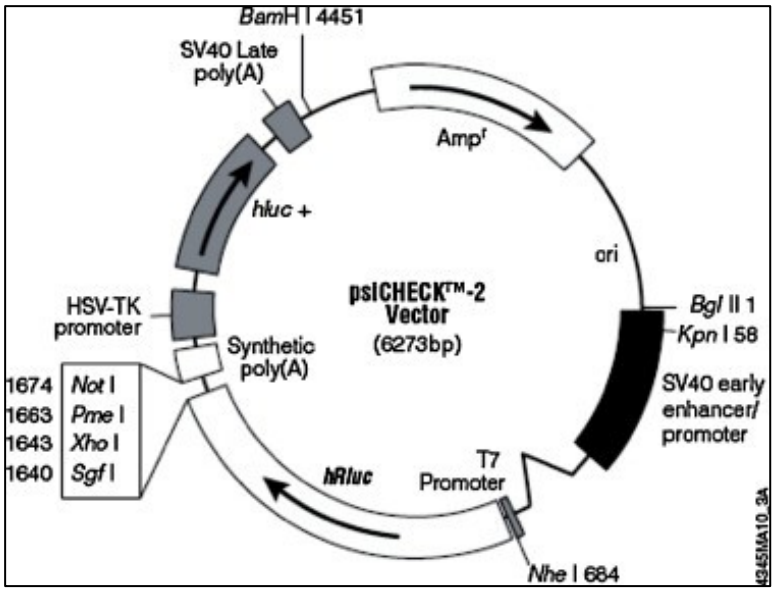

Figure 5: The psiCHECK^{TM}-2 vector map (Promega).
The psiCHECK^{TM}-2 vector was used for 3' UTR luciferase reporter gene assay.

Table 14:Cell lines used in this study.

Cell line	Species	Origin	Source
A172	human	glioblastoma	ATCC Manassas, Virginia
Hek293sw (APP695sw)	human	embryonic kidney	Lab S. Weggen, Düsseldorf
SH-SY5Y	human	neuroblastoma	Lab S. Weggen, Düsseldorf
T98G	human	glioblastoma	ATCC Manassas, Virginia

3 Methods

3.1 Molecular biological methods

3.1.1 Extraction of nucleic acids from brain tissue samples

The extraction of DNA, RNA and protein from the first set of Alzheimer's disease and control brain tissue samples of the grey matter (Table 1) was done by ultracentrifugation according to a published protocol (Van den Boom J 2003). These RNA samples were used for miRNA microarray analyses and validation of differential expression of miRNAs by real-time PCR.

The additional extraction of RNA from the first (Table 1) and second set (Table 2) of brain tissue samples was done by the miRNeasy Mini Kit according to manufacturer's protocol. These RNA samples were used for miRNA target gene validation by real-time PCR.

3.1.2 MiRNA microarray analyses

RNA of the first 20 samples (Table 1) was isolated by ultracentrifugation, labelled with a poly-A tail and biotin by the FlashTag™ Biotin HSR Labelling Kit according to manufacturer's protocol. The labelled RNA samples were hybridized on GeneChip® miRNA 2.0 Arrays with 830 human mature miRNAs, stained and scanned according to the protocol by Affymetrix® (Figure 6). The hybridization, staining and scanning were done by the BMFZ (Biologisch-Medizinisches Forschungszentrum), Heinrich-Heine-University, Düsseldorf. The bioinformatical analysis of the miRNA array data was done by Dipl.-Bioinform. Edith Willscher (Interdisciplinary Center for Bioinformatics, University of Leipzig) using the Gene Spring computer program and by Dr. Matthias Prucha (Illumina®, Munich) using the Partek program.

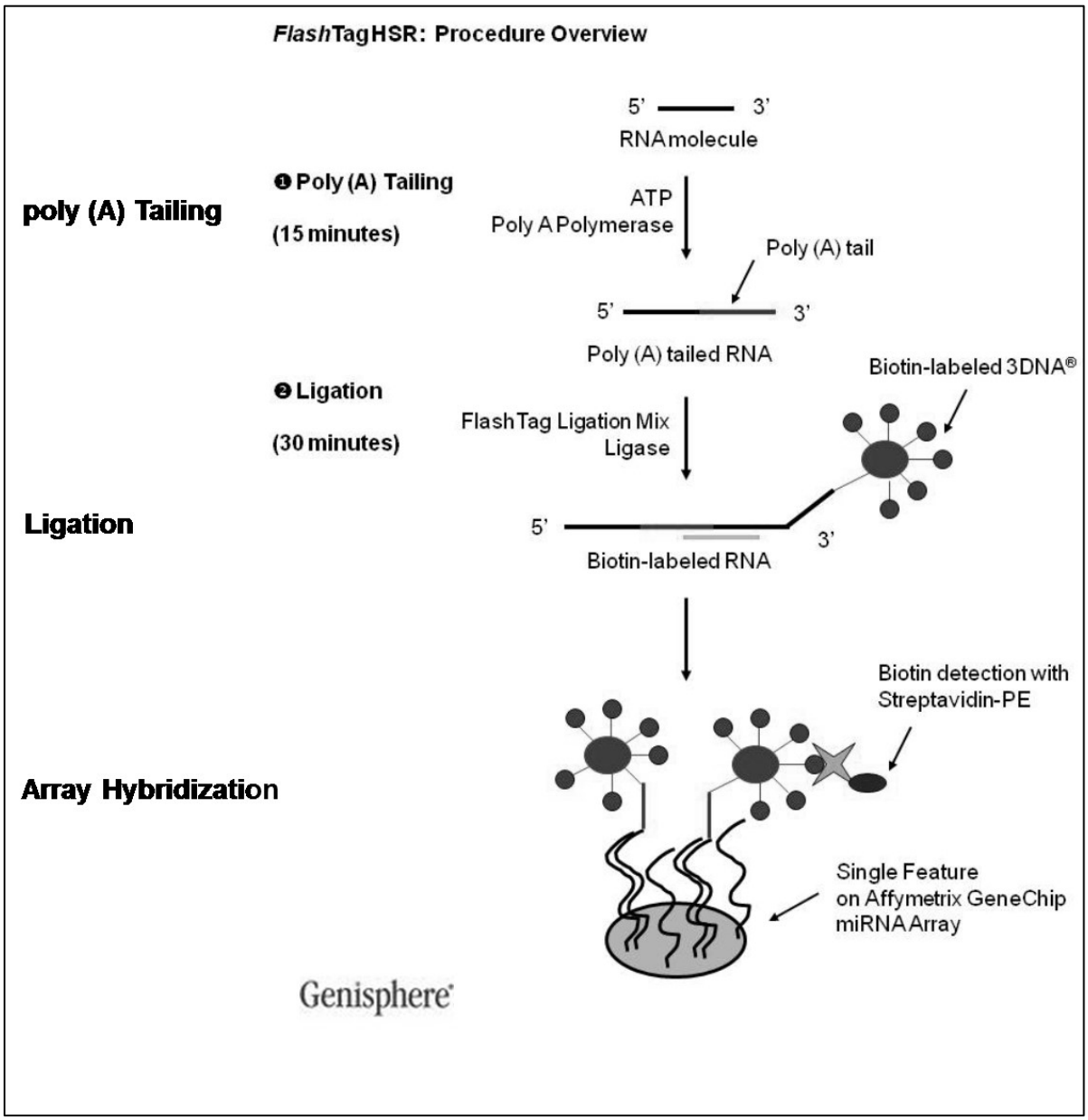

Figure 6: MiRNA expression profiling by miRNA microarray technique (Modified according to Genisphere)
First, a poly-A tail is added by poly-A polymerase to the miRNA molecules followed by ligation of the biotinylated signal molecule to the target RNA sample. After biotin-ligation the miRNAs are hybridized to the GeneChip® miRNA 2.0 Array and detected with Streptavidin.

3.1.3 Real-time RT-PCR analysis

3.1.3.1 Expression analysis of single mature miRNAs by real-time RT-PCR

For the detection of miRNA expression 20 ng/µl total RNA was reverse transcribed using the miRCURY LNA™ Universal RT microRNA PCR assay according to the manufacturer's protocol. Specific miRNAs were amplified by real-time PCR with microRNA LNA™ PCR primer sets (Figure 7).

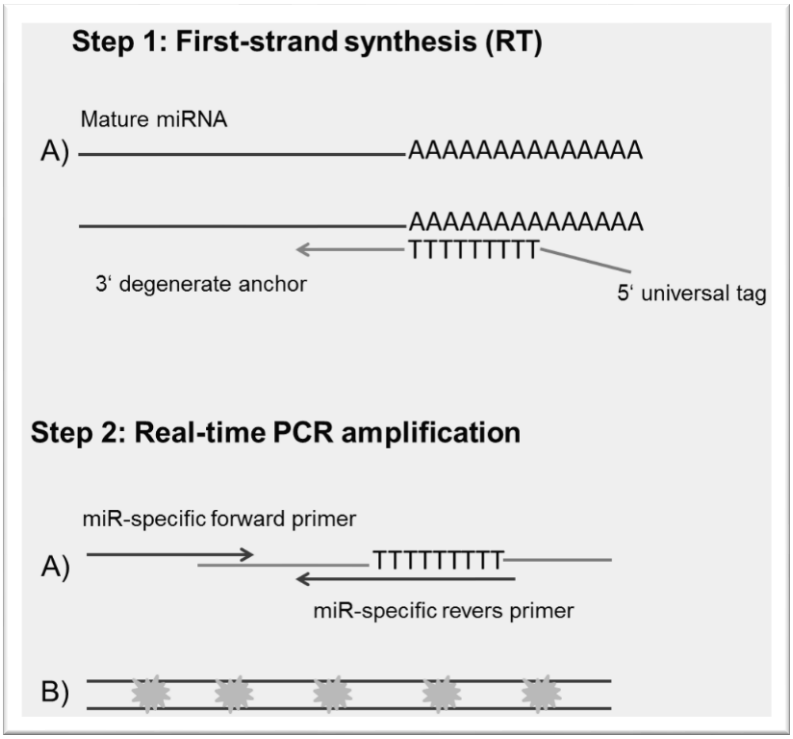

Figure 7: Schematic outline of the reverse transcriptase real-time PCR (Modified according to Exiqon.)
The first step is the universal reverse transcription which starts with adding a poly-A tail to the mature miRNA template. The cDNA is synthesized using poly-T primers with 5'universal tag and 3'degenerate anchor. In the second step the cDNA is amplified by real-time PCR using miRNA-specific and LNA™ enhanced forward and reverse primers. SYBR® GREEN is used for detection.

3.1.3.2 Expression analysis of mRNAs by real-time RT-PCR

The cDNA synthesis of RNA samples used for validation of miRNA target gene expression was done by reverse transcription using random-hexamer primer and real-time PCR using SYBR® GREEN as fluorescent dye. 3 µg RNA of each sample were diluted in 30.4 µl DEPC H_2O, incubated for 5 minutes at 70 °C and cooled on ice. After a brief centrifugation step 18.6 µl of master-mix is added to each RNA sample (Table 15).

Table 15: Master-mix and conditions for reverse transcription.

1 x Master-mix reverse transcription		Program	
0.4 µl	0.1 M DTT	42 °C	50 min
1.0 µl	RNAsin	80 °C	10 min
1.7 µl	BSA (1 mg/ml)	4 °C	∞
2.5 µl	dNTPs (25 mM)		
10.0 µl	5 x H-RT-buffer, first strand		
3.0 µl	pd(N_6) random hexamer primer (1.5 µg/µl)		
1.0 µl	Superscript Reverse Transcriptase II (200 U/µl)		

After reverse transcription an aliquot of the cDNA was diluted 1:25 with H_2O dest. and 5 µl of the diluted cDNA were used for real-time PCR. Table 16 contains the components of the master mix and conditions for the real-time PCR.

Table 16: Master-mix and conditions for real-time PCR.

1 x Master-mix real-time PCR		Program	
12.5 µl	SYBR® GREEN-Mix	95 °C	10 min
1.0 µl	forward primer (10 pmol)	95 °C	15 sec
1.0 µl	reverse primer (10 pmol)	60 °C	1 min
5.5 µl	H_2O	4 °C	∞

Real-time PCR analyses were performed on the StepOnePlus™ machine which converts the fluorescent data of SYBR® GREEN incorporation into cycle threshold data. Human universal reference (HU) RNA was used as a calibrator and U6 snRNA (miRNA) or ARF1 (mRNA) as reference transcripts. The fold change expression data relative to human universal reference RNA were calculated with the $2^{-\Delta\Delta Ct}$-method (Livak KJ 2001). Statistical analysis was performed using the software GraphPad Prism (www.graphpad.com).

3.2 3´UTR-luciferase reporter gene assay and transient transfection

The 3´UTR-luciferase reporter gene assay was used to prove the direct binding of the miRNA of interest to its putative target mRNA. Binding is permitted between the seed sequence of the miRNA and the complementary sequence in the 3´UTR of the mRNA. The part of the mRNA 3´UTR region surrounding the miRNA binding site, was cloned into the luciferase reporter psiCHECK^{TM}-2 vector. This vector contains two reporter genes, *Firefly* and *Renilla*. Measuring decreases in *Renilla* activity enables monitoring of the miRNA effect. The *Firefly* luciferase allows normalization of *Renilla* luciferase expression. Using transient transfection of the psiCHECK^{TM}-2 vector together with precursor-miRNAs (pre-miRNAs), the specificity of the binding can be determined. The quantification of the luminescent signal from the two reporter genes *Firefly* and *Renilla* luciferase was done by Dual-Glo® Luciferase Reporter Assay System with an ELISA reader (Paradigm TM) according to the manufacturer´s protocol.

3.2.1 Generation of the wild type 3' UTR fragment

PCR fragments containing parts of the target mRNAs with the predicted miRNA seed sequence were cloned into the psiCHECK^{TM}-2 vector as followed. The PCR fragments were synthesized using the respective primers (Table 9) and HotStar HiFidelity *Taq* DNA Polymerase at an annealing temperature of 58 °C for 40 cycles according to the manufacturer´s instructions. A mix of commercially available DNAs (Table 13) was used as template.

3.2.2 Direct deletion of the miRNA binding site in the 3`-UTR of target mRNA by Overlap-Extension Polymerase Chain Reaction (OE-PCR)

Generation of a 3' UTR fragment with deleted miRNA binding site was done by an overlap-extension-PCR (OE-PCR). Therefore, two PCR products, which overlap in the region to be deleted, were combined to get a longer hybrid gene without the miRNA binding site. The OE-PCR was done as described by Dr. Franziska Liesenberg (Liesenberg F 2012). Primers used for OE-PCR are listed in Table 9.

3.2.3 Cloning of the 3' UTR fragments in the psiCHECK^{TM}-2 vector

The PCR fragments were purified with the Jetquick PCR Purification Kit. Restriction enzymes *XhoI* and *NotI* were used to digest the purified PCR products and the psiCHECK^{TM}-2 vector according to the manufacturer´s protocol.

The DNA concentration of the PCR-product was determined with the Nanodrop 1000 spectrophotometer (PeqLap GmbH). The ligation was done with the T4-DNA-Ligase kit according to the manufacturer´s protocol. DNA was incorporated into competent *E. coli* cells by heat shock at 42 °C for 30 sec followed by incubation on ice for 2 min. 250 µl of antibiotic free LB-medium was added and cells were shaken for 1 hour at 37 °C. The transformed cells were plated on LB plates containing 100 µg/ml ampicillin. The bacteria were incubated overnight at 37 °C. The next day, single colonies were picked and transferred in 50 µl of sterile water. To test if the PCR fragment was inserted properly, a PCR of each colony dissolved in water was performed. Colony PCR was performed at 58 °C for 40 cycles with 5 µl of the bacterial cell solution, HotStar *Taq* DNA polymerase and primers encompassing the multicloning site of the psi-CHECK^{TM}-2 vector. Afterwards, PCR product sizes were analysed by agarose gel electrophoresis. Bacterial clones showing an insert of the expected size were inoculated in 3 ml LB-medium and grown over night at 37°C by shaking at 200 rpm. Plasmid DNA was extracted from overnight cultures using the peqGOLD Plasmid Miniprep Kit according the manufacturer´s protocol and eluted in 50 µl of H_2O dest. A control digest was performed with 5 µl of the plasmid DNA, 0.5 µl *NotI*, and 0.5 µl *XhoI* in a final volume of 20 µl for 1 h at 37 °C and analysed by agarose gel electrophoresis. The correct sequence of the inserted DNA was validated by sequencing (StarSEQ, Mainz) (http://www.starseq.com).

3.2.4 Transient transfection of T98G cells with vector constructs and pre-miRNA molecules

The precursor-miRNA (pre-miRNA) pre-miR-132-3p (Table 10) was overexpressed in T98G cells by transient transfection with Lipofectamine^{TM} 2000. To normalize for side-effects not caused by specific miRNA overexpression, cells were transfected with commercially available negative control oligonucleotides (NC#1). The 3' UTR fragments of the putative targets ERK1 and ERK2 containing the binding site(s) for *miR-132-3p* were cloned in the psiCHECK^{TM}-2 vector according to the protocol explained in 3.2.3 and also transiently transfected in the T98G cells.

24 h before transfection, 9000 T98G cells/well were seeded on a 96 well-plate in 100 µl/well DMEM containing 10 % (v/v) FCS and 1 % (v/v) penicillin G/streptomycin and incubated at 37 °C in a humidified atmosphere containing 5 % CO_2. The next day the medium was replaced by 50 µl/well DMEM containing 10 % (v/v) FCS but without penicillin G/streptomycin. Cells were transfected with 75 nM of pre-miR-132 or NC#1 together with 200 ng of the respective vector construct with Lipofectamine^{TM} 2000 as described in the manufacturer´s protocol. Afterwards, oligonucleotide solution together with

the vector constructs and transfection reagent were diluted in 25 µl OptiMEM each. Then both dilutions were mixed and incubated for 20 minutes at room temperature. Subsequently, 50 µl transfection mixture was added per well of T98G cells. 48 h post transfection the Dual-Glo® Luciferase Reporter Assay was used for determination of the *Renilla* and *Firefly* luciferase activities. Statistical analysis was performed using the software GraphPad Prism.

3.2.5 Transient transfection of Hek293sw (*APP*695sw) and SH-SY5Y cells with pre-miRNA and siRNA molecules

To analyze the effect of *miR-132-3p* on APP-processing, the cell line Hek293, which was stably transfected with *APP*695sw, was used for ELISA tests. The double mutation (sw) of *APP* (K595N/M596L) was originally found in a Swedish family with familial Alzheimer´s disease (Mullan M 1992).The cell line Hek293sw (*APP*695sw) produces about six to eight times more Aβ than wild type Hek293 cells.

The precursor-miRNA (pre-miRNAs) pre-miR-132-3p (Table 10) was overexpressed in Hek293sw (*APP*695sw) and SH-SY5Y cells by transient transfection with Lipofectamine™ 2000 according to the manufacturer´s protocol. 24 h before transfection, 1,000,000 Hek293sw (*APP*695sw) and SH-SY5Y cells/well were seeded on a 6 well-plate. Hek293sw (*APP*695sw) cells were transfected with either 75 nM pre-miR-132-3p or NC#2 while SH-SY5Y cells were transfected with either 50 nM pre-miR-132-3p or NC#2.

The Hek293sw (*APP*695sw) cells were also transiently transfected with siRNAs to inhibit the expression of ERK2 (22.5 nM siRNA) or both ERK1/2 (100 nM siRNA). To normalize for side-effects not caused by specific siRNA transfection, additional cells were transfected with respective amounts of commercially available signal silence control siRNA (Table 10).

72 h post transfection proteins were isolated through lysing the cells with Nonidet P-40 buffer according to 3.3.2 and RNA was isolated with TRIzol® according to 3.3.1. In addition, the toxicity of the transfected molecules was analysed with AlamarBlue® according to the manufacturer´s protocol. The cell culture supernatants were used for Enzyme-linked Immunosorbent Assay (ELISA) analyses as described in 3.4.3.

3.3 Cell based methods

3.3.1 RNA extraction from cells using TRIzol®-reagent

The cells in a 6 cm dish were first washed with DPBS, resuspended in 1 ml TRIzol®-reagent and RNA was extracted according to the manufacturer´s protocol. The RNA pellet was 10 minutes air dried and resuspended in 50 µl DEPC treated water. Finally the RNA was denatured at 50 °C for 5 minutes and incubated on ice for 5 minutes. The RNA concentration was measured at 260 nm by Nanodrop 1000 and the quality of the RNA was tested by running an aliquot on a 1 % (w/v) agarose gel.

3.3.2 Protein extraction from NP-40 lysis buffer-treated cells

The cells in a 6 cm dish were first washed with DPBS and then scraped with a cell scraper in 1 ml PBS and transferred into a tube. After 2 minutes centrifugation with 13,000 x g at 4 °C, the supernatant was discarded and the cells resuspended in 30 µl NP-40 lysis buffer. Then the tube was incubated on ice for 20 minutes while being vortexed every 5 minutes. After 15 minutes centrifugation with 13,000 x g at 4 °C, the supernatant was transferred to a fresh tube. The protein concentration was measured with BCA protein assay reagent according to the manufacturer´s protocol (Thermo Scientific, Rockford, IL).

3.3.3 ERK1/2-Inhibitor treatment of Hek293sw (*APP*695sw)

1,000,000 Hek293sw (*APP*695sw) cells/well were seeded on a 6-well-plate in 2 ml/well DMEM containing 10 % (v/v) FCS and 1 % (v/v) penicillin G/streptomycin and incubated at 37 °C in a humidified atmosphere containing 5 % CO_2. The next day the medium was replaced by 1 ml/well DMEM containing 10 % (v/v) FCS but without penicillin G/streptomycin. The cells were treated with 5 µM ERK1/2-Inhibitor. To normalize for side-effects not caused by specific ERK1/2-Inhibitor treatment, additional cells were treated with commercially available ERK-Inhibitor negative control (Table 10). After 24 h, the treatment procedure was repeated and after 48 h the cell culture supernatants were used for Enzyme-linked Immunosorbent Assay (ELISA) analyses as described in 3.4.2.

This inhibitor molecule of ERK1/2 was a cell permeable pyrazolopyridazinamine with the chemical formula $C_{18}H_{13}N_{7.}$ It acts as a potent, ATP-competitive inhibitor of ERK1 and ERK2 whereby their biological activity is controlled. The inhibitor negative control was a structural analog with the chemical formula $C_{18}H_{12}N_6O$. The structural formula of ERK1/2-Inhibitor and inhibitor-negative control are shown in Figure 8.

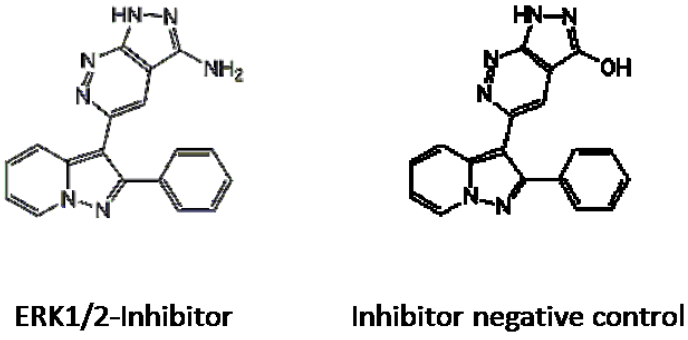

ERK1/2-Inhibitor Inhibitor negative control

Figure 8: Structural formulas of the ERK1/2 Inhibitor and inhibitor-negative control.

3.4 Protein-based methods

3.4.1 Sodium dodecyl sulfate polyacrylamide gel electrophoresis (SDS-PAGE), Western blot analysis and antigen-antibody reaction

A total amount of 15 µg proteins was separated by sodium dodecyl sulfate polyacrylamide gel electrophoresis (SDS-PAGE) according to their molecular weight as described (Laemmli 1970). The gels were run for 90 minutes at 180 V.

Afterwards the proteins were transferred from the gel onto a nitrocellulose membrane by Western blotting (Towbin H 1979). The transfer was run for 90 minutes at 250 mA and 4 °C. The membrane was stained in Ponceau S-solution for 2 minutes at RT to control the transfer, followed by washing with water. The destained membrane was incubated in 2.5 % BSA in TBS-Tween-20 for 1 h at RT to reduce unspecific background binding. The primary antibody (Table 12) was incubated with the membrane at a concentration recommend by the company over night at 4 °C. The secondary antibody (Table 12) was incubated for 1 h at RT. IRDye® secondary antibodies and the Odyssey Imager by Li-Cor® were used to detect the proteins by infrared fluorescence (Figure 9). Quantification of the western blots was done with the Li-Cor® Software. Statistical analysis was performed using the software GraphPad Prism.

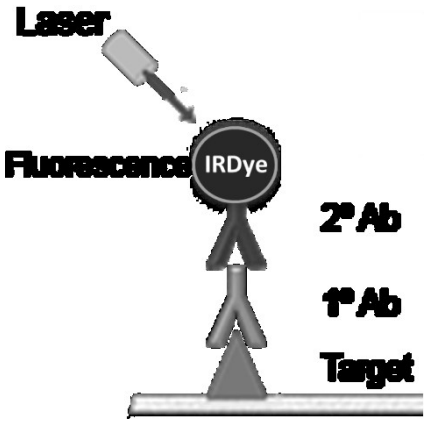

Figure 9: Schematic outline of the infrared fluorescent detection (modified according to Li-Cor®) The primary antibody binds its target onto the membrane and the labelled secondary antibody detects the primary antibody. The secondary antibodies are labelled with spectrally distinct IRDye® fluorescent dyes and were detected in independent fluorescence channels (700 and 800 nm).

3.4.2 Immunohistochemical staining of phosphorylated ERK1/2 in AD and non-AD tissue

To investigate the phosphorylated status of ERK1/2 (P-ERK1/2) in AD and non-AD brain tissue sections, three AD and one non-AD formalin-fixed and paraffin-embedded tissue samples were cut with a microtome and stained with an antibody against P-ERK1/2 in a

concentration of 1:400 at pH 6.1. For the antibody staining, the Ultra Vision LP Large Volume Detection System was used according to the manufacturer´s protocol without applying the Ultra Vision Block.

3.4.3 Enzyme-linked Immunosorbent Assay (ELISA)

To analyze the Aβ40 and Aβ42 protein expression in siRNA (ERK1/2) and pre-miR-132-3p transfected Hek293sw (*APP*695sw) cells, the cells were transfected as described in 3.2.5. After 72 h the cell culture supernatant was collected and analysed by enzyme-linked immunosorbent assay (ELISA) (Kemeny D 1994) (Hahn S 2011).

On the first day, a 96-well high-binding plate was coated with 100 µl/well capture antibody IC16, which was diluted 1:250 in 1 x PBS. This capture antibody IC16 binds amino acids 1-15 of the Aβ sequence. The plate was incubated overnight at 4 °C. The next day the capture antibody was poured off the plate and then 50 µl/well assay buffer was added. To generate standard curves, synthetic Aβ40 and Aβ42 were loaded in duplicates, 50 µl/well. 20 µl cell culture supernatant for Aβ40 and 120 µl cell culture for Aβ42 were loaded in triplicates. The HRP-coupled detection antibodies were diluted in assay buffer (Aβ40-HRP 1:1000 and Aβ42-HRP 1:500) and 50 µl of each were added to each well. The volume of each well was adjusted with assay buffer to 200 µl so that the plate was covered and incubated overnight at 4 °C. On the third day the antibodies were poured off and the wells were washed three times with 100 µl PBS-Tween and once with PBS. After removing the buffer completely, 50 µl TMB ELISA ultrasubstrate was added to each well. After 1-10 minutes incubation in the dark at RT, the reaction was stopped by adding 50 µl/well 2 M H_2SO_4. The absorbance was measured using a Paradigm microplate ELISA reader at 450 nm. The average of triplicate measurements from each experiment was normalized to DMSO control condition. Statistical analysis was performed using GraphPad Prism (GraphPad Software).

4 Results

4.1 Expression analysis of selected mouse miRNAs in human AD brain tissue samples

An earlier microarray-based analysis (performed by Dr. Petra Zipper, Department of Neuropathology, Heinrich Heine University Düsseldorf) of the *APP*655sw/PS1deltaExon9 transgenic mouse model of AD had provided evidence for 8 miRNAs showing differential expression when compared to wild type mouse brain tissue. The expression of these 8 miRNAs (*mmu-miR-96-5p, mmu-miR-141-3p, mmu-miR-182-5p, mmu-miR-183-5p, mmu-miR-200a-3p, mmu-miR-200c-3p, mmu-miR-429-3p, and mmu-miR-685*) was upregulated in the transgenic mouse brains compared to corresponding brain tissue samples of wild type mice.

To analyze the expression of these 8 murine miRNAs in human brains, real-time RT-PCR (3.1.3.1) was performed with 10 human brain tissue samples from AD patients compared to 10 aged-matched non-AD control samples (Table 1). The miRNAs *miR-96-5p, miR-141-3p, miR-183-5p* and *miR-429* were undetectable in human brain tissues. *Mmu-miR-685* was removed from the miRBase database (www.mirbase.org) because this mRNA has emerged as a fragment of RNase P RNA. The expression of the miRNAs *miR-182-5p, miR-200a-3p* and *miR-200c-3p* showed no significant differences in the human AD brain tissue samples compared to the control samples (Figure 10). These results suggested that the differential expression of these miRNAs is specific for the *APP*655sw/*PS1*deltaExon9 mouse model and may not be of relevance in AD patients.

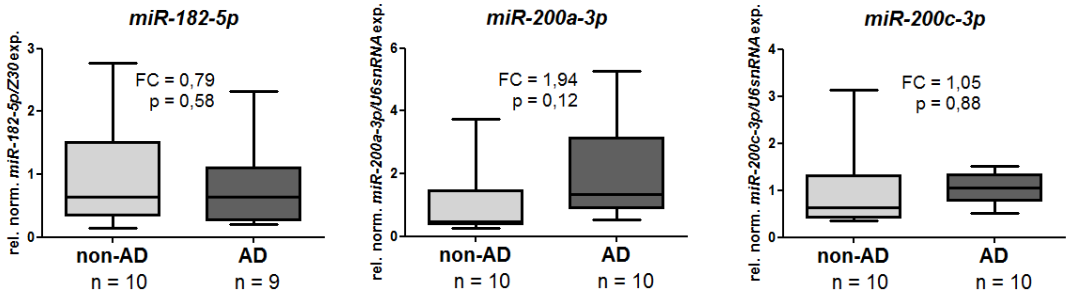

Figure 10: Real-time RT-PCR based expression analysis of *miR-182-5p, miR-200a-3p* and *miR-200c-3p* in AD brain tissue samples.
The expression of all three miRNAs was analyzed in autopsy brain tissue samples of AD patients versus normal brain samples from age-matched control subjects. Human universal reference RNA was used as a calibrator, and either U6 snRNA or Z30 were used as endogenous controls. The mean expression of the respective miRNAs in non-AD brain tissue samples was set to one. Box plots are depicted indicating median, lower and upper quartile, as well as sample maximum and sample minimum of normalized expression values. Statistics were performed by two-sided unpaired t-test. n, number of tissue samples; FC, fold change; p, p-value. Note absence of significant expression differences between AD and non-AD tissues.

4.1.1 First microarray-based screen of miRNA expression in human AD versus control brain tissue samples

To discover novel miRNAs that are differentially expressed in human AD brains, a miRNA microarray (GeneChip® miRNA 2.0 Array) analysis was performed to measure the expression of 830 human mature miRNAs in 10 human brain tissue samples from AD patients compared to 10 aged-matched non-AD control samples (Table 1) (3.1.1; 3.1.2.). The brain tissue samples originated from the medial frontal gyrus, and grey matter was preferentially used to enrich the samples for neuronal cell bodies. The bioinformatic analysis was performed by Edith Willscher using the software Genespring. Differentially expressed miRNAs with an absolute fold change (FC) greater than 2 and p values lower than 0.05 are shown in Table 17.

Table 17: Differentially expressed miRNAs in AD vs. non-AD tissue samples resulting from the first miRNA microarray hybridization. The underlined miRNAs were further investigated by real-time RT-PCR analysis (3.1.3). up, upregulated; down, downregulated. FC, fold change.

miRNA	FC absolute	p-value	miRNA-sequence	Regulated
hsa-miR-1184	5.05	0.0178	ccugcagcgacuugauggcuucc	up
hsa-miR-222	4.54	0.0162	agcuacaucuggcuacugggu	down
hsa-miR-138-5p	4.41	0.0164	agcuggugugugaaucaggccg	down
hsa-miR-107	4.36	0.0342	agcagcauuguacagggcuauca	down
hsa-miR-433-3p	3.57	0.0079	aucaugaugggcuccucggugu	down
hsa-miR-487b-3p	3.49	0.0087	aaucguacagggucauccacuu	down
hsa-miR-24-3p	3.42	0.0153	uggcucaguucagcaggaacag	down

hsa-miR-574-3p	3.26	0.0035	cacgcucaugcacacacccaca	down
hsa-miR-181b-5p	3.00	0.0343	aacauucauugcugucggugggu	down
hsa-miR-127-3p	2.79	0.0438	ucggauccgucugagcuuggcu	down
hsa-miR-874-3p	2.62	0.0019	cugcccuggcccgagggaccga	down
hsa-miR-370-3p	2.62	0.0097	gccugcugggguggaaccuggu	down
hsa-miR-139-3p	2.39	0.0025	uggagacgcggcccuguuggagu	down
hsa-miR-140-3p	2.29	0.0047	uaccacaggguagaaccacgg	down
hsa-miR-342-3p	2.19	0.0079	ucucacacagaaaucgcacccgu	down
hsa-miR-132-3p	2.18	0.0029	uaacagucuacagccauggucg	down

4.1.2 Real-time RT-PCR validation of the differentially expressed human miRNAs from the first microarray screen

The differential expression of nine selected miRNAs (underlined) was validated by real-time RT-PCR (3.1.3.1) in the same set of tissue samples (Table 1) with miRCURY LNA™ primer sets. All investigated miRNAs except *miR-1184* were expressed in human brain tissue. The expression of *miR-132-3p* showed a significant downregulation in the AD compared to the age-matched non-AD brain tissue samples, while the expression of *miR-222* was significantly upregulated (Figure 11). The expression of the other six miRNAs did not differ between AD and control samples. It is known that *miR-212-3p* and *miR-132-3p* share the same seed-region (Wanet A 2012). For this reason, the expression of *miR-212-3p* was also investigated and displayed a comparable downregulation in the AD brain tissue samples when compared to the age-matched control tissues (Figure 11).

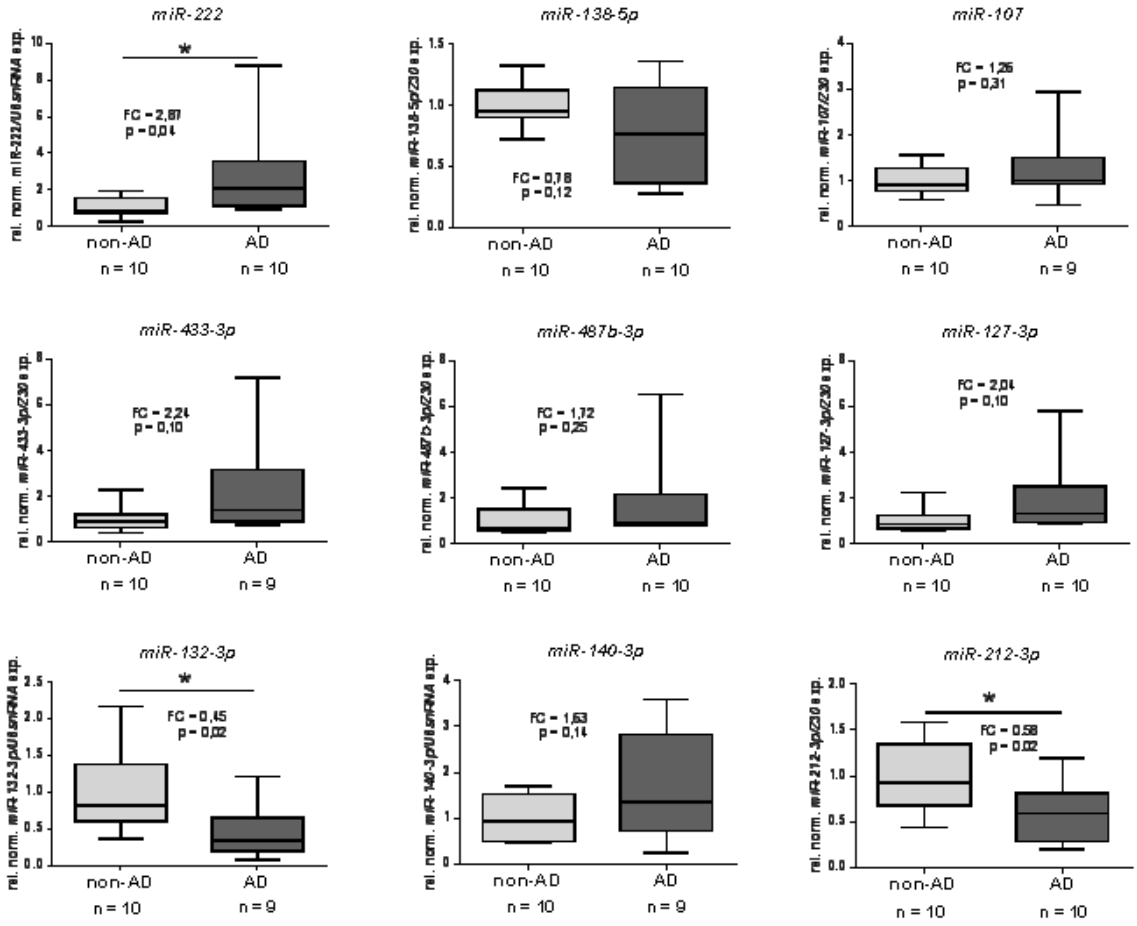

Figure 11: Real-time RT-PCR based expression analysis of nine selected miRNAs in brain tissue samples of AD patients versus non-AD controls.

The differential expression of miRNAs was validated in autopsy brain tissue samples of AD patients and age-matched control brain samples (non-AD). Human universal reference RNA was used as a calibrator, and either U6 snRNA or Z30 were used as endogenous controls. The mean expression of the respective miRNA in non-AD brain tissue samples was set to one. Box plots are depicted indicating median, lower and upper quartile as well as sample maximum and sample minimum of normalized expression values. Statistics were performed by two-sided unpaired t-test. *, significant expression differences ($p<0.05$). n, number of tissue samples; FC, fold change; p, p-value.

4.1.3 Second microarray screening of miRNA expression in human AD versus control brain tissue samples

The intensity of the miRNA signals in the first microarray screening was below the background level. One possible reason for this was the use of Amicon 0.5-ultra 10K filters to purify and enrich the miRNA before hybridization (3.1.2). Therefore, the signal intensity was tested again after the purification with filters of the RNEasy MinELUTE Cleanup kit, or without any purification. The highest signal intensity was observed using the unpurified RNA. Subsequently, the complete microarray analysis was repeated with unpurified RNA of the same 10 AD and 10 non-AD brain tissue samples. Various differentially regulated miRNAs were found depending on the analysis software used. The bioinformatic analysis was performed by Edith Willscher using the software Genespring or, alternatively, by Matthias Prucha with the software Partek. MiRNAs with an absolute fold change (FC) greater than 2 and a p-value smaller than 0.05 are shown in tables 18 (Genespring analysis) and 19 (Partek analysis).

Table 18: Differentially expressed miRNAs in AD versus non-AD tissue samples of the second miRNA microarray screening analysed with the software Genespring. The underlined miRNAs were further investigated by real-time RT-PCR analysis (3.1.3). up, upregulated; down, downregulated.

MiRNA	FC absolute	p-value	MiRNA-sequence	regulated
hsa-miR-212-3p	6.20	$5.45*10^{-5}$	uaacagucuccagucacggcc	down
hsa-miR-1274b	4,05	0,0430		up*
hsa-miR-505-5p	2.96	0.0203	gggagccaggaaguauugaugu	down
hsa-miR-138-2-3p	2.91	0.0117	gcuauuucacgacaccaggguu	down
hsa-miR-1250-5p	2.68	0.0047	acggugcuggauguggccuuu	down
hsa-miR-132-3p	2.61	$2.91*10^{-6}$	uaacagucuacagccauggucg	down
hsa-miR-625-5p	2.55	0.0001	agggggaaaguucuauagucc	down
hsa-miR-331-5p	2.35	0.0012	cuagguaugguccccagggaucc	down
hsa-miR-181c-3p	2.34	0.0103	aaccaucgaccguugaguggac	down
hsa-miR-668-5p	2.28	0.0139	ugcgccucgggugagcaug	down
hsa-miR-409-3p	2.27	0.0354	gaauguugcucggugaaccccu	down
hsa-miR-421	2.18	0.0363	aucaacagacauuaauugggcgc	down
hsa-miR-769-5p	2.04	0.0126	ugagaccucuggguucugagcu	down
hsa-miR-654-5p	2.04	0.0111	uggugggccgcagaacaugugc	down
hsa-miR-548a-3p	2.02	0.0087	caaaacuggcaauuacuuuugc	up
hsa-miR-490-3p	2.01	0.0413	caaccuggaggacuccaugcug	down
hsa-miR-1270	2.01	0.0477	cuggagauauggaagagcugugu	down

*The miRNA *hsa-miR-1274b* is a dead entry in miRBase: the putative mature *miR-1274* sequence is a fragment of a Lys tRNA (Schopman NC 2010).

Table 19: Differentially expressed miRNAs in AD versus non AD tissue samples of the second miRNA microarray screening analysed using the software Partek. The seed sequence is marked. down, downregulation.

MiRNA	FC	p-value	MiRNA-sequence	regulated
hsa-miR-132-3p	2.52	$1{,}51*10^{-5}$	uaacagucuacagccauggucg	down
hsa-miR-212-3p	5.57	$6{,}11*10^{-6}$	uaacagucuccagucacggcc	down

4.1.4 Real-time RT-PCR validation of the differential expression of *miR-132-3p* and *miR-212-3p* in a second set of brain tissue samples

The differential expression of the two miRNAs *miR-132-3p* and *miR-212-3p* was validated in a second set of brains consisting of 20 AD and 20 non-AD brain tissue samples (Table 2). Both miRNAs displayed a significant downregulation in the AD brain tissue samples compared to the age-matched non-AD samples (Figure 12).

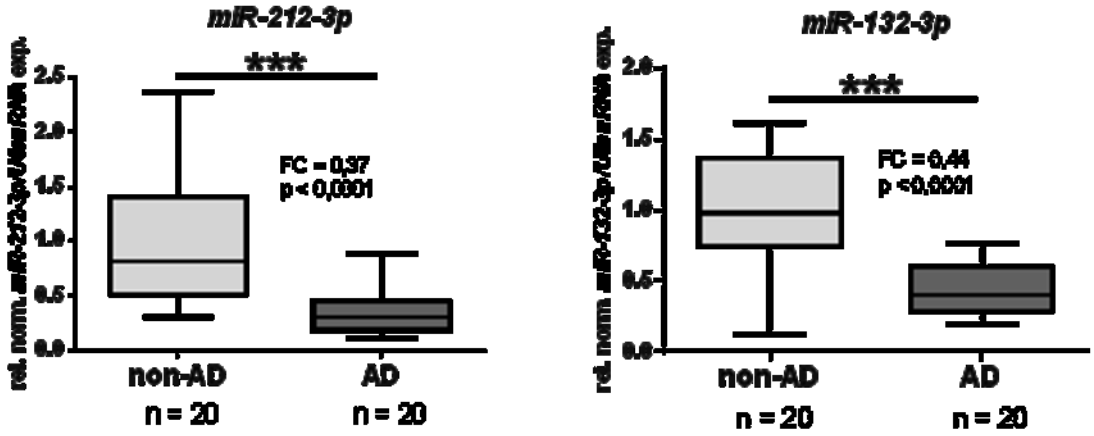

Figure 12: Real-time RT-PCR expression analysis of *miR-132-3p* and *miR-212-3p* in AD versus non-AD brain tissue samples.
The expression of *miR-132-3p* and *miR-212-3p* was investigated by real-time RT-PCR in a second set of 20 autopsy brain tissue samples of AD patients and 20 age-matched control brain samples (non-AD). Human universal reference RNA was used as a calibrator, and U6 snRNA as an endogenous control. The mean expression of the respective miRNAs in non-AD brain tissue samples was set to one. Box plots are depicted indicating median, lower and upper quartile as well as sample maximum and sample minimum of normalized expression values. Statistics were performed by two-sided unpaired t-test. *** significant expression differences ($p<0.0001$).

4.2 Identification and validation of putative *miR-132-3p* target genes

The miRNAs *miR-132-3p* and *miR-212-3p* share the same seed sequence (Wanet A 2012), similar mature sequences, and they may target the same mRNA sequences. Therefore, the following experiments were performed only for *miR-132-3p*.

4.2.1 First search for putative *miR-132-3p* target genes

To search for putative *miR-132-3p* targets, the target prediction programs Target Scan, Pictar, MiRanda, MiRDB and Microcosm were used. Putative targets of *miR-132-3p* predicted by all five programs were selected and are listed in Table 20.

Table 20: Putative targets of *miR-132-3p* selected with the target prediction programs Target Scan, Pictar, MiRanda, MiRDB and Microcosm. Shown are parts of the 3´UTR of the respective genes containing the putative *miR-132-3p* binding sites.

putative target	gene ID	3´UTR sequence part
OLFM1	10439	5´-agaggcgaggcaatgactgttg-3´
ATXN1	6310	5´-taaatatataaaatgactgttc-3´
WT1	7490	5´-atctccactgataagactgttt-3´
SIRT1	23411	5´-atttttacagtgaagactgttt-3´
		5´-gcatatgttttgtagactgttt-3´
FMR1	2332	5´-gcatcgctaatgccactgttc-3´
NR4A2	4929	5´-atgcagcagcttttgactgttt-3´
TMEM106B	54664	5´-tggtggagtaaaaagactgtta-3´
		5´-attactaccatgtagactgtta-3´
TIMM9	26520	5´-ttgtgtttaccagggactgttg-3´
		5´-caaccatctgtcatgactgttt-3´
		5´-gtttcttcaattgtgactgtta-3´

4.2.2 Real-time RT-PCR validation of putative targets of *miR-132-3p* in AD versus non-AD brain tissue samples

The mRNA expression of the 8 predicted *miR-132-3p* targets was analysed by real-time RT-PCR (3.1.3.2) in the first set of 10 AD and 10 non-AD brain tissue samples (Table 1) as shown in Figure 13. The results revealed only *FMR1* (fragile X mental retardation-1) as being significantly upregulated in the AD compared to non-AD brain tissue samples. The putative target *WT1* was undetectable in human brain tissue using real-time RT-PCR. The expression of the other six putative targets (*OLFM1*, *ATXN1*, *SIRT1*, *NR4A2*, *TMEM106B* and *TIMM9*) showed no significant differences between AD and non-AD samples (Figure 13).

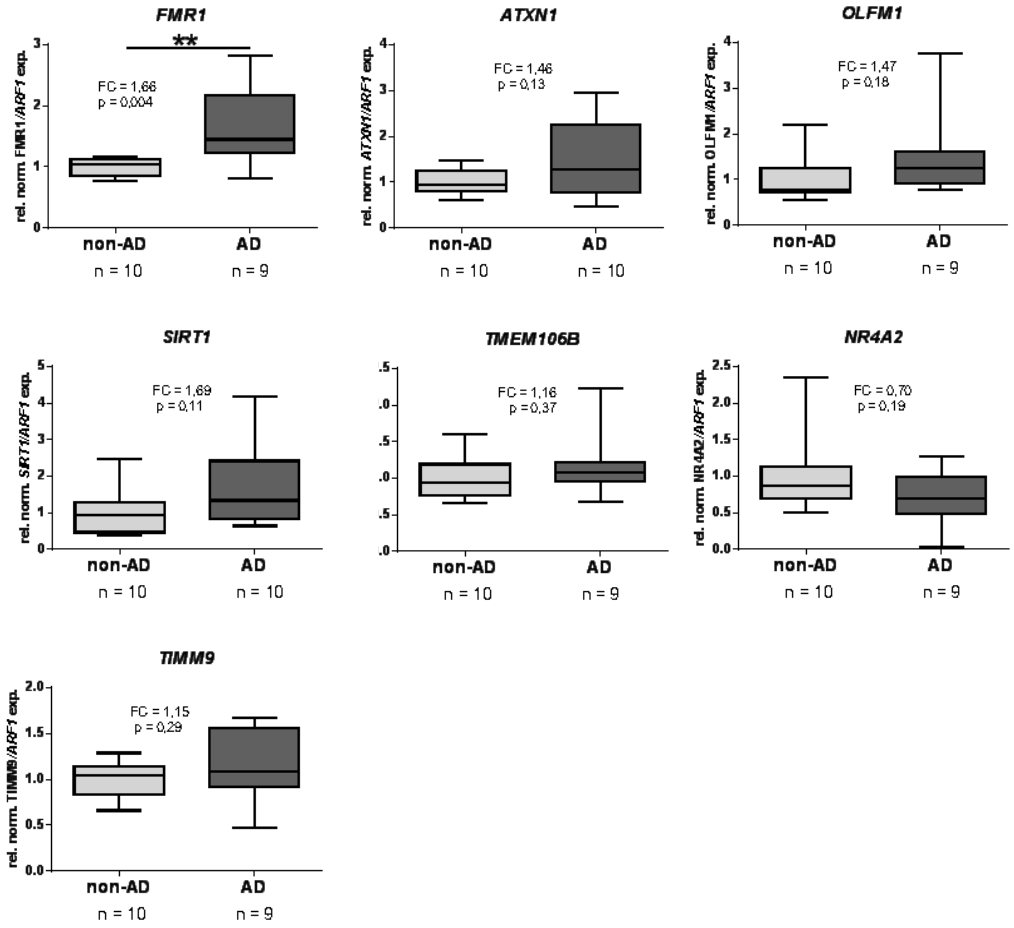

Figure 13: Real-time RT-PCR expression analysis of predicted *miR-132-3p* targets in brain tissue samples of AD patients and controls.
The expression of 7 predicted *miR-132-3p* targets was determined in autopsy brain tissue samples of AD patients and age-matched control brain samples (non-AD) by real-time RT-PCR. Human universal reference RNA was used as a calibrator, and *ARF1* as an endogenous control. The mean expression of the respective miRNA in non-AD brain tissue samples was set to one. Box plots are depicted indicating median, lower and upper quartile as well as sample maximum and sample minimum of normalized expression values. Statistics were performed by two-sided unpaired t-test. **, significant expression difference ($p<0.01$). n, number of tissue samples.

4.2.3 *FMR1* is not a direct target of *miR-132-3p*

To investigate the possible regulation of *FMR1* by binding of *miR-132-3p* to its 3´UTR, the mRNA expression of *FMR1* was investigated by real-time RT-PCR (3.1.3.2) with RNA extracted from *miR-132-3p* transfected T98G cells (these samples (3.2.5) were kindly provided by Dr. Franziska Liesenberg). However, in these experiments the expression of *FMR1* was unchanged in the *miR-132-3p* transfected cells compared to control transfected cells (pre-NC) as shown by Figure 14 A.

In addition, a luciferase reporter gene assay was performed (3.2) to investigate the direct binding of *miR-132-3p* to the 3´UTR of *FMR1*. The part of the *FMR1* 3´UTR sequence containing the predicted binding site of *miR-132-3p* was cloned into the psiCHECK^{TM}-2

vector (Figure 14, C). T98G cells were co-transfected with the psiCHECK^{TM}-2 *FMR1* 3´UTR vector and either precursor-miR-132-3p (pre-miR-132-3p) or precursor-negative control (pre-NC) oligonucleotides. The results showed that the luciferase expression was not downregulated in the *miR-132-3p* and psiCHECK^{TM}-2 *FMR1* 3´UTR co-transfected cells compared to control cells. Instead, the expression was significantly upregulated by up to 44 % (Figure 14, D). Hence, it was concluded that *FMR1* expression is not directly regulated by *miR-132-3p* neither at the mRNA level (Figure 14, A) nor at the protein level (Figure 14, D), and that *FMR1* is not a direct target of *miR-132-3p*.

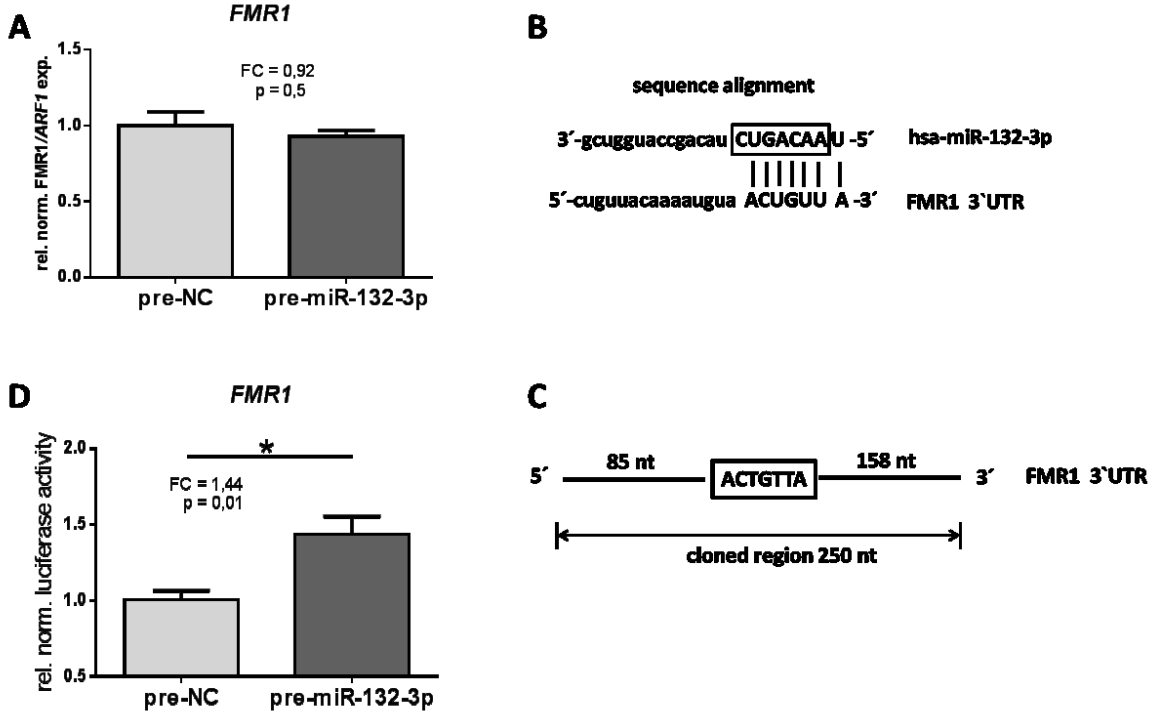

Figure 14: *FMR1* is not a direct target of *miR-132-3p*.
Real-time RT-PCR based analysis showed unchanged expression of *FMR1* in *miR-132-3p* transfected T98G cells compared to negative control (NC) transfected T98G cells. Bars represent the mean expression value of three independent experiments. Each independent experiment consists of five technical replicates. Error bars represent the standard deviation. Human universal reference RNA was used as a calibrator, and *ARF1* as an endogenous control **(A)**. Sequence alignment of the *miR-132-3p* seed sequence and part of the *FMR1* 3´UTR including the putative *miR-132-3p* binding site **(B)**. Scheme showing the part of the *FMR1* 3'UTR that was cloned into the luciferase reporter plasmid. **(C)**. T98G-cells were co-transfected with the luciferase reporter plasmid psiCHECK^{TM}-2 containing the *FMR1* 3´UTR sequence and either pre-miR-132-3p or scrambled oligonucleotides as a negative control (pre-NC). *Renilla* luminescence was normalized to *Firefly* luminescence. One experiment was performed, and the bars represent the mean of five technical replicates. The error bars represent standard deviation. The mean relative luminescence of the pre-NC transfected cells was set to one. Statistics were performed by two-sided unpaired t-test. *, significant expression difference ($p<0.05$); FC, fold change **(D)**.

4.2.4 Second search for putative *miR-132-3p* target genes

A second search for putative *miR-132-3p* target genes was performed with the target prediction program miRWalk. The generated list of putative *miR-132-3p* targets was compared with a previously published list of putatively AD-associated genes (Krauthammer KCA 2004). Table 21 shows only those genes that were listed as *miR-132-3p* targets in miRWalk and that were also previously identified by bioinformatic network analysis as AD candidate genes (Krauthammer KCA 2004).

Table 21: Putative targets of *miR-132-3p* listed in miRWalk. Shown are parts of the 3´UTR of the respective genes containing the putative *miR-132-3p* binding sites.

putative target	gene ID	3´UTR sequence part
EP300	2033	5´-tggatcactgtatagactgtta-3´
EPHB2	2048	5´-accaactcatgctggactgttg-3´
		5´-ataaggaaagcaatgactgttc-3´
		5´-gcttcccactccaggactgttg-3´
ERK1 (MAPK3)	5595	5´-cccctctcccgccagactgtta-3´
ERK2 (MAPK1)	5594	5´-ctgtaccctcgcatgactgtta-3´
		5´-ggacacagaaatgtgactgtta-3´
NCL	4691	5´-actctggggtttttactgtta-3
P21 (CDKN1A)	1026	5´-aacatactggcctggactgttt-3´
RB1	5925	5´-taatgctatgtcaagactgttg-3´
		5´-cacactccagttaggactgtta-3´
		5´-ttactccataaacagactgtta-3´

4.2.5 Real-time RT-PCR validation of putative targets of *miR-132-3p* in AD versus non-AD brain tissue samples

Using real-time RT-PCR, the expression of six putative targets of *miR-132-3p* was analysed in the second set of brain tissue samples (consisting of 20 AD and 20 non-AD samples), whereas the expression of *EPHB2* was analysed in the first set of brain tissue samples (consisting of 10 AD and 10 non-AD samples). The mRNA expression of *ERK1, ERK2, NCL* and *RB1* was significantly increased in the AD brain tissue samples compared to the non-AD samples (Figure 15). In contrast, the mRNA levels of *EP300, EPHB2* and *P21* exhibited no significant expression differences in AD versus non-AD brain tissue samples.

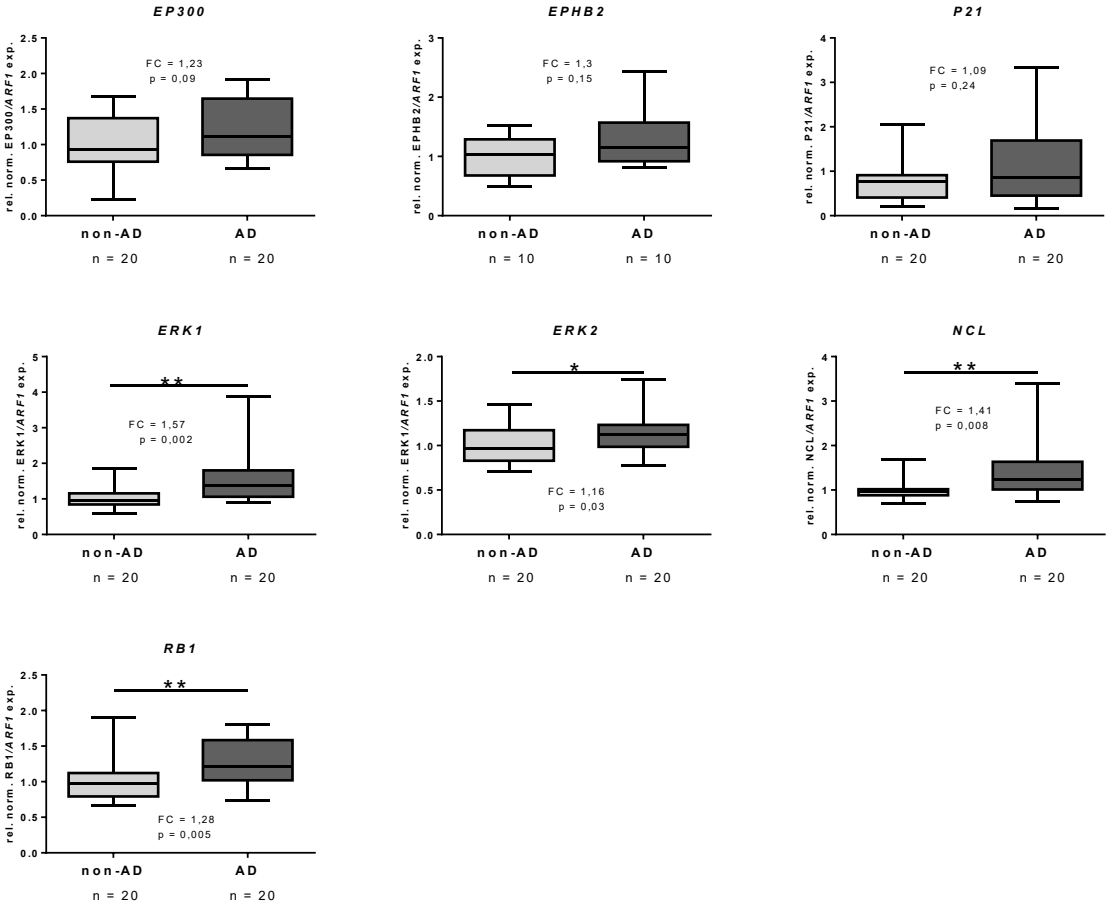

Figure 15: Real-time RT-PCR expression analysis of putative *miR-132-3p* target genes in brain tissue samples of AD patients.
The expression of seven putative targets was validated in autopsy brain tissue samples of AD patients compared to age-matched normal brain samples (non-AD). Human universal reference RNA was used as a calibrator, and *ARF1* as an endogenous control. The mean expression of the respective miRNAs in non-AD brain tissue samples was set to one. Box plots are depicted indicating median, lower and upper quartile as well as sample maximum and sample minimum of normalized expression values. Statistics were performed by two-sided unpaired t-test. Asterisks indicate significant expression differences (*, $p<0.05$; **, $p<0.01$); FC, fold change; n, number of tissue samples.

4.2.6 Expression of *RB1* and *ERK1/2 is* downregulated in pre-miR-132-3p transfected cells

The expression of the four putative *miR-132-3p* target genes *ERK1, ERK2, NCL* and *RB1* that were differentially expressed in AD brain tissue samples was further analysed in A172 and T98G cells transfected with pre-miR-132-3p or control oligonucleotides by real-time RT-PCR (3.1.3.2) (Figure 16). The mRNA expression of *NCL* showed no difference in the *miR-132-3p* transfected cells compared to control cells. *ERK1* and *RB1* mRNA levels were significantly downregulated in both cell lines, while *ERK2* displayed a significantly lower expression only in the T98G cells transfected with pre-miR-132-3p. The downregulation of these genes in the *miR-132-3p* transfected cells supports the possibility of a direct regulation by *miR-132-3p*.

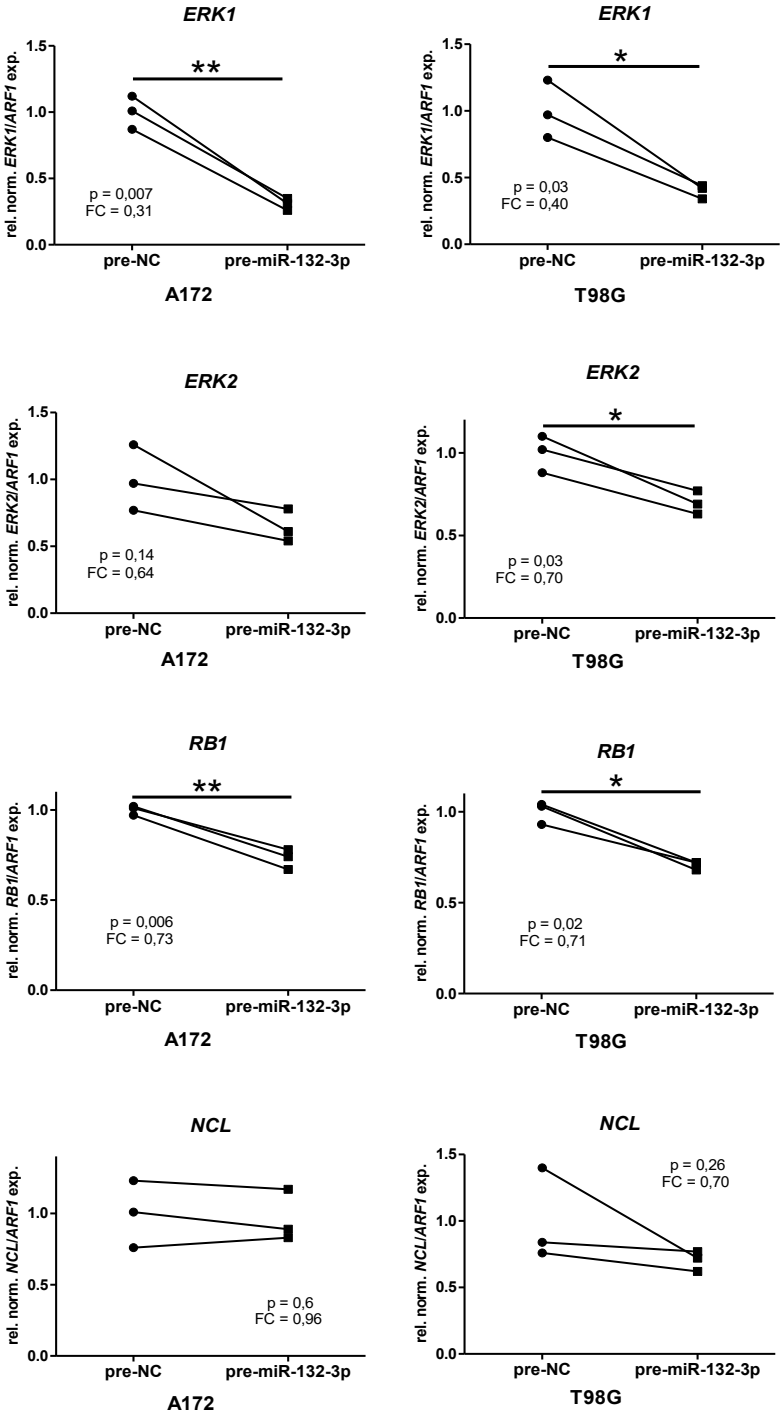

Figure 16: Real-time RT-PCR expression analysis of *ERK1*, *ERK2*, *RB1* and *NCL* in pre-miR-132-3p transfected cells.
The mRNA expression of the four putative *miR-132-3p* targets *ERK1*, *ERK2*, *RB1* and *NCL* was analysed in pre-miR-132-3p transfected A172 and T98G cells compared to negative control transfected cells (pre-NC). Human universal reference RNA was used as a calibrator, and *ARF1* as an endogenous control. The mean expression of the respective mRNAs in pre-NC transfected cells was set to one. Plots are depicted indicating the normalized expression values of three independent experiments. Statistics were performed by two-sided paired t-test. Asterisks indicate significant expression differences (*, $p<0.05$; **, $p<0.01$); FC, fold change.

4.2.7 *ERK1* and *ERK2* are direct targets of *miR-132-3p*

RB1 is a known target of *miR-132-3p* (Park JK 2011) and, therefore, it was not further validated by 3' UTR luciferase reported gene assays. The direct binding of *miR-132-3p* to the 3´UTR of *ERK1* (NM_002746.2) and *ERK2* (NM_002745.4) was investigated by a luciferase reporter gene assay (3.2). For these experiments, parts of the 3´UTR sequence of *ERK1* (Chr. 16p11.2) (Figure 17) or *ERK2* (Chr. 22q11.21-22q11.22) (Figure 18) containing the predicted binding sites for *miR-132-3p* were cloned into the psiCHECK^{TM}-2 vector. In control vectors, the binding sites were deleted from the 3'UTR sequences.

ERK1 has one putative binding site for *miR-132-3p*, which is complementary to the seed sequence "AACAGUC" (Figure 17 A). To investigate the direct binding of *miR-132-3p* to this putative binding site, two vector constructs were generated: the wild type (wt) construct "wt-luc-ERK1" contained a 636 bp fragment of the *ERK1* 3´UTR with the putative *miR-132-3p* binding site inserted into the multiple cloning site of the psiCHECK^{TM}-2 vector (Figure 17 B), while the construct "del-luc-ERK1" was identical except for a deletion (del) of the *miR-132-3p* binding site (Figure 17 C).

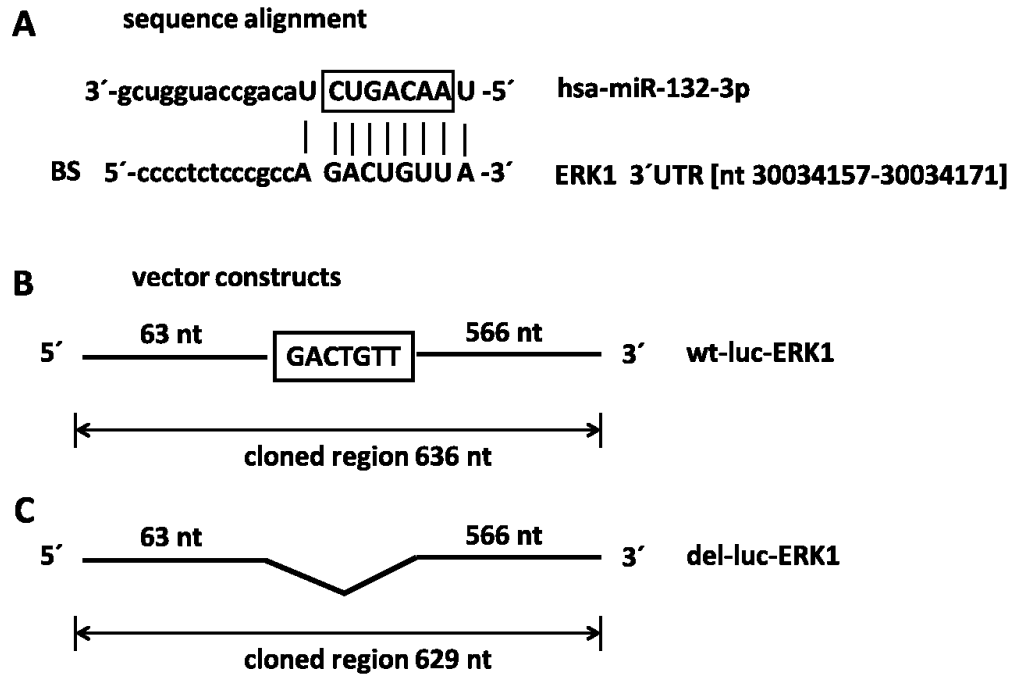

Figure 17: Sequence alignment of *miR-132-3p* with the *ERK1* 3´UTR and luciferase vector constructs.
The diagram depicts a sequence alignment of the *miR-132-3p* seed sequence with the part of the *ERK1* 3´UTR containing the putative *miR-132-3p* binding site (BS) **(A)**. Two constructs were generated by inserting a part of the *ERK1* 3'UTR into the psiCHECK^{TM}-2 vector. The wild type construct "wt-luc-ERK1" contained the *ERK1* 3´UTR with the putative *miR-132-3p* binding site **(B),** while in the mutant construct "del-luc-ERK1" this binding site was deleted **(C)**. nt, nucleotides.

In contrast, *ERK2* has two binding sites for *miR-132-3p* that are complementary to the seed sequence “AACAGUC” (Figure 18 A). For *ERK2*, four vector constructs were generated: The wild type construct “wt-luc-ERK2” contained a 1091 bp fragment of the *ERK2* 3´UTR with both putative *miR-132-3p* binding sites inserted into the multiple cloning site of the psiCHECK^{TM}-2 vector (Figure 18 B). The vector construct “del1-luc-ERK2” was identical except for a deletion of the first binding site (Figure 18 C), whereas in the vector construct “del2-luc-ERK2” the second binding site of *miR-132-3p* was deleted (Figure 18 D). A vector construct with a deletion of both *miR-132-3p* binding sites was named “del(1+2)-luc-ERK2” (Figure 18 E).

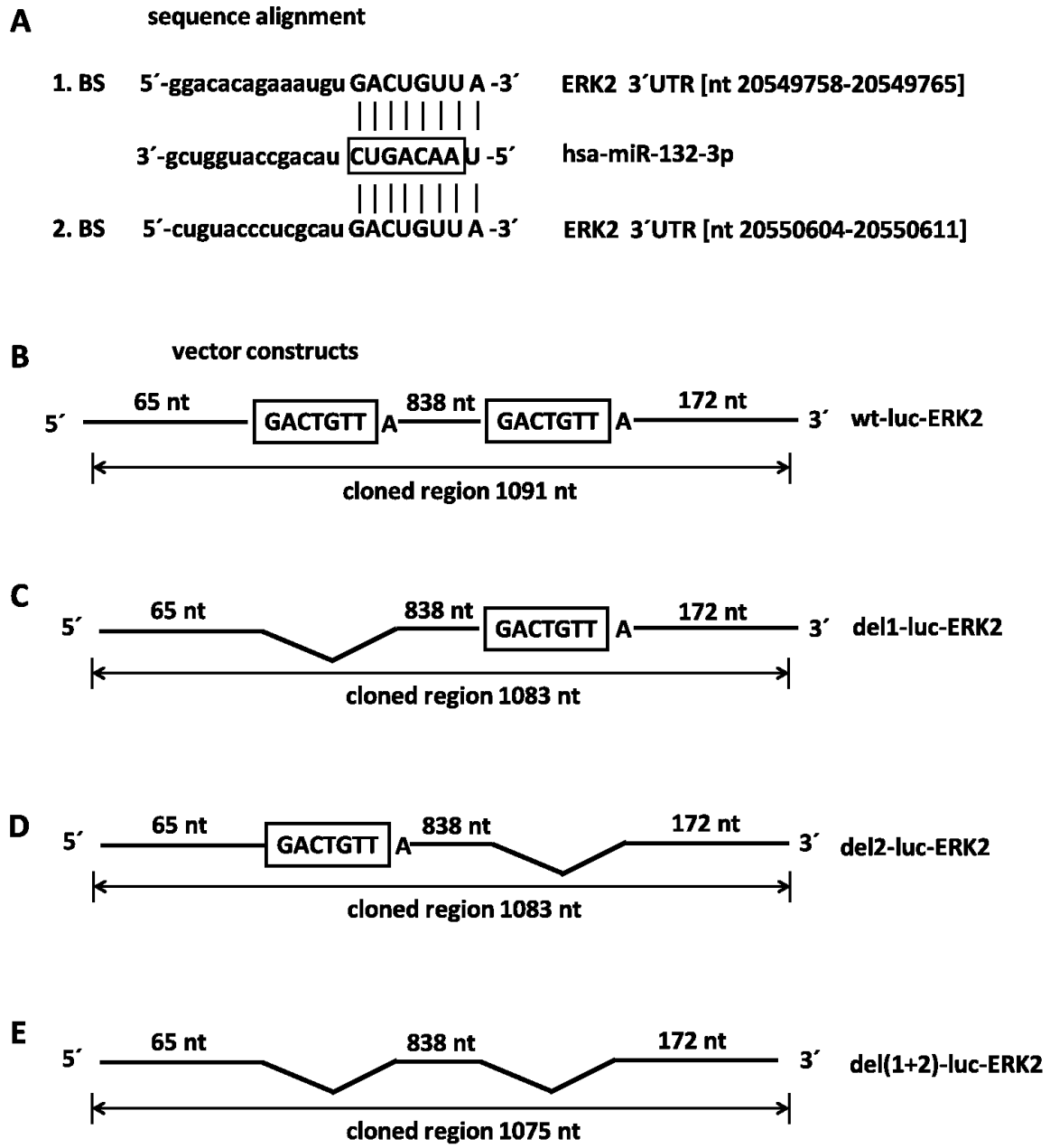

Figure 18: Sequence alignment of *miR-132-3p* with the *ERK2* 3´UTR and luciferase vector constructs.
The diagram depicts a sequence alignment of the *miR-132-3p* seed sequence with the part of the *ERK2* 3´UTR containing the two putative *miR-132-3p* binding sites (BS) **(A)**. Four vector constructs were generated by inserting a part of the ERK2 3´UTR encompassing the putative *miR-132-3p* binding sites into the psiCHECK™-2 vector. The wild type construct "wt-luc-ERK2" contained the *ERK2* 3´UTR with both putative *miR-132-3p* binding sites **(B)**. In the mutant construct "del1-luc-ERK2" the first binding site was deleted **(C),** whereas in the mutant construct "del2-luc-ERK2" the second binding site of *miR-132-3p* was deleted **(D)**. In the vector construct "del(1+2)-luc-ERK2" both binding sites were deleted **(E)**.

T98G cells were co-transfected with the psiCHECK^{TM}-2 luciferase vector constructs containing the wild type 3'UTR of *ERK1* or *ERK2* as shown in Figure 17 and Figure 18, and with either pre-miR-132-3p or pre-negative control (pre-NC) oligonucleotides. The results of the luciferase reporter gene assays showed a decreased luciferase activity by up to 46 % ("wt-luc-ERK1") and 27 % ("wt-luc-ERK2") compared to control transfected cells (Figure 19).

To prove the specificity of the putative *miR-132-3p* binding site in the *ERK1* 3´UTR sequence, T98G cells were co-transfected with the vector construct "del1-luc-ERK1", in which the *miR-132-3p* binding was deleted, and either pre-miR-132-3p or pre-NC oligonucleotides. The deletion of the binding site completely abolished the inhibitory effect of pre-miR-132-3p on the luciferase activity compared to the negative control (Figure 19, A).

To verify the putative *miR-132-3p* binding sites in the *ERK2* 3´UTR sequence, T98G cells were co-transfected with the vector constructs "del1-luc-ERK1" or "del2-luc-ERK1", in which the first or the second *miR-132-3p* binding site was deleted, and either pre-miR-132-3p or pre-NC oligonucleotides. The deletion of only one of the two binding sites partially reduced the effect of pre-miR-132-3p. However, the deletion of both binding sites completely abolished the inhibitory effect of pre-miR-132-3p on luciferase activity compared to negative control (Figure 19, B). This indicated that pre-miR-132-3p likely binds to both binding sites in the ERK2 3´UTR.

These results demonstrate that the *miR-132-3p* binding sites in the 3´UTR of *ERK1* and *ERK2* are functionally relevant, and provide experimental evidence that *miR-132-3p* directly targets the mRNAs of *ERK1* and *ERK2*.

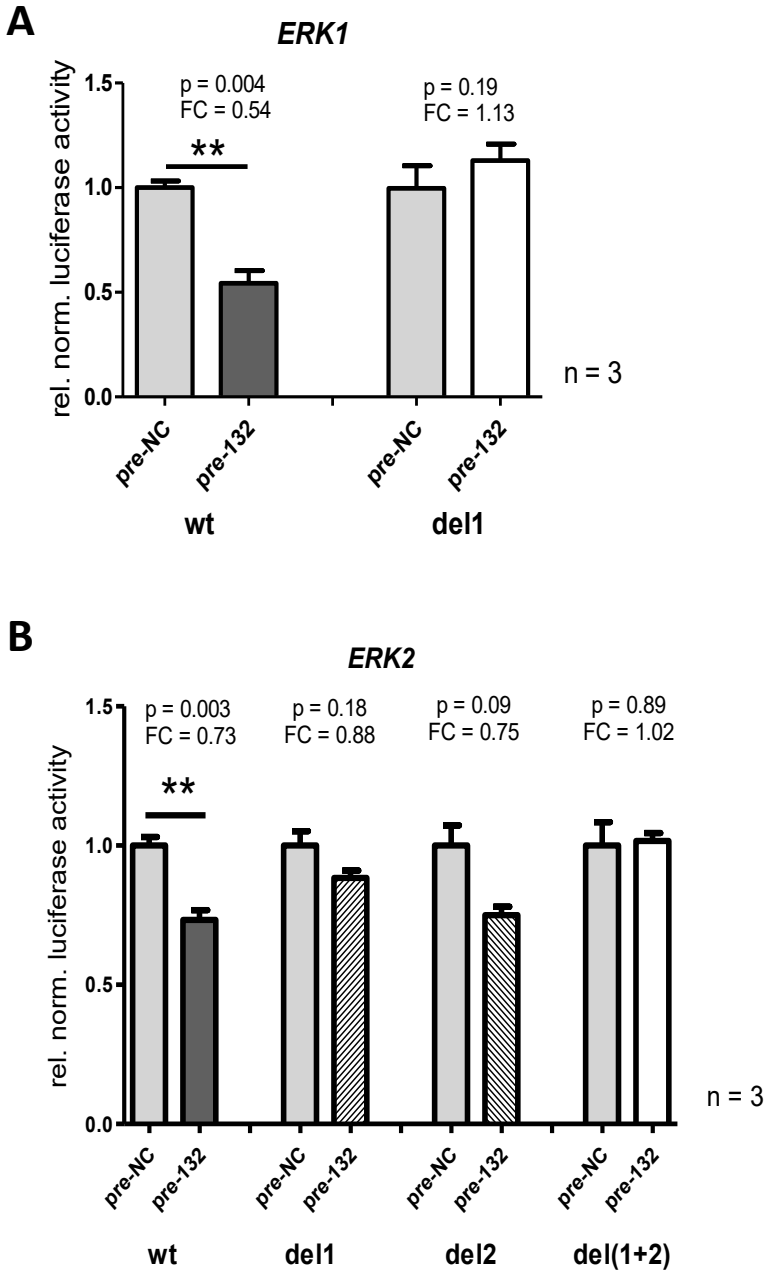

Figure 19: Functional relevance of *miR-132-3p* binding sites in the 3´UTRs of *ERK1* and *ERK2*. Human T98G cells were co-transfected with the luciferase reporter plasmid wt-luc-ERK1 containing part of the *ERK1* 3´UTR including the putative *miR-132-3p* binding site**,** and either pre-miR-132-3p (*pre-132*) or scrambled oligonucleotides as a negative control (pre-NC). The vector construct del-luc-ERK1 was identical except for a deletion of the *miR-132-3p* binding site **(A)**. Similar experiments were performed to test the relevance of the *miR-132-3p* binding sites in the *ERK2* 3'UTR. The vector wt-luc-ERK2 (wt) contained part of the *ERK2* 3'UTR including the two *miR-132-3p* binding sites. In the vector del1-luc-ERK2 (del1) the first *miR-132-3p* binding site was deleted, while in the vector del2-luc-ERK2 (del2) the second *miR-132-3p* binding site was deleted. In the vector del(1+2)-luc-ERK2 (del(1+2)) both *miR-132-3p* binding sites were deleted. *Renilla* luminescence was normalized to *Firefly* luminescence. Bars represent the mean of three independent experiments and error bars represent the standard deviation. The mean relative luminescence of the pre-NC transfected cells was set to one. Statistics were performed by two-sided paired t-test. **, significant expression differences ($p<0.01$).

4.2.8 Protein expression levels of total-ERK1/2 and p-ERK1/2 in *miR-132-3p* transfected HEK293-APP695sw and SH-SY5Y cells

The protein expression of ERK1/2 in *miR-132-3p* transfected cells was examined by Western blot analysis. Experiments were performed in two different cell lines to exclude cell line specific effects. Pre-miR-132-3p was used instead of anti-miR-132-3p because real-time RT-PCR experiments showed an approximately 8-fold lower *miR-132-3p* expression in the HEK293-APP695sw and SH-SY5Y cell lines compared to normal human brain tissue (nb) (3.1.3.1) (Figure 20).

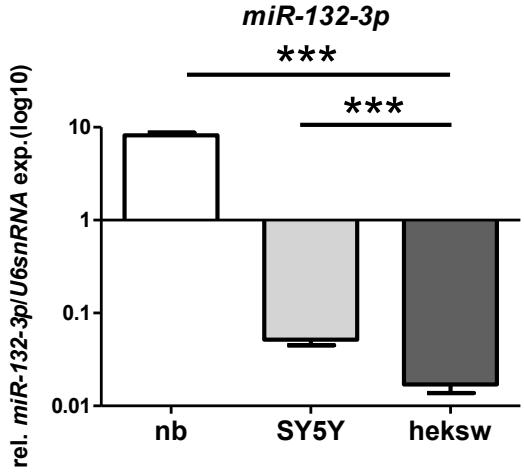

Figure 20: Real-time RT-PCR based expression analysis of *miR-132-3p* in HEK293-APP695sw and SH-SY5Y cell lines.
The expression of *miR-132-3p* was measured in HEK293-APP695sw (heksw) and SH-SY5Y (SY5Y) cell lines compared to three different normal brain tissue samples (nb). Human universal reference RNA was used as a calibrator and U6 snRNA as an endogenous control. Error bars indicate standard deviations (SD). Statistics were calculated by two-sided unpaired t-test. ***, significant expression differences ($p<0.001$).

The cell lines HEK293-APP695sw (Figure 21) and SH-SY5Y (Figure 22) were transiently transfected with pre-miR-132-3p or scrambled oligonucleotides as negative control (pre-NC) (3.2.5). Protein lysates of these cells were generated (3.3.2) and Western blot analysis with antibodies against total ERK1/2 and phosphorylated ERK1/2 (p-ERK1/2) was performed (3.4.1). This revealed a trend for decreased expression of total ERK1/2 and p-ERK1/2 in pre-miR-132-3p transfected HEK293-APP695sw cells (Figure 21). However, only total ERK1 displayed statistically significant decreased expression by about 77 % in pre-miR-132-3p transfected HEK293-APP695sw cells in three independent experiments.

Efficient transfection of the cells was controlled by real-time RT-PCR analysis of pre-miR-132-3p transfected HEK293-APP695sw cells compared with pre-NC transfected cells. The expression of *miR-132-3p* was about 1000 -times higher in the pre-miR-132-3p transfected cells than in the pre-NC transfected cells (data not shown).

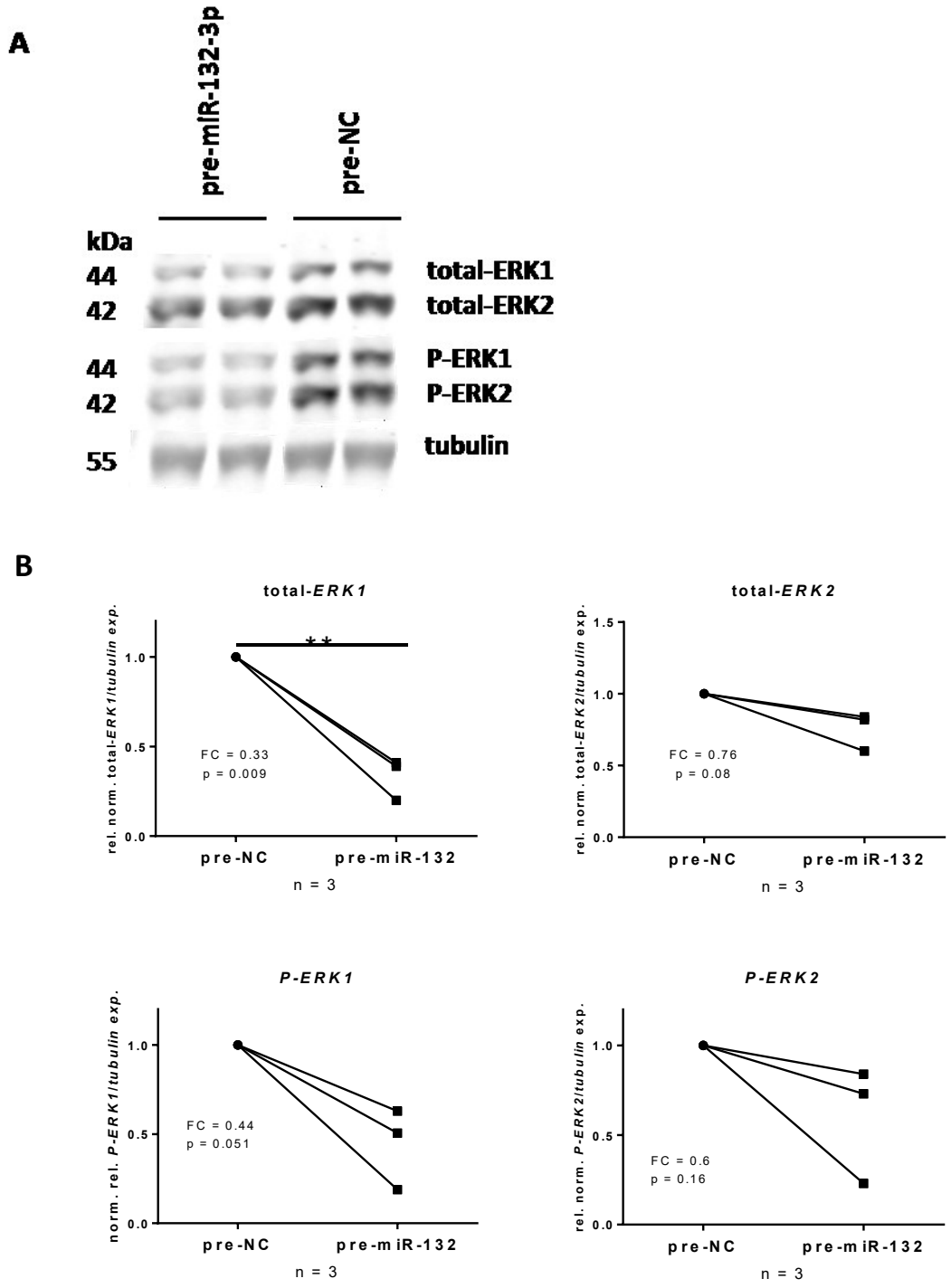

Figure 21: Western blot analysis of total ERK1/2 and phosphorylated ERK1/2 (p-ERK1/2) protein expression in pre-miR-132-3p transfected HEK293-APP695sw cells.
The Western blots were probed with antibodies against total ERK1/2 and p-ERK1/2 and against tubulin as a loading control **(A)**. Quantification of Western blotting results of total ERK1/2 and p-ERK1/2 protein expression levels relative to tubulin levels. The expression data of three independent experiments was normalized to the control condition (pre-NC transfection), which was set to one. Statistics were calculated by one sample t-test. **, significant expression difference ($p<0.01$) **(B)**.

Western blot analysis also revealed a trend for decreased expression of total ERK1/2 and p-ERK1/2 in pre-miR-132-3p transfected SH-SY5Y cells compared to pre-NC transfected control cells (Figure 22). However, these differences did not reach statistical significance (Figure 22).

Additionally, ERK1/2 mRNA expression in pre-miR-132-3p transfected HEK293-APP695sw cells was analysed by real-time RT-PCR. The expression of ERK1 was nearly 50 % lower compared to pre-NC transfected cells while ERK2 expression was only about 20 % lower, largely consistent with the results in A172 and T98G cells shown in Figure 16 (data not shown).

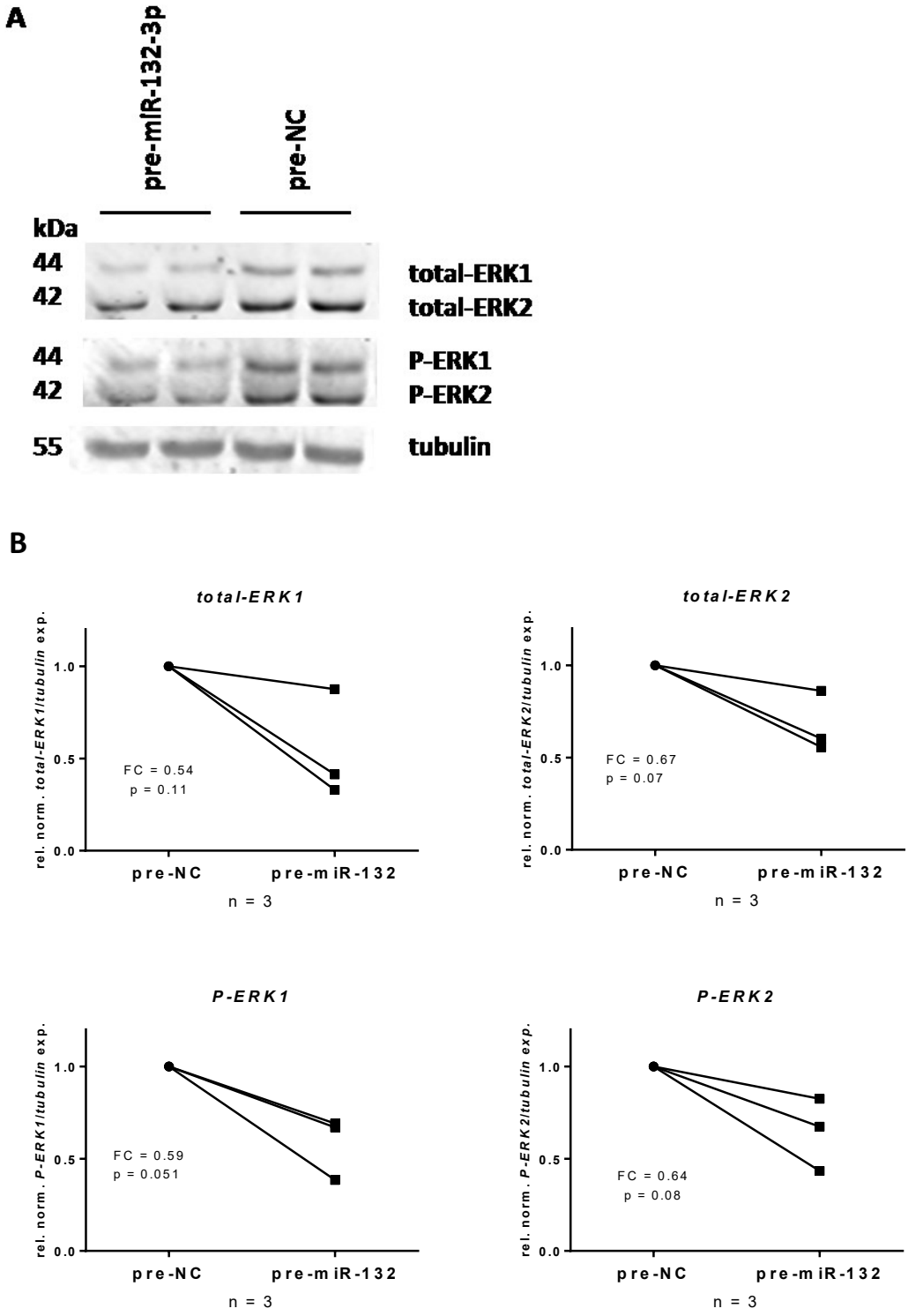

Figure 22: Western blot analysis of total ERK1/2 and phosphorylated ERK1/2 (p-ERK1/2) protein expression in pre-miR-132-3p transfected SH-SY5Y cells.
The Western blots were probed with antibodies against total ERK1/2 and p-ERK1/2 and against tubulin as a loading control **(A)**. Quantification of Western blotting results of total ERK1/2 and P-ERK1/2 protein expression levels relative to tubulin levels. The expression data of three independent experiments was normalized to the control condition (pre-NC transfection), which was set to one. Statistics were calculated by one sample t-test. **(B)**

4.2.9 Progressive neuronal *p-ERK1/2* immunoreactivity in AD brain tissue samples of increasing Braak stages

Upregulation of p-ERK1/2 levels in AD brains has been reported previously and was found to be co-distributed with the progressive accumulation of neurofibrillary tangles (Pei JJ 2002). Based on these findings, immunohistochemical stainings for p-ERK1/2 in the hippocampus (Ammon's horn region, area CA2) of three AD and one non-AD brain tissue samples was perfomed (3.4.2). The autopsy brain tissue samples were fixed in formalin and embedded in paraffin. While the brain tissue of non-AD individuals showed no p-ERK1/2 immunoreactivity, AD brain tissue displayed progressive immunoreactivity with increasing Braak stages (2, 3 and 5) (Figure 23). This immunoreactivity was associated with neurons and frequently with cells that appeared to contain neurofibrillary tangles. However, this would need to be confirmed by colocalization studies for p-ERK1/2 and tau protein.

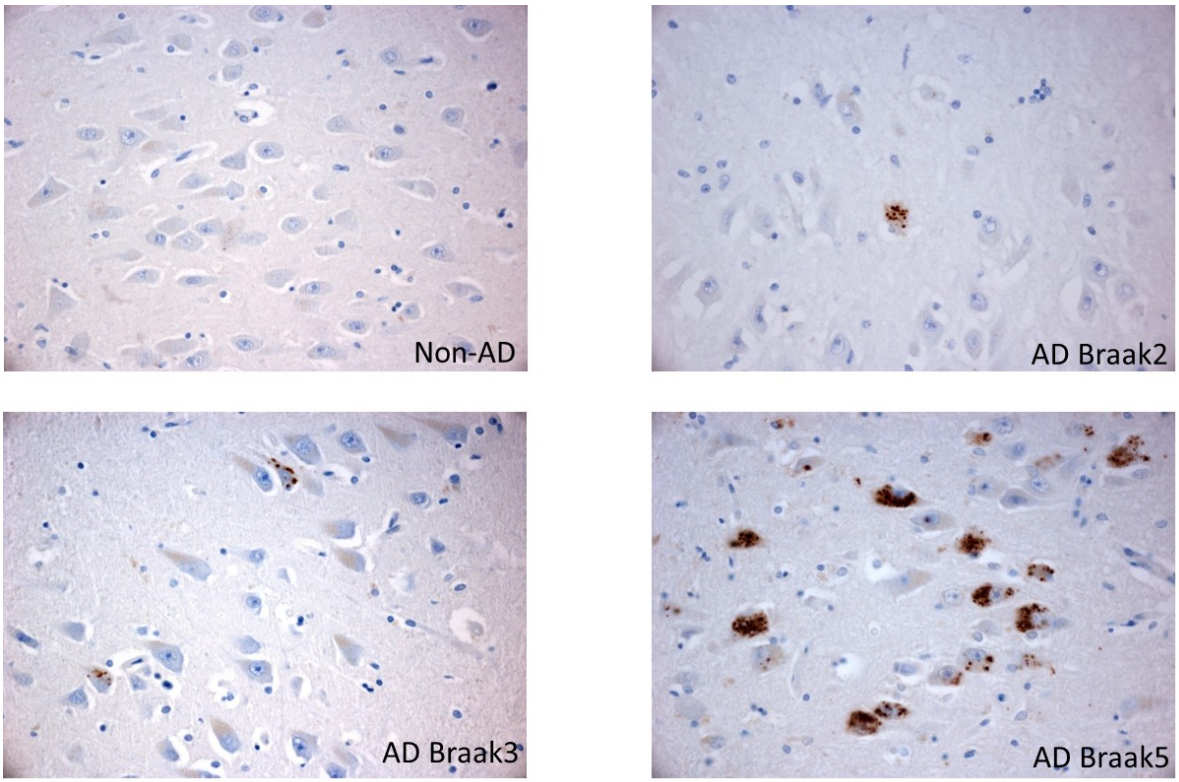

Figure 23: Increased numbers of nerve cells with immunoreactivity for phosphorylated ERK1/2 in the hippocampus of AD patients compared to non-AD patients.
Immunoreactivity for phosphorylated ERK1/2 in cells with neuronal morphology in the hippocampus (area CA2) of AD patients (Braak stages 2, 3, and 5). No immunoreactivity was observed in brain samples of non-AD control individuals. Pictures are exemplary.

4.3 Functional experiments to investigate the role of *miR-132-3p* and ERK1/2 in APP processing and Aβ generation

4.3.1 Downregulation of Aβ40 and Aβ42 levels in pre-miR-132-3p transfected HEK293-APP695sw cells

To address the question of a functional relationship of *miR-132-3p* and ERK1/2 expression with the processing of APP leading to Aβ generation, tissue culture supernatants of pre-miR-132-3p transfected HEK293-APP695sw cells were investigated by ELISA (3.4.3) (Figure 24 A). Additionally, HEK293-APP695sw cells were transfected with siRNA against ERK2 (Figure 24 B), siRNA against ERK1/2 (Figure 24 C) and scrambled siRNA as negative control (siRNA-NC) (3.2.5). Furthermore, HEK293-APP695sw cells were treated with small molecule inhibitors of ERK1/2 (ERK1/2-inhibitor) or a control compound (inhibitor-NC) (3.3.3) (Figure 24 D).

Results of three independent experiments showed a significant downregulation of Aβ40 and Aβ42 levels in the supernatants of pre-miR-132-3p transfected HEK293-APP695sw cells (Figure 24 A). In pre-miR-132-3p transfected cells, the mean level of Aβ40 was 85 % lower than in negative control (pre-NC) transfected cells. Similarly, the mean level of Aβ42 in pre-miR-132-3p transfected cells was 73 % lower than in the pre-NC transfected control cells.

The effects of siRNA transfection against ERK2 (Figure 24 B) and ERK1/2 (Figure 24 C) were not as strong as the effect of pre-miR-132-3p transfection with regard to Aβ40 and Aβ42 levels. The levels of both Aβ40 and Aβ42 showed a trend towards downregulation after siRNA ERK2 and siRNA ERK1/2 transfection compared to siRNA-NC transfected cells, while the downregulation of Aβ42 levels in siRNA ERK2 transfected cells reached statistical significance. The difference in Aβ42 levels between siRNA ERK2 and siRNA-NC transfected cells was 26 % (Figure 24 B).

There was no effect on Aβ40 or Aβ42 levels after treatment of HEK293-APP695sw cells with ERK1/2 inhibitors compared to control cells (Figure 24 D).

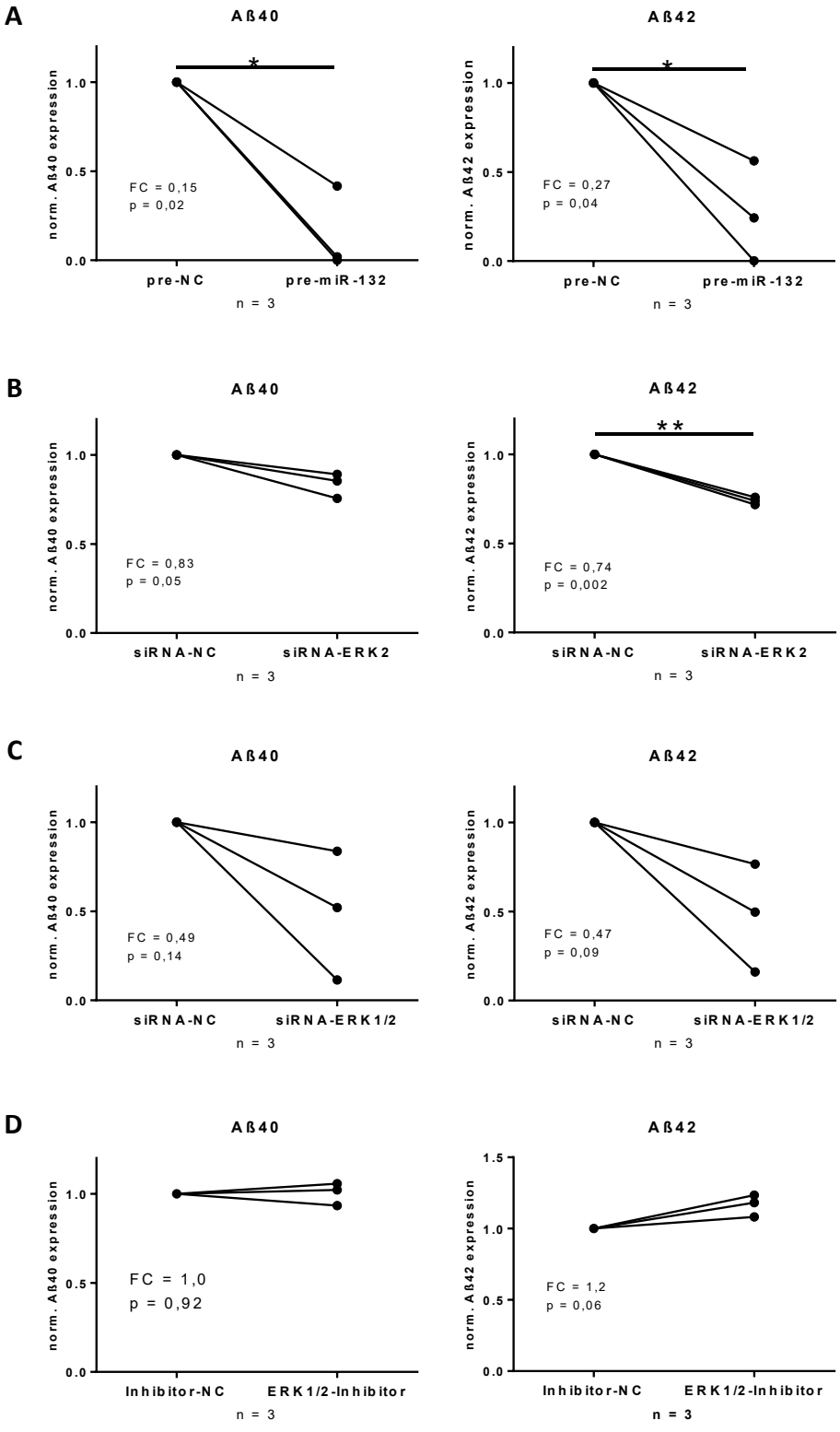

Figure 24: Aβ40 and Aβ42 levels in tissue culture supernatants of HEK293-APP695sw cells after transfection with pre-miR-132-3p (A) or downregulation of ERK1/2 activity by siRNA transfection (B, C) or small molecule inhibitors of ERK1/2 (D).
The data of three independent experiments were normalized to pre-NC, siRNA-NC or inhibitor-NC controls, which were set to one. Statistics were perfomed by one sample t-test. Asterisks indicate significant difference in Aβ levels (*, p<0.05; **, p<0.001); FC, fold change.

To ensure that the transfection with pre-miR-132-3p or siRNAs against ERK1/2 or the treatment with ERK1/2 inhibitors (3.3.3) had no toxic effects on the HEK293-APP695sw cells, AlamarBlue® toxicity assays were performed (3.2.5.). In this assay, the non-fluorescent dye resazurin is converted to the red–fluorescent compound resorufin by metabolically active cells. No toxic effects were observed (Figure 25 A-C).

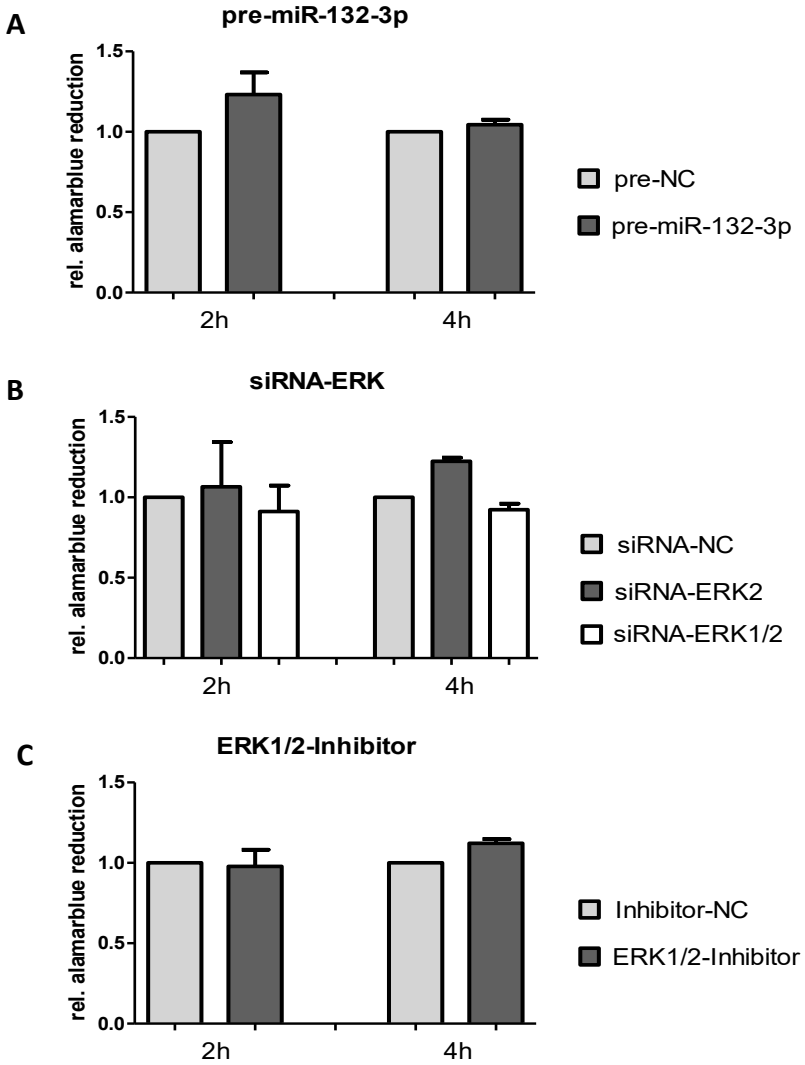

Figure 25: No toxic effects after transfection of HEK293-APP695sw cells with pre-miR-132-3p (A), siRNA against ERK1/2 (B), or treatment with ERK1/2 inhibitor (C).
AlamarBlue® reagent was added, and fluorescence was measured 2 h or 4 h later.

4.3.2 Downregulation of sAPPβ and total-sAPP levels after pre-miR-132-3p transfection of HEK293-APP695sw cells

To identify a potential explanation for the reduced Aβ40 and Aβ42 levels in tissue culture supernatants of HEK293-APP695 cells after transfection with pre-miR-132-3p, the proteolytic processing of APP in these cells was investigated. The HEK293-APP695 cells were transfected with pre-miR-132-3p or pre-NC as described above. Cell lysates and tissue culture supernatants were subsequently investigated by Western blotting (3.4.1). The cell lysate was used to detect total APP with the polyclonal antibody CT15 against the C-terminus of APP, whereas the culture supernatant was investigated with a mixture of the monoclonal antibodies IG7/5A3 recognizing both sAPPα and sAPPβ (= total-sAPP), or with a polyclonal antibody specific for the sAPPβ isoform of the APP ectodomain (Figure 26). The sAPPβ ectodomain is generated by β-secretase (BACE1) cleavage of APP while the sAPPα ecotodomain is generated by α-secretase.

The Western blot analysis revealed a significant reduction in the levels of both total-sAPP and sAPPß in the tissue culture supernatants of pre-miR-132-3p transfected cells (Figure 26, A). The protein levels of total-sAPP and sAPPβ were 32 % and 78 % lower in pre-miR-132-3p transfected cells compared to pre-NC transfected cells (Figure 26, B). The levels of APP in the cell lysates displayed no difference in the pre-miR-132-3p transfected cells compared to pre-NC transfected cells.

In contrast, HEK293-APP695sw cells transfected with siRNA against ERK1/2 demonstrated no differences in the levels of cellular APP, total-sAPP and sAPPβ compared to siRNA-NC transfected control cells (Figure 26, A).

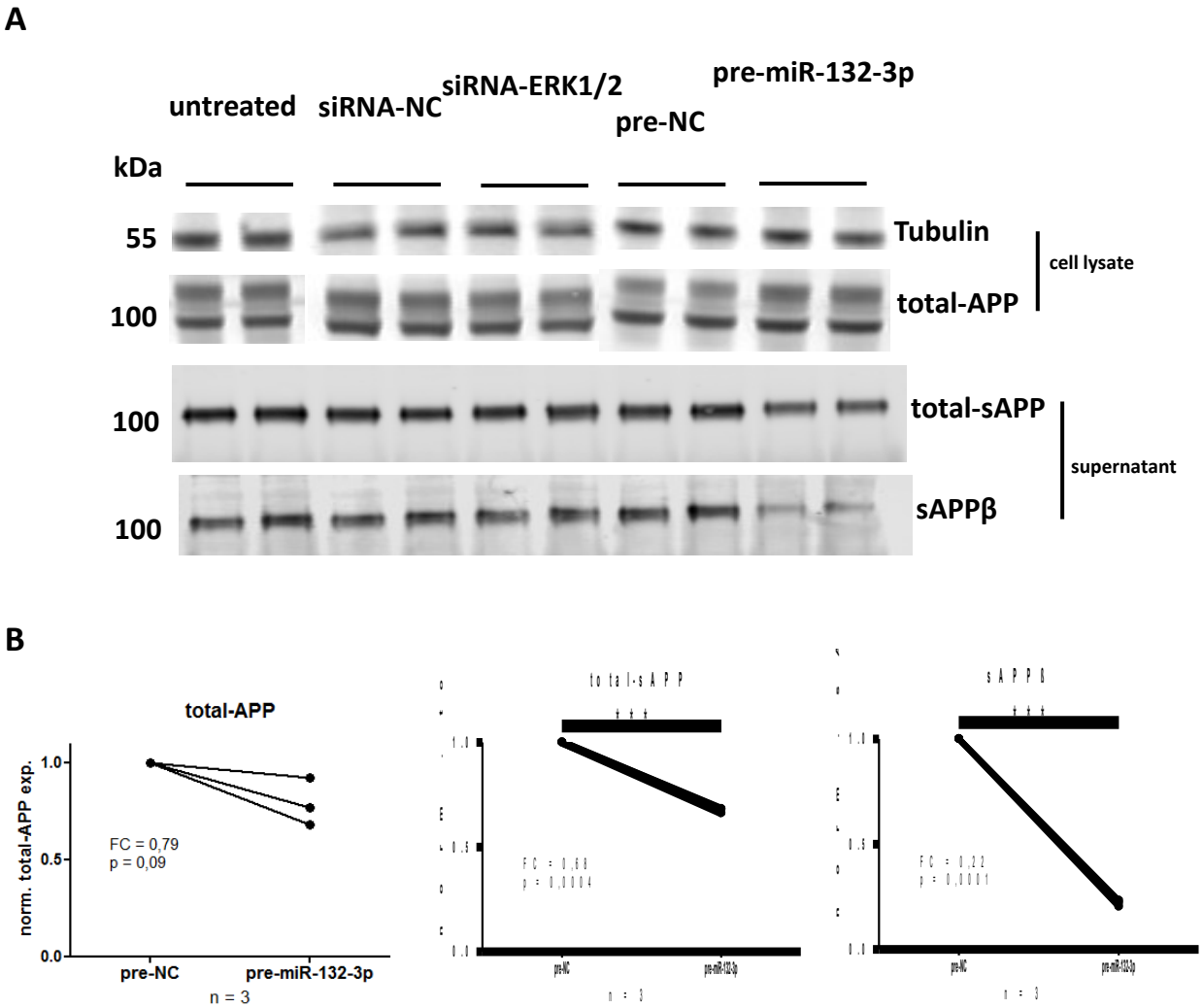

Figure 26: Significantly lower levels of total-sAPP and sAPPβ but no difference in cellular APP levels in pre-miR-132-3p transfected HEK293-APP695sw cells.
HEK293-APP695sw cells were transfected with pre-miR-132-3p or pre-NC, or siRNA against ERK1/2 or siRNA-NC. Cell lysates and tissue culture supernatants were collected. The Western blots were probed with antibodies against APP, total-sAPP and sAPPβ **(A)**. Quantification of the Western blotting results for APP, total-sAPP and sAPPβ after transfection with pre-miR-132-3p. The data of three independent experiments was normalized to pre-NC transfected control cells, which was set to one. Statistics were performed by one sample t-test. ***, significant expression differences (p<0.001) **(B)**. FC, fold change.

4.3.3 The mRNA expression of BACE1 is significantly downregulated in pre-miR-132-3p transfected HEK293-APP695sw cells

Transfection of HEK293-APP695sw cells with pre-miR-132-3p caused a reduction in both Aβ and sAPPβ in tissue culture supernatants. These are both proteolytic products of APP generated by β-secretase (BACE1) cleavage. Therefore, to identify a potential regulatory effect of *miR-132-3p* on BACE1 expression, HEK293-APP695sw cells were transfected with pre-miR-132-3p or pre-NC negative control (3.2.5) and BACE1 mRNA levels were determined by real-time RT-PCR 72 h post transfection (3.1.3.2). In pre-miR-132-3p transfected cells, BACE1 mRNA expression was significantly downregulated by 24 % compared to control transfected cells (Figure 27).

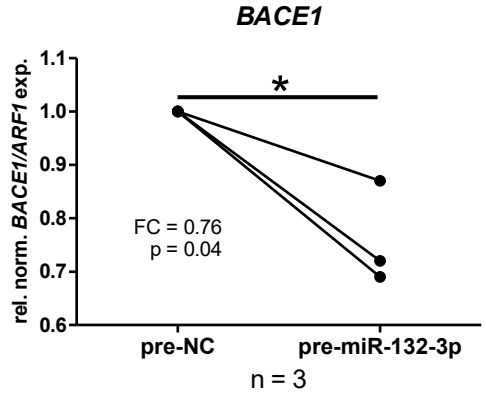

Figure 27: BACE1 mRNA expression is significantly downregulated in pre-miR-132-3p transfected HEK293-APP695sw cells.
BACE1 mRNA levels in pre-miR-132-3p or control transfected (pre-NC) HEK293-APP695sw cells were determined by real-time RT-PCR analyses. Human universal reference RNA was used as calibrator and *ARF1* mRNA as endogenous control. The expression data were normalized to the pre-NC control condition, which was set to one. Statistics were performed by one-sample t-test. *, significant expression differences ($p<0.05$).

5 Discussion

5.1 The miRNAs *miR-132-3p* and *miR-212-3p* are downregulated in brain tissue samples from AD patients

In the last couple of years, several investigations have found differentially expressed miRNAs in brain tissue from AD patients and mouse models of AD, and their targets have often been linked to AD related pathology (Chunmei W 2014, Van den Hove DL 2014). Previous results of a miRNA microarray based experiment (performed by Dr. Petra Zipper, Department of Neuropathology) with brain tissue from the *APP*655sw/*PS1*deltaExon9 mouse model of AD had demonstrated that 8 miRNAs were differentially expressed in the transgenic mouse brain tissue samples compared to corresponding brain samples of wild type mice. However, the expression of these 8 miRNAs was not significantly different in brain tissue samples from AD patients compared to non-AD brain tissue samples. It was therefore concluded that the differential expression of these 8 miRNAs was specific for the *APP*655sw/*PS1*deltaExon9 mouse model but had no relevance for human AD.

For this reason, a miRNA microarray analysis of 830 human mature miRNAs was performed with 10 autopsy brain tissue samples from the medial temporal gyrus of AD patients and 10 matched non-AD brain tissue samples. The screening result showed differential expression of 16 miRNAs in the AD versus non-AD brain tissue samples. However, only the downregulation of *miR-132-3p* and *miR-222* expression in the AD brain samples could be validated by real-time RT-PCR in the same tissue samples. It is known that *miR-132-3p* and *miR-212*-3p share the same seed-region (Wanet A 2012). Hence, the expression of *miR-212-3p* was also analysed in the same tissue samples and displayed significant downregulation in the AD versus non-AD brain tissue samples. In addition, a second microarray screening of the same set of brain tissue samples was performed because the miRNA signals in the first microarray screening were below the background. The results of the second miRNA microarray showed 17 differentially expressed miRNAs in the AD versus non-AD brain samples. The only miRNA, which was detected as differentially expressed in both miRNA microarray experiments was *miR-132-3p*. The second microarray experiment further indicated downregulated expression of *miR-212-3p*. Downregulated expression of these two miRNAs could be also validated by real-time PCR in a second set of human brains consisting of 20 AD and 20 non-AD brain tissue samples from the superior frontal gyrus.

Controversial results concerning the expression of *miR-132-3p* and *miR-212-3p* in AD brains have been reported in the literature. While Lukiw et al. found no significant change of *miR-132-3p* expression in AD brain samples (Lukiw WJ 2007), Cogswell et al. showed that

miR-132-3p and *miR-212-3p* were significantly downregulated (Cogswell JP 2008). In 2011, Wang et al. reported only *miR-212-3p* but not *miR-132-3p* expression as downregulated in AD (Wang WX 2011). In 2013, the downregulation of both miRNAs in AD brain samples was confirmed by Wong et al. (Wong HKA 2013). In 2013, another research group demonstrated the downregulation of *miR-132-3p* in AD brain tissue samples by miRNA microarray and real-time PCR (Lau P 2013). Similar to us, this group used two independent sets of AD brain tissue samples from the hippocampus and the prefrontal gyrus and patient cohorts of a comparable size. Overall, these previous studies and our own microarray and real-time PCR validation experiments provide compelling evidence for the downregulation of *miR-132-3p* and *miR-212-3p* in AD brain tissue samples, a finding recently confirmed in an independent investigation of the AD microRNAnome (Pichler S 2017).

An important question is whether the reduction of *miR-132-3p* and *miR-212-3p* expression levels in AD brains was due to their specific downregulation in neurons or just a consequence of the fact that AD brains have less neurons relative to non-AD brain tissue samples. Measurements of total protein levels in our AD and non-AD brain tissue samples did not show any consistent differences (data not shown). This would indicate that these brain tissue samples contained similar numbers of viable cells but the cellular composition meaning the number of neurons versus other brain cells is unknown. Recently, Wong et al. were able to demonstrate more directly that *miR-132-3p* and *miR-212-3p* expression is downregulated in AD neurons. These authors laser-captured neuronal cell bodies from the hippocampal CA1 region and measured the expression of *miR-132-3p* and *miR-212-3p* in the isolated neurons (Wong HKA 2013). Consistent with the results described above, they observed a downregulation of *miR-132-3p* and *miR-212-3p* expression in AD versus non-AD neurons.

MiR-132-3p (miRBase accession: MI0000449) and *miR-212-3p* (miRBase accession: MIMAT0000269) are tandem miRNAs, which means they originate from the same primary transcript and share the same seed region (Remenyi J 2010). It is very likely that they regulate the same targets and, for that reason, follow-up experiments in this study were only performed for *miR-132-3p*. Both miRNAs are enriched in the brain and they are located in an intergenic region on chromosome 17p13.3 in humans. The maturation of *miR-132-3p* and *miR-212-3p* generates two additional miRNAs, *miR-132-5p* and *miR-212-5p*, which are nearly complementary to the other two miRNAs (Wanet A 2012). Their expression has also been shown to be downregulated in AD (Lau P 2013). The *miR-132/212* locus is regulated by the transcription factor CREB (cAMP-response element binding protein) in neurons and by REST (repressor element 1 silencing transcription factor) in non-neuronal cells (Vo N 2005)

(Conaco C 2006). The *miR-132-3p* appears to play an important role in the development, maturation and function of neurons (Wanet A 2012). Overexpression of *miR-132-3p in vitro* has been shown to modulate short-term synaptic plasticity (Lambert TJ 2010), and *in vivo* it increased dendritic spine density (Hansen KF 2010). *In vivo* knockdown of *miR-132-3p* in the hippocampus of mice caused impaired fear memory (Wang RY 2013). Another study in *miR-132-3p/212-3p* knockout mice has confirmed the importance of *miR-132-3p* in memory formation (Hernandez-Rapp 2015). The *miR-132-3p* expression profile in the suprachiasmatic nucleus is light dependent and appears to influence circadian rhythms (Cheng H Y 2007). Additionally, *miR-132-3p* might play a role in the regulation of mRNA targets in the tau network since Lau et al. identified the transcription factor FOXO1a as a target of *miR-132-3p* (Lau P 2013). Deregulated expression of *miR-132-3p* has also been associated with other brain-related disorders besides AD. For example, *miR-132-3*p has been demonstrated to be downregulated in Huntington´s disease (Johnson R 2009), in the tauopathy progressive supranuclear palsy (Smith 2011), and in schizophrenia and bipolar disorder (Perkins DO 2007).

In addition, *miR-132-3p* might play an important role outside the nervous system. For example, the expression of *miR-132-3p* is deregulated in different cancer types like chronic lymphoblastic leukaemia (Calin G A 2004), squamous cell carcinoma of the tongue (Wong 2008), pancreatic cancer (Park JK 2011, Zhang S 2011), and in tumor-associated endothelia promoting neovascularization (Anand S 2010). Finally, *miR-132-3p* has been designated as a “neurimmiR”, a class of miRNAs which play a role in both neuronal and immune functions (Soreq H 2011).

MiRNAs are often found to be epigenetically regulated like *miR-34a, miR-34b/c, miR-107, miR-124, miR-125b, miR-137 and miR-181c* (Van den Hove DL 2014). A feedback loop between epigenetic mechanisms and *miR-132-3p* has been proposed because *miR-132-3p* targets methyl CpG binding protein 2 (MeCP2) and sirtuin-1 (SIRT1) (Strum JC 2009). Furthermore, it is known that the *miR-132-3p* promoter is hypermethylated in hepatocellular carcinomas (Wei X 2013) and that ischaemic events can lead to epigenetic silencing of the *miR-132-3p* promoter (Hwang JY 2014). Hence, it might be useful to determine DNA and histone modifications like methylation and acetylation in the *miR-132-3p* promoter in AD brain tissue samples. Such an epigenetic analysis could be informative to find out why the expression of miR-132-3p is downregulated in AD.

5.2 *ERK1* and *ERK2* are direct targets of *miR-132-3p*

MiRNAs mostly bind in the 3'UTR region of their target mRNAs, which leads to inhibition of translation or degradation of the corresponding mRNA. The miRNA bases 2-7 are called "seed sequence" and must be a perfect complement to the 3'UTR region of the target mRNA sequence to define target specificity (Doench JG 2004). A few targets of *miR-132-3p*, which might play a role in AD, have already been validated: *EP300* (E1A binding protein p300) (Lagos D 2010), *PTEN* (Phosphatase and tensin homolog), *FOXO3a* (Forkhead box O3A) (Wong HKA 2013) and *FOXO1a* (Forkhead box O1A) (Lau P 2013). Additionally, *miR-132-3p* targets the mRNA of AChE (acetylcholinesterase), which degrades the neurotransmitter acetylcholine (Shaked I 2009). Shaked et al. have demonstrated an upregulation of AChE levels in transgenic mice expressing a 3'UTR-deficient AChE transgene, which was accompanied by reduced acetylcholine levels and enhanced peripheral inflammation. This means that *miR-132-3p* could be responsible for limiting inflammation in the periphery and could, potentially, regulate ACh levels in the brain, which are insufficient in AD patients (Kihara T 2004).

In this study, putative *miR-132-3p* target genes were initially identified by computational analysis, which predicts the presence of putative binding sites for the miRNA. Several different target prediction programs were used. The mRNA expression of one predicted target, *FMR1*, was found to be significantly upregulated in AD versus to non-AD brain tissue samples. The *FMR1* gene encodes a protein FMRP, which has been proposed to regulate mRNA transport and the translation of target mRNAs at the synapse (Oostra BA 2009). A trinucleotide repeat expansion mutation in the 5′UTR of the *FMR1* gene is responsible for the disease fragile X syndrome (Verkerk AJ 1991). Evidence indicates that *miR-132-3p* functionally interacts with FMRP in the mouse brain (Edbauer D 2010). Interestingly, FMRP binds to the *APP* mRNA and regulates its translation, which suggests a potential link between AD and fragile X syndrome (Westmark CJ 2007). To confirm *FMR1* as a target of *miR-132-3p*, a luciferase reporter gene assay was performed to investigate the direct binding of *miR-132-3p* to the 3´UTR of *FMR1*. However, the results were negative leading to the conclusion that *FMR1* expression is not directly regulated by *miR-132-3p*.

After the conclusion that *FMR1* expression was not directly regulated by *miR-132-3p*, a second target search was performed. This time the generated list of putative *miR-132-3p* targets was compared with a published list of putative AD associated genes (Krauthammer KCA 2004). This comparison resulted in a list of seven putative targets: *EP300, EPHB2, P21, ERK1, ERK2, NCL* and *RB1*. The mRNA expression of these putative targets was predicted to be upregulated in AD versus non-AD brain tissue samples. Real-time PCR expression

analysis of these putative targets demonstrated significantly upregulated mRNA expression in AD brain samples only for *ERK1*, *ERK2*, *NCL* and *RB1*.

The first step to determine whether these four upregulates genes were direct targets of *miR-132-3p* was to analyze their expression in pre-miR-132-3p transfected cells. The expression of putative target genes should be downregulated in pre-miR-132-3p compared to control transfected cells. Indeed, the mRNA expression of *ERK1*, *ERK2* and *RB1* but not *NCL* was significantly downregulated in pre-miR-132-3p transfected cells. However, due to the fact that *RB1* was an already known target of *miR-132-3p* (Park JK 2011), further experiments in this study focused on *ERK1* and *ERK2*.

Next, to determine whether or not the predicted target sites for *miR-132-3p* in the 3´UTR of the *ERK1* and *ERK2* mRNAs were responsible for the mRNA downregulation, 3´UTR luciferase reporter gene assays were carried out. The results demonstrated that the *miR-132-3p* binding sites in the 3´UTR of *ERK1* and *ERK2* were functionally relevant and they provided experimental evidence that *miR-132-3p* directly targets and degrades the mRNAs of *ERK1* and *ERK2.* This study is the first to have demonstrated that *ERK1* and *ERK2* are direct targets of *miR-132-3p*.

ERK1 and *ERK2* are the final effector kinases of the mitogen-activated protein kinase/extracellular signal-regulated kinase (MAPK/ERK) pathway (Robinson MJ 1997). The MAPK/ERK pathway belongs to the MAPK pathway family, which includes the Big MAP kinase-1 (BMK-1), the c-Jun N-terminal kinase (JNK), and the p38 signaling families (Cossa G 2013). All these four kinase families are organized in the same way and are each composed of two serine/threonine kinases and one threonine/tyrosine kinase, which sequentially phosphorylate and activate each other (Dhanasekaran NE 1998). In the cytoplasm, ERKs phosphorylate proteins of the cytoskeleton, which influence cell migration and movement (Pullikuth AK 2007), as well as substrates involved in cell adhesion, cell metabolism and the regulation of other signaling pathways (Ma L 2005). In the nucleus, active ERKs phosphorylate various transcription factors, which promote cell-cycle progression (Zassadowsk F 2012, Sigoillot FD 2002). Consequently, the activation of the MAPK/ERK pathway can stimulate proliferation and invasion, and cellular survival as well as apoptosis, and the oncogene or tumor-suppressor functions of kinases in the MAPK/ERK pathway depend on the tissue-specific tumor environment (Burotto MD 2014).

The two isoforms ERK1 (MAPK3, p44) and ERK2 (MAPK1, p42) share about 90 % homology (Boulton TG 1990) but the expression of ERK2 seems to be higher in neurons of the rat hippocampus (Giovanni MG 2001) and in other brain areas. In addition, ERK2 appears to be more critical for memory processes (Sweatt JD 2001). Whereas knock-out (KO) mice for

ERK1 are viable and neurologically healthy (Selcher JC 2001), KO mice for ERK2 are embryonically lethal at day 6.5 (Saba-El-Leil MK 2003). Using the ERK2 KO mice it was shown that ERK2 is an essential protein for long-term memory (Satoh Y 2007).

Previous studies have demonstrated unchanged or slightly reduced levels of total ERK1/2 in AD versus non-AD brain tissue. However, these studies measured either ERK protein levels or mRNA levels with methods that are difficult to quantify (*in situ* hybridization) in only a small number of brains (Trojanewski JQ 1993, Hyman BT 1994, Perry G 1999). Hence, these studies are not easily comparable to the ERK1/2 mRNA level measurements by real-time RT-PCR performed in this study. In contrast, several studies have shown that levels of p-ERK1/2, the phosphorylated and activated forms of ERK1/2, are markedly increased in AD brain tissue versus controls (Perry G 1999, Zhu X 2001, Ferrer I 2001), which is consistent with our observation that ERK1/2 mRNA expression levels were increased in a larger collection of AD versus non-AD brains.

ERK can be activated by the neurotransmitters glutamate (Peavy RD 1998, Zhu JJ 2002) and noradrenalin (Watabe AM 2000), by growth factors (Castillo D V 2011), and by the sex steroid hormones 17β-estradiol and progesterone (Orr PT 2012). Additionally, it is known that ACh released from cholinergic fibers activates nicotinic and muscarinic ACh receptors followed by downstream activation of ERK (Giovannini MG 2008). Other experiments have demonstrated that ERK1 (Hébert SS 2012) and ERK2 (Zhu 2002) are major kinases for neuronal tau phosphorylation, in addition to p38 and JNK (Zhu 2002) as well as GSK3, CDK5 and CaMK-II (Ca2+/calmodulin-dependent protein kinase) (Churcher I 2006). In AD patients the MAPK/ERK pathway appears to be activated in neurons vulnerable to neurofibrillary tangle formation (Zhu 2002). Upregulation of p-ERK1/2 was found to be co-distributed with the progressive accumulation of neurofibrillary tangles in AD (Pei JJ 2002).

Based on these findings, we also performed immunohistochemical stainings for p-ERK1/2 in the hippocampus (Ammon's horn region, area CA2) of AD and non-AD brain tissue samples. While the brain tissue of non-AD controls showed very low immunoreactivity for p-ERK1/2, AD brain tissue displayed increasing immunoreactivity in neurons with increasing Braak stages (2, 3 and 5). These results fit well to the findings by Pei et al. (Pei JJ 2002).

In summary, all this evidence indicates that the MAPK/ERK pathway might be involved in the pathogenesis of AD. We observed a significant downregulation of *miR-132-3p* in AD brain tissue samples, while *ERK1* and *ERK2* as direct targets of *miR-132-3p* were upregulated (Figure 28). Low expression of *miR-132-3p* in AD could affect memory processes and neurofibrillary tangle formation through upregulation of *ERK1* and *ERK2*. Follow-up experiments were designed to investigate whether downregulation of *miR-132-3p* might also affect APP processing and Aβ formation.

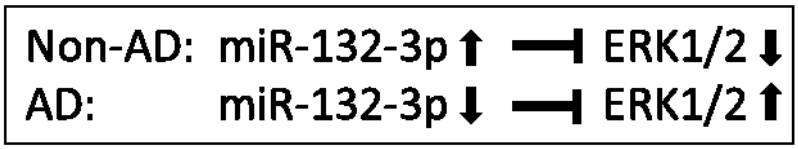

Figure 28: Low expression of *miR-132-3p* in AD leads to upregulation of ERK1/2 activity.

5.3 Possible role of *miR-132-3p* in APP processing and Aβ formation

Several studies have demonstrated an important role of the ERK signaling pathway in APP processing (Mills J 1997, Desdouits-Magnen J 1998). It is known that activation of the ERK pathway can stimulate APP shedding leading to the release of the soluble APP ectodomain (sAPP) into the extracellular space (Manthey D 2001, Mills J 1997). In turn, it has been demonstrated that sAPP when applied to cells can activate the ERK1/2 pathway (Greenberg SM 1994), forming a potential feedback loop. Enhanced non-amyloidogenic processing of APP through the α-secretase pathway can limit Aβ generation and amyloid plaque formation in APP-transgenic mouse models of AD (Postina R 2004). On the other hand, upregulation of β-secretase (BACE1) expression or activity could enhance Aβ generation. Furthermore, although contradictory findings have been published, Aβ peptides at physiological concentrations have been shown to activate the ERK1/2 pathway in rat hippocampal slice cultures (Dineley KT 2001, Zhu 2002), and an ERK1/2 inhibitor was able to block the toxicity of synthetic Aβ in primary hippocampal neuron cultures (Rapoport M 2000), indicating that ERK1/2 activation might be an essential downstream effect of Aβ toxicity (Zhu 2002). Finally, a recent publication demonstrated that ERK1/2 activation might enhance the secretion of the Aβ-degrading protease neprilysin leading to Aβ clearance (Yamamoto N 2016). Therefore, we asked the question whether *miR-132-3p* might affect APP processing and/or Aβ levels, possibly through modulation of ERK1/2 signaling.

To investigate this question, the levels of Aβ40 and Aβ42 were analyzed in tissue culture supernatants of HEK293-APP695sw cells transfected with pre-miR-132-3p by ELISA. Importantly, the results demonstrated a significant downregulation of Aβ40 and Aβ42 levels by about 85 % and 73 %, indicating that *miR-132-3p* might regulate Aβ generation and that reduced *miR-132-3p* expression in AD could potentially lead to increased Aβ levels. However, this phenotype was only partially mimicked by transfection of HEK293-APP695sw cells with siRNA against ERK1/2. While trends for reduced Aβ levels were observed, only the transfection of siRNA against ERK2 caused a statistically significant downregulation of Aβ42 levels. Furthermore, treatment of HEK293-APP695sw cells with an ERK1/2 inhibitor had no effects on either Aβ40 or Aβ42 levels. Overall, these tissue culture experiments indicate that overexpression of pre-miR-132-3p reduces extracellular Aβ levels but that this effect is not or only partially mediated by downregulation of ERK1/2 protein levels and activity.

Therefore, with the intention to find another mechanism how *miR-132-3p* could interfere with Aβ generation, APP processing was investigated in more detail. For this, the expression levels of cellular APP in cell lysates, the total levels of the secreted APP ectodomain (sAPPα

+ sAPPβ), and the levels of sAPPβ generated by β-secretase (BACE1) cleavage of APP were analyzed in pre-miR-132-3p transfected HEK293-APP695sw cells. While the expression of cellular APP showed no difference, total sAPP levels (32 %) and especially sAPPβ levels (78 %) demonstrated a significant downregulation in pre-miR-132-3p transfected cells compared with control transfected cells. This finding indicated that *miR-132-3p* might reduce the β-secretase (BACE1) cleavage of APP. Reduced β-secretase processing of APP could also result in reduced levels of the γ-secretase substrate APP-CTF99, which might explain the lower Aβ levels in tissue culture supernatants of pre-miR-132-3p transfected cells (Figure 29). Consistent with the Aβ data, the levels of total sAPP and sAPPβ were unchanged in cells transfected with siRNA against ERK1/2. This demonstrated again that the changes in APP processing and Aβ levels after *miR-132-3p* transfection were likely not mediated by ERK1/2. As an alternative explanation, *miR-132-3p* might directly or indirectly target the expression of BACE1. Therefore, the mRNA expression of BACE1 was examined in pre-miR-132-3p transfected cells. Indeed, the results demonstrated a significantly reduced expression of BACE1 (24 %) in pre-miR-132-3p transfected cells compared with control transfected cells.

Recent literature underlines the important role of the *miR-132/212* cluster in the metabolism of tau and amyloid-β. Downregulation of *miR-132/212* may induce tau phosphorylation via its target NOS1 (neuronal nitric oxide synthase) and thereby may contribute to the pathogenesis of AD and other tauopathies (Wang Y 2017). *MiR-212/132* deficiency in triple transgenic AD mice (3xTg-AD) promotes Aβ production and plaque formation (Hernandez-Rapp J 2016) as well as tau expression, phosphorylation and aggregation (Smith P 2015). This corresponds to the own result as it was shown that overexpression of *miR-132-3p* reduced the levels of secreted Aβ peptides. Interestingly, the level of *miR-132* correlates with Aβ-load, soluble tau and cognitive impairment in humans (Hernandez-Rapp J 2016, Smith P 2015). In addition, it was shown that treatment of AD mice with *miR-132* mimics could restore in part memory function and tau metabolism (Smith P 2015). Another publication demonstrated the functional implication of *miR-132* loss on amyloid and tau pathology in AD (Salta E 2016). The authors showed that *miR-132* is a potent early regulator of Aβ and tau pathology via its target ITPKB (inositol 1,4,5-triphosphate 3-kinase B). The kinase ITPKB activates ERK1/2 which leads to increased BACE1 activity and tau phosphorylation (Salta E 2016). Salta et al. suggested that restoring *miR-132* levels in human diseased brain might represent a new therapeutic strategy in AD. This hypothesis is supported by the treatment of AD mice with *miR-132* mimics, which in part restored memory function (Smith P 2015).

The downregulation of the cluster *miR-212/132* in AD brain tissue observed in the own experiments is additionally supported by a recent miRNome-wide study (Pichler S 2017). The authors observed downregulation of *miR-132* and *miR-212* in temporal and prefrontal cortex with a stronger decrease in gray matter AD samples.

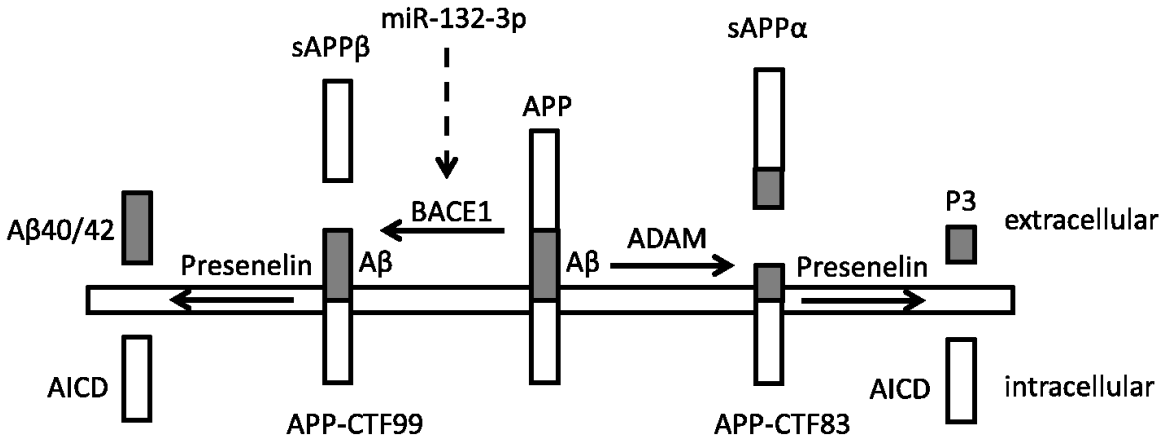

Figure 29: This model demonstrates the possible steps of intervention of *miR-132-3p* in the APP processing pathway.

Taken together, our findings provide clear evidence that *miR-132-3p* expression is downregulated in brain tissue of AD patients. One consequence of this is the upregulation of ERK1 and ERK2, which were shown to be direct targets of *miR-132-3p*. In tissue culture experiments, overexpression of *miR-132-3p* reduced the levels of secreted Aβ peptides. The reduction in Aβ levels was likely not mediated by ERK1/2 but accompanied by changes in APP processing suggestive of reduced β-secretase cleavage. Consistent with this mechanism, a significant reduction in BACE1 mRNA levels following pre-miR-132-3p transfection was observed, but additional experiments are required to demonstrate a reduction in BACE1 protein levels and to prove that BACE1 is a direct target of *miR-132-3p*. Based on these and findings from other groups (Salta E 2016, Smith P 2015), loss of *miR-132-3p* expression might contribute to the amyloid pathology in AD and restoration of *miR-132-3p* expression levels could provide a possible way to reduce Aβ levels and to treat AD.

6 Abstract

The aims of this thesis project were the identification and functional characterization of microRNAs (miRNAs) with altered expression in the brains of Alzheimer's disease patients. MiRNAs are small, non-coding RNA molecules that posttranscriptionally regulate gene expression in a sequence-dependent manner. Dysregulation of miRNA expression has been observed in many diseases including Alzheimer's disease, which is by far the most common neurodegenerative disease responsible for 60-80 % of all cases of dementia. The disease process in Alzheimer's disease is believed to start decades before the onset of clinical symptoms with the accumulation of amyloid-β (Aβ) peptides in the brain, which then form neurotoxic protein aggregates and trigger detrimental downstream events like neuroinflammation, tau aggregation and widespread synaptic and neuronal loss resulting in cognitive decline.

To discover novel differentially expressed miRNAs in human Alzheimer's disease brains, a microarray analysis covering 830 human mature miRNAs was performed with brain tissue samples from 10 Alzheimer patients and 10 aged matched control samples. The expression of the miRNA cluster *miR-212/132* was found to be significantly downregulated in Alzheimer patients, a finding that was confirmed in a second, independent set of 20 Alzheimer brain samples compared to 20 age-matched control brain samples. Subsequently, putative target genes of *miR-132-3p* were determined using prediction algorithms and their expression was investigated by real time reverse transcription PCR. Aside from the known *miR-132-3p* target gene *RB1*, the extracellular signal-regulated kinases ERK1 and ERK2 were found to be upregulated in Alzheimer brain samples and confirmed as direct *miR-132-3p* target genes by 5'-UTR luciferase reporter gene assays. To address the relevance of reduced *miR-212/132* expression in AD, the processing of the amyloid precursor protein (APP) and Aβ levels were investigated in human HEK293 cells after overexpression of pre-miR-132-3p. Transfection of pre-miR-132-3p significantly reduced Aβ levels that were accompanied by changes in APP processing, indicating reduced cleavage by β-secretase (BACE1), which is the rate-limiting enzyme for Aβ production. Consistent with this mechanism, a significant reduction in BACE1 mRNA levels was observed following transfection of pre-miR-132-3p. However, treatment with ERK1/2 inhibitors or siRNA mediated knock-down of ERK1/2 did not mimic the effects of pre-miR-132-3p overexpression indicating that the reduction in Aβ levels was likely mediated by other target genes. Finally, eight miRNAs found to be upregulated in an APP-transgenic mouse model of Alzheimer's disease (APPswe/PSEN1ΔE9) were validated in human Alzheimer brain tissue samples and controls. Expression of these miRNAs was either undetectable or unchanged in Alzheimer patient brains, thus questioning the utility of the mouse models for miRNA analysis.

In summary, this study provided clear evidence that *miR-212/132* expression is downregulated in brain tissue of Alzheimer patients. Loss of *miR-132-3p* expression might contribute to the amyloid pathology in Alzheimer's disease by promoting Aβ accumulation in the brain. Consequently, restoration of *miR-132-3p* expression could possibly provide an alternative way to therapeutically reduce Aβ levels in Alzheimer's disease.

7 Zusammenfassung

Das Ziel der vorliegenden Arbeit war es, microRNAs (miRNAs) zu finden und funktionell zu charakterisieren, deren Expression im Gehirngewebe von Patienten mit der Alzheimer-Krankheit verändert ist. MiRNAs sind kleine, nicht-kodierende RNA-Moleküle, die an der posttranskriptionalen Regulation der Genexpression beteiligt sind. Es ist bekannt, dass sie eine wichtige Rolle in neurodegenerativen Krankheiten wie der Alzheimer-Krankheit spielen. Die Alzheimer-Krankheit ist mit 60-80 % die häufigste Form der Demenz. Man geht davon aus, dass die pathologischen Prozesse Jahrzehnte vor den ersten klinischen Symptomen mit einer Amyloid-β-Akkumulation im Gehirn beginnen, woraus sich neurotoxische Proteinaggregate formen. Diese wiederum bewirken Neuroinflammation, Tau- Aggregation sowie Synapsen und Neuronen-Verluste, was den kognitiven Abbau begründet.

Um neue differentiell bei der Alzheimer-Krankheit exprimierte miRNAs zu finden, wurde eine Microarray-basierte Expressionsanalyse von 830 humanen miRNAs in autoptischen Hirngewebeproben von 10 Alzheimer-Patienten und 10 altersgleichen Kontrollproben ohne Alzheimer-Krankheit durchgeführt. Die Expression des miRNA Clusters *miR-212/132* war in den Hirngewebeproben der Alzheimer-Patienten signifikant erniedrigt. Dieser Befund ließ sich in einer zweiten, unabhängigen Untersuchungsgruppe von 20 Alzheimer- und 20 Kontroll-Gewebsproben bestätigen. Anschließend wurden putative Zielgene der Micro-RNA *miR-132-3p* mittels bioinformatischer Vorhersageprogramme identifiziert und deren Expression in den Hirngewebeproben durch quantitative Real-time Reverse Transkriptase-PCR bestimmt. Neben dem bereits bekannten *miR-132-3p* Zielgen *RB1* zeigten die durch extrazelluläre Signale regulierten Kinasen ERK1 und ERK2 eine im Vergleich zu normalen Hirngewebe erhöhte Expression in den Alzheimer-Gewebeproben. Mittels 5'-UTR Luciferase-Reportergen-Assays wurden *ERK1* und *ERK2* als direkte Zielgene von *miR-132-3p* bestätigt. Um die funktionelle Bedeutung der verminderten *miR-132-3p* Expression bei der Alzheimer-Krankheit zu untersuchen, wurden die Prozessierung des Amyloid-Vorläuferproteins (APP) sowie das Amyloid-β (Aβ)-Level in HEK293 Zellen nach Überexpression von pre-miR-132-3p bestimmt. Es zeigten sich signifikant reduzierte Aβ-Level sowie Veränderungen der APP-Prozessierung mit Hinweisen auf eine reduzierte Spaltung von APP durch β-Secretase (BACE1), welches das limitierende Enzym für die Aβ-Produktion darstellt. Übereinstimmend mit diesem Mechanismus fand sich nach pre-miR-132-3p Überexpression eine signifikante Reduktion der BACE1 mRNA-Expression. Allerdings konnte der Effekt der pre-miR-132-3p Überexpression durch die Behandlung mit ERK1/2 Inhibitoren oder durch siRNA-mediierten Knock-down von ERK1/2 nicht nachgestellt werden, was dafür spricht, dass die nach pre-miR-132-3p Überxpression beobachtete Reduktion der Aβ-Level durch Beeinflussung weiterer Ziel-Gene mitbedingt ist. In weiteren Experimenten ließ sich eine differentielle Expression von acht miRNAs, die in einem APP-transgenen Maus-Model (APPswe/PSEN1ΔE9) eine aberrante Expression zeigten, in Hirngewebeproben von Alzheimer-Patienten nicht validieren. Dies stellt den Nutzen dieses Maus-Models für Untersuchungen zur Rolle von miRNAs in der Pathogenese der Alzheimer-Krankheit in Frage.

Zusammenfassend lässt sich sagen, dass die in der vorliegenden Doktorarbeit erzielten Ergebnisse eine verminderte Expression von *miR-132-3p* und *miR-212-3p* im Hirngewebe von Alzheimer-Patienten belegen. Die erniedrigte Expression dieser miRNAs trägt möglicherweise zu der für diese Erkrankung typischen Amyloid-Pathologie durch Förderung

der Aβ-Akkumulation im Gehirn bei. Eine gezielte Erhöhung der *miR-132-3p* Expression könnte demnach ein potentieller Weg zur therapeutischen Aβ-Reduzierung bei der Alzheimer-Krankheit darstellen.

8 References

Alzheimer A. “Über eine eigenartige Erkrankung der Hirnrinde.” *Allgemeine Zeitschrift für Psychiatrie.*, 1907.

Ambros V. "A hierarchy of regulatory genes controls a larva-to-adult developmental switch in C. elegans." *Cell*, 1989: 49-57.

Anand S, Majeti B K, Acevedo L M, Murphy E A, Mukthavaram R, Scheppke L, Huang M, Shields D J, Lindquist J N, Lapinski P E. “MicroRNA-132-mediated loss of p120RasGAP activates the endothelium to facilitate pathological angiogenesis.” *Nat. Med.,*, 2010, 16,909–914. ed.

Avila J, Lucas JJ, Perez M, Hernandez F. “Role of tau protein in both physiological and pathological conditions.” *Physiol. Rev.*, 2004.

Bakota L, Brandt R. “Tau Biology and Tau-Directed Therapies for Alzheimer's Disease.” *Drugs.*, 2016.

Bard F, Cannon C. “Peripherally administered antibodies against amyloid beta-peptide enter the central nervous system and reduce pathology in a mouse model of Alzheimer disease.” *Nat Med*, 2000, 6(8): 916-9 ed.

Bateman R J, Aisen P S, De Strooper B, Xiong C. “Autosomal-dominant Alzheimer’s disease: a review and proposal for the prevention of Alzheimer’s disease.” *Alzheimer’s Research & Therapy*, 2011, 3:1 ed.

Bates D, Liang R L N, Wang E. "The ompact of noncoding RNA on the biochemical and molecular mechanism of aging." *Biochim.Biophys. Acta*, 2009.

Berezikov, E., Chung, W., Willis, J., Cuppen, E., Lai, E. "Mammalian mirtron genes." *Mol. Cell.*, 2007: 328–336.

Bertram L, Tanzi R. "Alzheimer's disease: one disorder, too man genes?" *Hum. Mol. Genet.*, 2004: R 135- R 141.

Bettens K, Sleegers K, Van Broeckhoven C. "Current status on Alzheimer disease molecular genetics: from past, to present, to future." *Human Molecular Genetics*, 2010: R4-R11.

Blennow K, Mattsson N, Schöll M, Hansson O, Zetterberg H. “Amyloid biomarkers in Alzheimer’s disease.” *Trends in Pharmacological Sciences*, 2015, 1217, 1-13 ed.

Bohnsack MT, Czaplinski K, Gorlich D. "Exportin 5 is a RanGTP-dependent dsRNA-binding protein that mediates nuclear export of pre-miRNAs." *RNA*, 2004: 185–191.

Boulton TG, Yancopoulos G D, Gregory J S, Slaughter C, Moomaw C, Hsu J. “An insulin-stimulated protein kinase similar to yeast kinases involved in cell cycle control.” *Science,*, 1990, 249, 64–67. ed.

Braak H, Braak E. "Neuropathological stageing of Alzheimer-related changes." *Acta Neuropathol.*, 1991: 239-259.

Burotto MD, Chiou VL, Lee JM, Kohn EC. “The MAPK Pathway Across Different Malignancies: A New Perspective.” *Cancer*, 2014, 120:3446-56. ed.

Cacace R, Sleegers K, Van Broeckhoven C. “Molecular genetics of early-onset Alzheimer disease revisited.” *Alzheimer´s and Dementia*, 2016, DOI: http://dx.doi.org/10.1016/j.jalz.2016.01.012 ed.

Caceres A, Kosik K S. “Inhibition of neurite polarity by tau antisense oligonucleotides in primary cerebellar neurons.” *Nature*, 1990.

Cai X, Hagedorn C, Cullen B. "Human microRNAs are processed from capped, polyadenylated transcripts that can also function as mRNAs." *RNA*, 2004: 1957–1966.

Calin G A, Liu C G, Sevignani C, Ferracin M, Felli N, Dumitru C D, Shimizu M, Cimmino A, Zupo S, Dono M. “MicroRNA profiling reveals distinct signatures in B cell chronic lymphocytic leukemias.” *Proc. Natl Acad. Sci*, 2004, 101, 11755–11760. ed.

Castillo D V, Escobar M L. “A role for MAPK and PI-3K signaling pathways in brain-derived neurotrophic factor modification of conditioned taste aversion retention.” *Behavioural Brain Research*, 2011, 217, 248–252. ed.

Cavallini A, Brewerton S, Bell A, Sargent S, Glover S, Hardy C, Moore R, Calley J, Ramachandran D, Poidinger M, Karran E, Davies P, Hutton M, Szekeres P, Bose S. “An Unbiased Approach to Identifying Tau Kinases That Phosphorylate Tau at Sites Associated with Alzheimer Disease.” *J Biol Chem.*, 2013, 288(32): 23331–23347 ed.

Chalfie M, Horvitz H, Sulston J. "Mutations that lead to reiterationes in the cell lineages of C. elegans." *Cell*, 1981: 59-69.

Cheng H Y, Papp J W, Varlamova O, Dziema H, Russell B, Curfman J P, Nakazawa T, Shimizu K, Okamura H, Impey S. “microRNA modulation of circadian-clock period and entrainment.” *Neuron*, 2007, 54, 813–829. ed.

Chunmei W, Bingyuan J, Baohua C, Jing C, Bo B. “Neuroprotection of microRNA in neurological disorders.” *Biomedical Reports*, 2014, 2: 611-619 ed.

Churcher I. “Tau therapeutic strategies for the treatment of Alzheimer's disease.” *Curr Top Med Chem.*, 2006, 6(6):579-95 ed.

Citron M. “Alzheimer's disease: strategies for disease modification.” *Nat Rev Drug Discov.*, 2010, 9(5):387-98 ed.

Citron, M, Diehl T, Gordon G, Biere A, Seubert P, Selkoe D. "Evidence that the42- and 40- amino acid forms of amyloid beta protein are generated from the beta-amyloid precursor protein by different protease activities." *Proc. Natl. Acad. Sci.*, 1996: 13170-13175.

Cogswell JP, Ward J, Taylor IA, Waters M, Shi Y, Cannon B. “Identification of miRNA changes in Alzheimer’s disease brain and CSF yields putative biomarkers and insights into disease pathways.” *J. Alzheimer’sDis*, 2008, 14, 27–41 ed.

Conaco C, Otto S, Han J J, Mandel G. “Reciprocal actions of REST and a microRNA promote neuronal identity.” *Proc. Natl Acad. Sci. USA,*, 2006, 103, 2422–2427. ed.

Corder E H, Saunders A M, Strittmatter W J, Schmechel D E, Gaskell P C, Small G W, Roses A D, Haines J L, Pericak-Vance M A. “Gene dose of apolipoprotein E type 4 allele and the risk of Alzheimer's disease in late onset families.” *Science*, 1993, 13;261(5123):921-3 ed.

Coric V, Salloway S, van Dyck CH, Dubois B, Andreasen N, Brody M, Curtis C, Soininen H, Thein S, Shiovitz T, Pilcher G, Ferris S, Colby S, Kerselaers W, Dockens R, Soares H, Kaplita S, Luo F, Pachai C, Bracoud L, Mintun M, Grill. “Targeting Prodromal Alzheimer Disease With Avagacestat: A Randomized Clinical Trial.” *JAMA Neurol.*, 2015, 72(11):1324-33 ed.

Cossa G, Gatti L, Cassinelli G, Lanzi C, Zaffaroni N, Perego P. “Modulation of sensitivity to antitumor agents by targeting the MAPK survival pathway.” *Curr Pharm Des.*, 2013, 19:883-894. ed.

Crowther, R A. “Straight and paired helical filaments in Alzheimer disease have a common structural unit.” *Proc Natl Acad Sci USA.*, 1991.

Cruchaga, Karch, Jin, Benitez , Cai, Guerreiro , Harari , Norton, Budde, Bertelsen , Jeng, Cooper, Skorupa , Carrell, Levitch , Hsu, Choi, Ryten , UK Brain Expression Consortium, Sassi, Bras, Gibbs, Hernandez , Lupton , Powell , Forabosco , Ridge, Corcor. “Rare coding variants in the phospholipase D3 gene confer risk for Alzheimer’s disease.” *Nature*, 2014, 505(7484):550-4. ed.

Cummings J, Aisen PA, DuBois B, Frölich L, Clifford R J, Jones RW, Morris JC, Raskin J, Dowsett SA, Scheltens P. “Drug development in Alzheimer´s disease: the path to 2025.” *Alzheimers Res Ther.*, 2016, 8: 39. ed.

De Strooper B, Saftig P, Craessaerts K, Vanderstichele H, Guhde G, Annaert W, Von Figura K, Van Leuven F. "Deficiency of presenilin-1 inhibits the normal cleavage of amyloid precursor protein." *Nature*, 1998: 387-390.

De Strooper B., Simons M, Multhaup G, Van Leuven F, Beyreuther K, Dott C. "Production of intracellular amyloid-containing fragments in hippocampal neurons expressing human amyloid precursor protein and protection against amyloidogenesis by subtle amino acid substitution in the rodent sequence." *EMBO*, 1995: 4932-4938.

Denli A, Tops BB, Plasterk RH, Ketting RF, Hannon GJ. "Processing of primary microRNAs by the Microprocessor complex." *Nature*, 2004: 231–235.

Desdouits-Magnen J, Desdouits F, Takeda S. “Regulation of secretion of Alzheimer amyloid precursor protein by the mitogen-activated protein kinase cascade.” *J Neurochem*, 1998, 70:524–530. ed.

Dhanasekaran NE, Premkumar R. “Signaling by dual specificity kinases.” *Oncogene.*, 1998, 17:1447-1455. ed.

Dimitrov M, Alattia JR, Lemmin T, Lehal R, Fligier A, Houacine J. “Alzheimer’s disease mutations in APP but not gamma-secretase modulators affect epsilon-cleavage-dependent AICD production.” *Nat. Commun*, 2013, 4:2246 ed.

Dineley KT, Westerman M, Bui D, Bell K, Ashe KH, Sweatt JD. “Beta-amyloid activates the mitogen-activated protein kinase cascade via hippocampal alpha7 nicotinic acetylcholine receptors: In vitro and in vivo mechanisms related to Alzheimer's disease.” *J Neurosci.*, 2001, 15;21(12):4125-33. ed.

Doench JG, Sharp PA. "Specificity of microRNA target selection in translational repression." *Genes Dev.*, 2004: 504–511.

Doench, JG, Sharp PA. "Specificity of microRNA target selection in translational repression." *Genes Dev.*, 2004: 504–511.

Doody RS, Raman R, Farlow M, Iwatsubo T, Vellas B, Joffe S, Kieburtz K, He F, Sun X, Thomas RG, Aisen PS, Alzheimer's Disease Cooperative Study Steering Committee, Siemers E, Sethuraman G, Mohs R Group., Semagacestat Study. “A phase 3 trial of semagacestat for treatment of Alzheimer's disease.” *N Engl J Med.*, 2013, 25;369(4):341-50. ed.

Easow G, Teleman AA, Cohen SM. "Isolation of microRNA targets by miRNP immunopurification." *RNA*, 2007.

Edbauer D, Neilson JR, Foster KA, Wang CF, Seeburg DP, Batterton MN. “Regulation of Synaptic Structure and Function by FMRP-Associated MicroRNAs miR-125b and miR-132.” *The Cell*, 2010, Neuron 65, 373–384. ed.

Esch F, Keim P, Beattie E, Blacher R, Culwell A, Oltersdorf T, McClure D, Ward P. "Cleavage of amyloid beta peptide during constitutive processing of it's precursor." *Science*, 1990: 1122-1124.

Fabian MR, Sonenberg N, Filipowicz W. "Regulation of mRNA translation and stability by miRNAs." *Annu. Rev. Biochem.*, 2010: 351-79.

Farrer L, Cupples L, Haines J, Hyman B, Kukull W, Mayeux R, Myers R, Pericak-Vance M, Risch N, Van Duijn C. "Effects of age, sex, and ethnicity on the association between apolipoprotein E genotype and Altheimer's disease. A meta-analysis." *JAMA*, 1997: 1349-1356.

Femminella GD, Ferrara N, Rengo G. “The emerging role of microRNAs in Alzheimer’s disease.” *Frontiers in Physiology*, 2015, 6 (40) 1-5 ed.

Ferrer I, Blanco R, Carmona M. “Phosphorylated map kinase (ERK1, ERK2) expression is associated with early tau deposition in neurones and glial cells, but not with increased nuclear DNA vulnerability and cell death, in Alzheimer disease, Pick’s disease, progressive supranuclear palsy an.” *Brain Pathol*, 2001, 11:144–158. ed.

Folch J, Petrov D, Ettcheto M, Abad S, Sánchez-López E, García ML, Olloquequi J, Beas-Zarate C, Auladell C, Camins A. “Current Research Therapeutic Strategies for Alzheimer's Disease Treatment.” *Neural Plast.*, 2016, 2016:8501693. ed.

Förstl H, Kurz A. "Clinical features of Alzheimer's disease." *European Archives of Psychiatry and Clinical Neuroscience.*, 1999: 288-290.

Franks TM, Lykke-Andersen J. "The control of mRNA decapping and P-body formation." *Mol. Cell.*, 2008: 605–615.

Friedman R, Farh K, Burge C, Bartel D. "Most mammaliam mRNAs are conserved targets of microRNAs." *Genome Res.*, 2009: 92-105.

Geekiyanage H, Jicha GA, Nelson PT, ChanC. “Blood serum miRNA:non-invasive biomarkers for Alzheimer’s disease.” *Exp.Neurol.*, 2012, 235, 491–496. ed.

Giovanni MG, Blitzer RD, Wong T, Asoma K, Tsokas P, Morrison JH. “Mitogen-activated protein kinase regulates early phosphorylation and delayed expression of Ca2+/calmodulin-dependent protein kinase II in longterm potentiation.” *Journal of Neuroscience*, 2001, 21, 7053–7062. ed.

Giovannini MG, Cerbai F, Bellucci A, Melani C, Grossi C, Bartolozzi C. “Differential activation of mitogen-activated protein kinase signalling pathways in the hippocampus of CRND8 transgenic mouse, a model of Alzheimer’s disease.” *Neuroscience*, 2008, 153, 618–633. ed.

Goodall EF, Heath PR, Bandmann O, Kirby J, Shaw PJ. “Neuronal dark matter: the emerging role of microRNAs in neurodegeneration.” *Front.Cell.Neurosci.*, 2013, 7:178. ed.

Greenberg SM, Koo EH, Selkoe DJ, Qiu WQ, Kosik KS. “Secreted beta-amyloid precursor protein stimulates mitogen-activated protein kinase and enhances tau phosphorylation.” *Proc Natl Acad Sci USA*, 1994, 91:7104–7108 ed.

Hahn S, Bruning T, Ness J, Czirr E, Baches S, Gijsen H, Korth C, Pietrzik CU, Bulic B, Weggen S. “Presenilin-1 but not amyloid precursor protein mutations present in mouse models of Alzheimer's disease attenuate the response of cultured cells to gamma secretase modulators regardless of their potency and structure.” *J. Neurochem.*, 2011, 116 ed.

Hammond SM, Boettcher S, Caudy AA, Kobayash R, Hannon GJ. "Argonaute2, a link between genetic and biochemical analyses of RNAi." *Science*, 2001: 1146–1150.

Han J, Lee Y, Yeom KH, Kim YK, Jin H, Kim VN. "The Drosha-DGCR8 complex in primary microRNA processing." *Genes. Dev.*, 2004: 3016–3027.

Hansen KF, Sakamoto K, Wayman GA, Impey S, Obrietan K. "Transgenic miR132 alters neuronal spine density and impairs novel object recognition memory." *PloS one*, 2010, e15497. ed.

Hardy J, Selkoe DJ. "The amyloid hypothesis of Alzheimer's disease: progress and problems on the road to therapeutics." *Science*, 2002, 297, 353–356 ed.

Hebert SS, Horre K, Nicolai L, Papadopoulou AS, Mandemakers W, Silahtaroglu AN. "Loss of microRNA cluster miR-29a/b-1 in sporadic Alzheimer's disease correlates with increased BACE1/beta-secretase expression." *Proc.Natl.Acad.Sci.U.S.A.*, 2008, 105, 6415–6420 ed.

Hébert SS, Sergeant N, Buée L. "MicroRNAs and the Regulation of Tau Metabolism." *International Journal of Alzheimer's Disease*, 2012, 1-6 ed.

Heneka MT, Carson MJ, El Khoury J, Landreth GE, Brosseron F, Feinstein DL, Jacobs AH, Wyss-Coray T, Vitorica J, Ransohoff RM, Herrup K, Frautschy SA, Finsen B, Kummer MP. "Neuroinflammation in Alzheimer's disease." *Lancet Neurol.*, 2015, 14: 388–405 ed.

Hernandez-Rapp J, Rainone S, Goupil C, Dorval V, Smith PY, Saint-Pierre M, Vallée M, Planel E, Droit A, Calon F, Cicchetti F, Hébert SS. "microRNA-132/212 deficiency enhances Aβ production and senile plaque deposition in Alzheimer's disease triple transgenic mice." *Sci Rep.*, 2016, 6: 30953. ed.

Hernandez-Rapp, J, Smith PY, Filali M, Goupil C, Planel E, Magill ST, Goodman RH, Hébert SS. "Memory formation and retention are affected in adult miR-132/212 knockout mice." *Behav Brain Res.*, 2015, 287:15-26 ed.

Hochgräfe K, Sydow A, Mandelkow EM. "Regulatable transgenic mouse models of Alzheimer disease: onset, reversibility and spreading of Tau pathology." *FEBS J*, 2013, 280(18):4371-81 ed.

Hooper C, Meimaridou E,Tavassoli M, Melino G, Lovestone S, Killick R. "p53 is upregulated in Alzheimer's disease and induces tau phosphorylation in HEK293a cells." *Neurosci.Lett.*, 2007, 418, 34–37 ed.

Hutvagner G, Zamore PD. "A microRNA in a multiple-turnover RNAi enzyme complex." *Science*, 2002: 2056–2060.

Hwang JY, Kaneko N, Noh KM, Pontarelli F, Zukin RS. "The gene silencing transcription factor REST represses miR-132 expression in hippocampal neurons destined to die." *J Mol Biol.*, 2014, 9;426(20):3454-66. ed.

Hyman BT, Elvehage TE, Reiter J. "Extracellular signal regulated kinases. Localization of protein and mRNA in the human hippocampal formation in Alzheimer´s disease." *Am J Pathol*, 1994, 144:565-572. ed.

Jack C, Knopman D, Jagust W. "Hypothetical model of dynamic biomarkers of the Alzheimer's pathological cascade." *Lancet Neurol.*, 2010: 119.

Johnson R, Buckley NJ. “Gene dysregulation in Huntington’s disease: REST, microRNAs and beyond.” *Neuromolecular Med.,*, 2009, 11, 183–199. ed.

Kemeny D. *ELISA- des Enzyme Linked Immunosorbent Assay im biologisch/medizinischen Labor.* Stuttgart: Gustav Fischer Verlag, 1994.

Kennedy ME, Stamford AW, Chen X, Cox K, Cumming JN, Dockendorf MF, Egan M, Ereshefsky , Hodgson RA, Hyde LA, Jhee S, Kleijn HJ, Kuvelkar R, Li W, Mattson BA, Mei H, Palcza J, Scott JD, Tanen M, Troyer MD, Tseng JL, Stone JA, Park. “The BACE1 inhibitor verubecestat (MK-8931) reduces CNS β-amyloid in animal models and in Alzheimer's disease patients.” *Sci Transl Med.*, 2016, 2;8(363):363ra150. ed.

Kerantzoulis S, Galvin J. "Distinguishing Alzheimer's disease from other major forms of dementia." *CME*, 2011: 1579-1591.

Ketting RF, Fischer SE, Bernstein E, Sijen T, Hannon GJ, Plasterk RH. "Dicer functions in RNA interference and in synthesis of small RNA involved in developmental timing in C. elegans." *Genes. Dev.*, 2001: 2654–2659.

Khvorova A, Reynolds A, Jayasena SD. "Functional siRNAs and miRNAs exhibit strand bias." *Cell*, 2003: 209–216.

Kihara T, Shimohama S. “Alzheimer's disease and acetylcholine receptors.” *Acta Neurobiol Exp (Wars).*, 2004, 64(1):99-105. ed.

Kim J, Yoon H, Ramirez CM, Lee SM, Hoe HS, Fernandez-Hernando C. “MiR-106b impairs cholesterol efflux and increases Abeta levels by repressing ABCA1 expression.” *Exp.Neurol.*, 2012, 235, 476–483 ed.

Klafki H, Abramows D, Swoboda R, Paganetti P, Staifenbiel M. "The carboxyl termini of beta-amyloid peptides 1-40 and 1-42 are generated by distinct gamma-secretase activities." *J. Bio. Chem.*, 1996: 28655-28659.

Krauthammer KCA, Kaufmann T, Gilliam C, Rzhetsky A. “Molecular triangulation: Bridging linkage and molecular-network information for identifying candidate genes in Alzheimer's disease.” *Proc Natl Acad Sci U S A*, 2004, 101 ed.

Krek A, Grun D, Poy MN, Wolf R, Rosenberg L, Epstein EJ. "Combinatorial microRNA target predictions." *Nat. Genet.*, 2005: 495-500.

Krichevsky AM, King K S, Donahue CP, Khrapko K, Kosik KS. “A microRNA array reveals extensive regulation of microRNAs during brain development.” *RNA 9*, 2003, 1274–1281 ed.

Kwak PB, Tomari Y. "The N domain of Argonaute drives duplex unwinding during RISC assembly." *Nat Struct Mol Biol*, 2012: 145–151.

Laemmli, UK. “Cleavage of structural proteins during the assembly of the head of bacteriophage T4.” *Nature*, 1970, 15;227(5259):680-5 ed.

Lagos D, Pollara G, Henderson S, Gratrix F, Fabani M, Milne RS, Gotch F, Boshoff C. “miR-132 regulates antiviral innate immunity through suppression of the p300 transcriptional co-activator.” *Nat. Cell Biol.*, 2010, 12, 513–519. ed.

Lambert TJ, Storm DR, Sullivan JM. “MicroRNA132 modulates short-term synaptic plasticity but not basal release probability in hippocampal neurons.” *PloS one*, 2010, 5, e15182. ed.

Lander E, Kruglyak L. "Genetic dissection of complex traits: guidelines for interpreting and reporting linkage results." *Nat. Genet.*, 1995: 241-247.

Lannfelt L, Relkin NR, Siemers ER. “Amyloid-ß-directed immunotherapy for Alzheimer's disease.” *J Intern Med.*, 2014, 275(3):284-95. ed.

Lau P, Bossers K, Janky R, Salta E, Frigerio CS, Barbash S, Swaab DF, Aerts S, De Strooper B. “Alteration of the microRNA network during the progression of Alzheimer’s disease.” *EMBO Mol Med*, 2013, 5, 1613–1634 ed.

Lee R, Feinbaum R, Ambros V. "The C. elegans heterochronic gene lin-4 encodes small RNAs with antisense complementarity to lin-14." *Cell*, 1993: 843-854.

Lee, Y., Jeon, K., Lee, J.T., Kim, S., Kim, V.N. "MicroRNA maturation: stepwise processing and subcellular localization." *EMBO J.*, 2002: 4663-70.

Leuchtenberger S, Maler J, Czirr E, Ness J, Lichtenthaler SF, Esselmann H, Pietrzik CU, Wiltfang J, Weggen S. "Nonsteroidal anti-inflammatory drugs and ectodomain shedding of the amyloid precursor protein." *Neurodegener Dis.*, 2009.

Lewczuk P, Mroczko B, Fagan A, Kornhuber J. “Biomarkers of Alzheimer’s disease and mild cognitive impairment: A current perspective.” *Advances in Medical Sciences*, 2015, 60, 76–82 ed.

Liesenberg F. “Aberrant expression of microRNA in gliomas: Molecular mechanisms, functional consequences and clinical significance.” *Dissertation*, 2012.

Livak KJ, Schmittgen TD. "Analysis of relative gene expression data using real-time quantitative PCR and the 2(-Delta Delta C(T)) Method." *Methods*, 2001, 25(4):402-8 ed.

Lukiw WJ. “Micro-RNA speciation in fetal, adult and Alzheimer's disease hippocampus.” *Neuroreport.*, 2007, 18(3):297-300. ed.

Ma L, Chen Z, Erdjument-Bromage H, Tempst P, Pandolfi PP. “Phosphorylation and functional inactivation of TSC2 by Erk implications for tuberous sclerosis and cancer pathogenesis.” *Cell.*, 2005, 121:179-193. ed.

Manthey D, Heck S, Engert S, Behl C. “Estrogen induces a rapid secretion of amyloid beta precursor protein via the mitogen-activated protein kinase pathway.” *Eur J Biochem.*, 2001, 268:4285–4291. ed.

McShane R, Areosa Sastre A, Minakaran N. “Memantine for dementia [update of Cochrane Database Syst Rev.2005;(3):CD003154].” *Cochrane Database of Systematic Reviews.*, 2006.

Medina M, Hernández F, Avila J. “New Features about Tau Function and Dysfunction.” *Biomolecules.*, 2016.

Mills J, Laurent Charest D, Lam F. “Regulation of amyloid precursor protein catabolism involves the mitogen-activated protein kinase signal transduction pathway.” *J Neurosci*, 1997, 17:9415–9422. ed.

Morlando M, Ballarino M, Gromak N, Pagano F, Bozzoni I, Proudfoot NJ. "Primary microRNA transcripts are processed co-transcriptionally." *Nat. Struct. Mol. Biol.*, 2008: 902–909.

Mullan M, Houlden H, Windelspecht M, Fidani L, Lombardi C, Diaz P, Rossor M, Crook R, Hardy J, Duff K. “A locus for familial early-onset Alzheimer's disease on the long arm of chromosome 14, proximal to the alpha 1-antichymotrypsin gene.” *Nat Genet.*, 1992, Dec;2(4):340-2. ed.

Müller-Schiffmann A, Herring A, Abdel-Hafiz L, Chepkova AN, Schäble S, Wedel D, Horn AH, Sticht H, de Souza Silva MA, Gottmann K, Sergeeva OA, Huston JP, Keyvani K, Korth C. “Amyloid-β dimers in the absence of plaque pathology impair learning and synaptic plasticity.” *Brain.*, 2016, 139(Pt 2):509-25. ed.

Nelson PT, Wang WX. “MiR-107 is reduced in Alzheimer’s disease brain neocortex: validation study.” *J. Alzheimer’s Dis.*, 2010, 21, 75–79. ed.

Noble W, Planel E, Zehr C, Olm V, Meyerson J, Suleman F, Gaynor K, Wang L, LaFrancois J, Feinstein B. “Inhibition of glycogen synthase kinase-3 by lithium correlates with reduced tauopathy and degeneration in vivo.” *Proc. Natl. Acad. Sci. USA*, 2005.

Nowak JS, Michlewski G. “miRNAs in development and pathogenesis of the nervous system.” *Biochem Soc Trans*, 2013, 41(4):815e20 ed.

O' Carrol D, Schaefer A. "General principals of miRNA biogenesis and regulation in the brain." *Neuropsychopharmocology*, 2012: 1-16.

Okamura K, Hagen JW, Duan H, Tyler DM, Lai EC. "The mirtron pathway generates microRNA-class regulatory RNAs in Drosophila." *Cell*, 2007: 89–100.

Oostra BA, Willemsen R. “FMR1: a gene with three faces.” *Biochim Biophys Acta.*, 2009, 1790(6): 467–477. ed.

Orom UA, Nielsen FC, Lund AH. "MicroRNA-10a binds the 5'UTR of ribosomal protein mRNAs and enhances their translation." *Mol. Cell*, 2008: 460–471.

Orom, UA, Nielsen FC, Lund AH. "MicroRNA-10a binds the 5'UTR of ribosomal protein mRNAs and enhances their translation." *Mol. Cell*, 2008: 460–471.

Orr PT, Rubin AJ, Fan L, Kent BA, Frick K M. “The progesterone induced enhancement of object recognition memory consolidation involves activation of the extracellular signal-regulated kinase (ERK) and mammalian target of rapamycin (mTOR) pathways in the dorsal hippocampus.” *Hormones and Behavior*, 2012, 61, 487–495. ed.

Park JK, Henry JC, Jiang J, Esau C, Gusev Y, Lerner MR, Postier RG, Brackett DJ, Schmittgen TD. “miR-132 and miR-212 are increased in pancreatic cancer and target the retinoblastoma tumor suppressor.” *Biochem Biophys Res Commun*, 2011, 25;406(4):518-23 ed.

Peavy RD, Conn PJ. “Phosphorylation of mitogen-activated protein kinase in cultured rat cortical glia by stimulation of metabotropic glutamate receptors.” *Journal of Neurochemistry*, 1998, 71, 603–612. ed.

Pei JJ, Braak H, An WL, Winblad B, Cowburn RF, Iqbal K, Grundke-Iqbal I. “Up-regulation of mitogen-activated protein kinases ERK1/2 and MEK1/2 is associated with the progression of neurofibrillary degeneration in Alzheimer's disease.” *Brain Res Mol Brain Res.*, 2002, 109(1-2):45-55 ed.

Perkins DO, Jeffries CD, Jarskog LF, Thomson JM, Woods K, Newman MA, Parker JS, Jin J, Hammond SM. “microRNA expression in the prefrontal cortex of individuals with schizophrenia and schizoaffective disorder.” *Genome Biol.,*, 2007, 8, R27. ed.

Perry G, Roder H, Nunomura A. “Activation of neuronal extracellular receptor kinase (ERK) in Alzheimer´s diesase links oxidative stress to abnormal phosphorylation.” *Neuoreport*, 1999, 10:2411-2415 ed.

Peterson R. "Mild cognitive impairment as a diagnostic entity." *J. Internal Med.*, 2004: 183-194.

Pichler S, Gu W, Hartl D, Gasparoni G, Leidinger P, Keller A, Meese E, Mayhaus M, Hampel H, Riemenschneider M. “The miRNome of Alzheimer's disease: consistent downregulation of the miR-132/212 cluster.” *Neurobiol Aging.*, 2017, 50:167.e1-167.e10 ed.

Postina R, Schroeder A, Dewachter I, Bohl J, Schmitt U, Kojro E, Prinzen C, Endres K, Hiemke C, Blessing M, Flamez P, Dequenne A, Godaux E, van Leuven F, Fahrenholz F. “A disintegrin-metalloproteinase prevents amyloid plaque formation and hippocampal defects in an Alzheimer disease mouse model.” *J Clin Invest.*, 2004, 113(10):1456-64. ed.

Priller C, Bauer T, Mitteregger G, Krebs B, Kretzschmar HA, Herms J. “Synapse Formation and Function Is Modulated by the Amyloid Precursor Protein.” *The Journal of Neuroscience*, 2006, 26(27): 7212-7221 ed.

Pullikuth AK, Catling AD. “Scaffold mediated regulation of MAPK signaling and cytoskeletal dynamics: a perspective.” *Cell Signal.*, 2007, 19:1621-1632. ed.

Rademarkers R, Cruts M, Van Broeckhoven C. "Genetics of Early-Onset Alzheimer Dementia." *The Scientific World J.*, 2003: 497-519.

Rapoport M, Ferreira A. “PD98059 prevents neurite degeneration induced by fibrillar beta-amyloid in mature hippocampal neurons.” *J Neurochem.*, 2000, 74(1):125-33. ed.

Reisberg B, Doody R, Stöffler A, Schmitt F, Ferris S, Möbius HJ. "Memantine Study Group. Memantine in moderater-to-severe Alzheimer's disease." *New Engl. J. Med.*, 2003: 1333-41.

Remenyi J, Hunter CJ, Cole C, Ando H, Impey S, Monk CE, Martin KJ, Barton GJ, Hutvagner G,Arthur JS. “Regulation of the miR-212/132 locus by MSK1 and CREB in response to neurotrophins.” *Biochem. J.*, 2010, 428:281–291 ed.

Robinson MJ, Cobb MH. “Mitogen-activated protein kinase pathways.” *Curr Opin Cell Biol.*, 1997, 9:180-186. ed.

Rodriguez A, Griffiths-Jones S, Ashurst J, Bradley A. "Identification of mammalian microRNA host genes and transcription units." *Genome Res.*, 2004: 1902-1910.

Ruby JG, Jan CH, Bartel, DP. "Intronic microRNA precursors that bypass Drosha processing." *Nature*, 2007: 83–86.

Saba-El-Leil MK, Vella FD, Vernay B, Voisin L, Chen L, Labrecque N. “An essential function of the mitogen-activated protein kinase Erk2 in mouse trophoblast development.” *EMBO Reports*, 2003, 4, 964–968. ed.

Salmon D, Bondi M. "Neuropsychology of Alzheimer's disease." *Alzheimer Disease*, 1999: 39-56.

Salta E, Sierksma A, Vanden Eynden E, De Strooper B. “miR-132 loss de-represses ITPKB and aggravates amyloid and TAU pathology in Alzheimer's brain.” *EMBO Mol Med.*, 2016, 1;8(9):1005-18 ed.

Satoh Y, Shogo E, Toshio I, Kazuyuki Y, Masataka I, Masahiko K, Takeshi H, Osamu I, Yasushi K, Yasuhiro W, Shigeyoshi I, Kunio T. “Extracellular Signal-Regulated Kinase 2 (ERK2) Knockdown Mice Show Deficits in Long-Term Memory; ERK2 Has a Specific Function in Learning and Memory.” *The Journal of Neuroscience*, 2007, 27(40): 10765-10776 ed.

Schenk D, Barbour R. “Immunization with amyloid-beta attenuates Alzheimer-disease like pathology in the PDAPP mouse.” *Nature*, 1999, 400(6740): 173-7 ed.

Schneider LS, Mangialasche F, Andreasen N, Feldman H, Giacobini E, Jones R, Mantua V, Mecocci P, Pani L, Winblad B, Kivipelto M. “Clinical trials and late-stage drug development for Alzheimer’s disease: an appraisal from 1984 to 2014.” *J Intern Med.*, 2014.

Schonrock N, Humphreys DT, Preiss T, Götz J. “Target gene repression mediated by miRNAs miR-181c and miR-9 both of which are down-regulated by amyloid-β.” *J Mol Neurosci.*, 2012, 46(2):324-35 ed.

Schopman NC, Heynen S, Haasnoot J, Berkhout B. “A miRNA-tRNA mix-up: tRNA origin of proposed miRNA.” *RNA Biol.*, 2010, 7(5):573-6 ed.

Selcher JC, Nekrasova T, Paylor R, Landreth GE, Sweatt J D. “Mice lacking the ERK1 isoform of MAP kinase are unimpaired in emotional learning.” *Learning & Memory*, 2001, 8, 11–19. ed.

Selkoe D, Hardy J. *The amyloid hypothesis of Alzheimer.* EMBO Molecular Medicine, 2016.

Sethi P, Lukiw WJ. “Micro-RNA abundance and stability in human brain:specific alterations in Alzheimer’s disease temporal lobe neocortex.” *Neurosci.Lett.*, 2009, 459, 100–104 ed.

Sevigny J, Chiao P, Bussière T, Weinreb PH, Williams L, Maier M, Dunstan R, Salloway S, Chen T, Ling Y, O'Gorman J, Qian F, Arastu M, Li M, Chollate S, Brennan MS, Quintero-Monzon O, Scannevin RH, Arnold HM, Engber T, Rhodes K, Ferrer. “The antibody aducanumab reduces Aβ plaques in Alzheimer's disease.” *Nature.*, 2016, 1;537(7618):50-6. ed.

Shaked I, Meerson A, Wolf Y, Avni R, Greenberg D, Gilboa-Geffen A Soreq H. “MicroRNA-132 Potentiates Cholinergic Anti-Inflammatory Signaling by Targeting Acetylcholinesterase.” *Immunity*, 2009, 31, 965–973 ed.

Sheth U, Parker R. "Decapping and decay of messenger RNA occur in cytoplasmic processing bodies." *Science*, 2003: 805–808.

Sigoillot FD, Evans DR, Guy HI. “Growth-dependent regulation of mammalian pyrimidine biosynthesis by the protein kinase A and MAPK signaling cascades.” *J Biol Chem.*, 2002, 277:15745-15751. ed.

Smalheiser N, Lugli G, Torvik V, Mise N, Ikeda R, Abe K. "Natural antisense transcripts are co-expressed with sense mRNAs in synaptoneurosomes of adult mouse forebrain." *Neurosci Res*, 2008: 236–239.

Smith P, Hernandez-Rapp J, Jolivette F, Lecours C, Bisht K, Goupil C, Dorval V, Parsi S, Morin F, Buée L, Tremblay ME, Calon F, Hébert SS. “miR-132/212 deficiency impairs tau metabolism and promotes pathological aggregation in vivo.” *Hum Mol Genet.*, 2015, 1; 24(23): 6721–6735. ed.

Smith, P.Y., Delay,C., Girard,J., Papon,M.A., Planel,E. Sergeant,N., Bue´e,L. and Hebert,S.S. “MicroRNA-132 loss is associated with tau exon 10 inclusion in progressive supranuclear palsy.” *Hum. Mol. Genet.,* , 2011, 20, 4016–4024. ed.

Smith-Vikos T, Slack FJ. “MicroRNAs and their roles in aging.” *J Cell Sci.*, 2012, 125(Pt 1):7-17 ed.

Soreq H, Wolf Y. “NeurimmiRs: microRNAs in the neuroimmune interface.” *Trends Mol. Med.,*, 2011, 17, 548–555. ed.

Sperling R, Aisen P, Becket L. "The diagnosis of mild cognitive impairment due to Alzheimer's disease: recommendations from the National Institute on Aging-Alzheimr's Association workgrous on diagnostic guidelines for Alzherimer's disease." *Alzheimer's Dement.*, 2001: 270-279.

Streffer J. 2015, http://www.alzforum.org/news/conference-coverage/adpd-meeting-new-bace-inhibitor-struts-its-stuff ed.

Strittmatter W, Saunders A, Schmechel D, Pericak-Vance M, Enghild J, Salvesen G, Roses A. "Apolipoprotein E: high-avidity binding to beta-amyloid and increased freuency of type 4 allele in late-onset familial AD." *Proc. Natl. Acad. Sci.*, 1993: 1977-1981.

Strum JC, Johnson JH, Ward J, Xie H, Feild J, Hester A, Alford A, Waters KM. “MicroRNA 132 regulates nutritional stress-induced chemokine production through repression of SirT1.” *Mol. Endocrinol.*, 2009, 23, 1876e1884. ed.

Sweatt JD. “The neuronal MAP kinase cascade: A biochemical signal integration system subserving synaptic plasticity and memory.” *Journal of Neurochemistry*, 2001, 76, 1–10. ed.

Towbin H, Staehelin T, Gordon J. “Electrophoretic transfer of proteins from polyacrylamide gels to nitrocellulose sheets: procedure and some applications.” *Proc Natl Acad Sci U S A*, 1979, 76(9): 4350–4354 ed.

Trojanewski JQ, Mawal-Dewan M, Schmidt ML, Martin J, Lee VM. “Localization of the mitogen activated protein kinase ERK2 in Alzheimer´s disease neurofibrillary tangles and senile plaque neurites.” *Brain Res.*, 1993, 618:333-337 ed.

Turner PR, O’Connor K, Warren PT, Abraham WC. “Roles of amyloid precursor protein and its fragments in regulating neural activity, plasticity and memory.” *Progress in Neurobiology.*, 2003, 70, 1 (1–32) ed.

Van den Boom J, Wolter M, Kuick R, Misek DE, Youkilis AS, Wechsler DS, Sommer C, Reifenberger G, Hanash SM. “Characterization of Gene Expression Profiles Associated with Glioma Progression Using Oligonucleotide-Based Microarray Analysis and Real-Time Reverse Transcription-Polymerase Chain Reaction.” *Am J Pathol.*, 2003, 163(3): 1033–1043 ed.

Van den Hove DL, Kompotis K, Lardenoije R, Kenis G, De Strooper B, Rutten BPF. “Epigenetically regulated microRNAs in Alzheimer’s disease.” *Neurobiology of Aging*, 2014, 35, 731-745 ed.

Van den Hove, DL, Kompotis K, Lardenoije R, Kenis G, Mill J, Steinbusch HW, Lesch KP, Fitzsimons CP, De Strooper B, Rutten BP. “Epigenetically regulated microRNAs in Alzheimer's disease.” *Neurobiol Aging.*, 2014 , 35(4):731-45. ed.

Vasudeva S, Tong Y, Steitz JA. "Switching from repression to activation: miRNAs can upregulate translation." *Science*, 2007: 1931-34.

Vasudeva, S, Tong Y, Steitz J A. "Switching from repression to activation: miRNAs can upregulate translation." *Science*, 2007: 1931-34.

Verkerk AJ, Pieretti M, Sutcliffe JS, Fu YH, Kuhl DP, Pizzuti A, Reiner O, Richards S, Victoria MF,. "Identification of a gene (FMR-1) containing a CGG repeat coincident with a breakpoint cluster region exhibiting length variation in fragile X syndrome." *Cell*, 1991, 65:905–914. ed.

Vo N, Klein ME, Varlamova O, Keller DM, Yamamoto T, Goodman RH, Impey S. "A cAMP-response element binding protein-induced microRNA regulates neuronal morphogenesis." *Proc. Natl Acad. Sci. USA,*, 2005, 102, 16426–16431. ed.

Wanet A, Tacheny A, Arnould T, Renard P. "miR-212/132 expression and functions: within and beyond the neuronal compartment." *Nucleic Acids Res.*, 2012, 40(11):4742-53 ed.

Wang RY, Phang RZ, Hsu PH, Wang WH, Huang HT, Liu IY. "In vivo knockdown of hippocampal miR-132 expression impairs memory acquisition of trace fear conditioning." *Hippocampus*, 2013, 23, 625e633. ed.

Wang WX, Qingwei H, Yanling H, Stromberg AJ, Nelson PT. "Patterns of microRNA expression in normal and early Alzheimer's disease human temporal cortex: white matter versus gray matter." *Acta Neuropathol.*, 2011, 121(2): 193–205. ed.

Wang Y, Veremeyko T, Wong AH, El Fatimy R, Wei Z, Cai W, Krichevsky AM. "Downregulation of miR-132/212 impairs S-nitrosylation balance and induces tau phosphorylation in Alzheimer's disease." *Neurobiol Aging.*, 2017, 51:156-166. ed.

Warwick D, Payami H, Nemens E, Nochlin D, Bird T, Schellenberg G, Wijsman E. "The number of trait loci in late-onset Alzherimer's disease." *Am. J. Hum. Genet.*, 2000: 196-204.

Watabe AM, Zaki PA, O'Dell TJ. "Coactivation of beta-adrenergic and cholinergic receptors enhances the induction of long-term potentiation and synergistically activates mitogen-activated protein kinase in the hippocampal CA1 region." *Journal of Neuroscience*, 2000, 20, 5924–5931. ed.

Wei X, Tan C, Tang C, Ren G, Xiang T, Qiu Z, Liu R, Wu Z. "Epigenetic repression of miR-132 expression by the hepatitis B virus x protein in hepatitis B virus-related hepatocellular carcinoma." *Cell Signal.*, 2013, 25(5):1037-43. ed.

Westmark CJ, Malter JS. "FMRP Mediates mGluR5-Dependent Translation of Amyloid Precursor Protein." *PLoS Biology*, 2007, 5(3): e52. ed.

Wilcock GK, Gauthier S, Frisoni GB, Jia J, Hardlund JH, Moebius HJ, Bentham P, Kook KA, Schelter BO, Wischik DJ, Davis CS, Staff RT, Vuksanovic V, Ahearn T, Wischik CM. "Potential of Low Dose Leuco-Methylthioninium Bis(Hydromethanesulphonate) (LMTM) Monotherapy for Treatment

of Mild Alzheimer's Disease: Cohort Analysis as Modified Primary Outcome in a Phase III Clinical Trial." *J Alzheimers Dis.*, 61(1): 435–457. 2017.

Wong HKA, Veremeyko T, Patel N, Lemere CA, Walsh DM, Esau C, Vanderburg C, Krichevsky AM. "De-repression of FOXO3a death axis by microRNA-132 and -212 causes neuronal apoptosis in Alzheimer's disease." *Human Molecular Genetics*, 2013, 1–16 ed.

Wong, T.S., Liu,X.B., Wong,B.Y., Ng,R.W., Yuen,A.P. and Wei,W.I. "Mature miR-184 as potential oncogenic microRNA of squamous cell carcinoma of tongue." *Clin. Cancer Res.,* , 2008, 14, 2588–2592. ed.

Yamamoto N, Fuji Y, Kasahara R, Tanida M, Ohora K, Ono Y, Suzuki K, Sobue K. "Simvastatin and atorvastatin facilitates amyloid β-protein degradation in extracellular spaces by increasing neprilysin secretion from astrocytes through activation of MAPK/Erk1/2 pathways." *Glia*, 2016, 64: 952–962. ed.

Yanamandra K, Kfoury N, Jiang H, Mahan TE, Ma S, Maloney SE, Wozniak DF, Diamond MI, Holtzman DM. "Anti-tau antibodies that block tau aggregate seeding in vitro markedly decrease pathology and improve cognition in vivo." *Neuron.*, 2013, 16;80(2):402-14. ed.

Yekta S, Shih IH, Bartel DP. "MicroRNA-directed cleavage of HOXB8 mRNA." *Science*, 2004: 594–596.

Zassadowsk F, Rochette-Egly C, Chomienne C, Cassinat B. "Regulation of the transcriptional activity of nuclear receptors by the MEK/ERK1/2 pathway." *Cell Signal.*, 2012, 24:2369-2377. ed.

Zhang B, Gaiteri C, Bodea L-G. "Integrated systems approach identifies genetic nodes and networks in late-onset Alzheimer's disease." *Cell*, 2013, 153: 707–20. ed.

Zhang J, Hu M, Teng Z, Tang YP, Chen C. "Synaptic and cognitive improvements by inhibition of 2-AG metabolism are through upregulation of microRNA-188-3p in a mouse model of Alzheimer's disease." *J Neurosci.*, 2014, 5;34(45):14919-33. ed.

Zhang S, Hao J, Xie F, Hu X, Liu C, Tong J, Zhou J, Wu J Shao C. "Downregulation of miR-132 by promoter methylation contributes to pancreatic cancer development." *Carcinogenesis,*, 2011, 32, 1183–1189. ed.

Zhu JJ, Qin Y, Zhao M, Van Aelst L, Malinow R. "Ras and Rap control AMPA receptor trafficking during synaptic plasticity." *Cell*, 2002, 110, 443–455. ed.

Zhu X, Castellani RJ, Takeda A. "Differential activation of neuronal ERK, JNK/SAPK and p38 in Alzheimer disease: The 'two hit' hypothesis." *Mech Ageing Dev*, 2001, 123:39–46 ed.

Zhu, X, Lee HG, Raina AK, Perry G, Smith MA. "The role of mitogen-activated protein kinase pathways in Alzheimer's disease." *Neurosignals*, 2002, 11(5):270-81. ed.

Zovoilis A, Agbemenyah HY, Agis-Balboa RC, Stilling RM, Edbauer D, Rao P. "microRNA-34c is a novel target to treat dementias." *EMBO J.*, 2011, 30, 4299–4308 ed.

9 Danksagung

Als erstes möchte ich Herrn Prof. Dr. Guido Reifenberger für die Möglichkeit danken, im Institut für Neuropathologie der Heinrich-Heine-Universität Düsseldorf meine Dissertation durchführen zu dürfen sowie für die Überlassung des interessanten Promotionsthemas und die fundierte Beratung während der Durchführung dieser Arbeit.

Bei Herrn Prof. Dr. Dieter Willbold bedanke ich mich für die freundliche Übernahme der Betreuung meiner Dissertation seitens der Mathematisch-Naturwissenschaftlichen Fakultät der Heinrich-Heine-Universität Düsseldorf und die Erstellung des Korreferats.

Ich möchte mich ganz besonders bei Herrn Prof. Dr. Sascha Weggen für die freundliche und fachliche Beratung besonders zum Thema der Alzheimer-Krankheit sowie den funktionalen Experimenten bei dieser Arbeit bedanken.

Mein ausgesprochen herzlicher Dank gilt Frau Dr. Marietta Wolter für ihre geduldige Betreuung meiner Arbeit von Beginn an, ihr Engagement, ihre Expertise, besonders im Labor, und dass sie mir in allen Belangen mit Rat und Tat zur Seite stand. Auch die entspannten Yogastunden und unterhaltsamen Treffen zum Plätzchen backen werde ich nie vergessen. Eine hilfreichere, ehrlichere, klügere und lustigere Betreuerin kann man sich während seiner Promotion wirklich nicht wünschen.

Ich möchte auch dem gesamten Institut der Neuropathologie für die praktische Unterstützung der experimentellen Arbeiten und für die zahlreichen Ratschläge und die angenehme Arbeitsatmosphäre Danke sagen. Insbesondere gilt mein Dank Isabella Ogorek und Sandra Baches für die Unterstützung bei den ELISA-Assays, einigen Western-Blots und einigen Arbeiten in der Zellkultur. Außerdem danke ich Frau Dr. Franziska Liesenberg, Frau Dr. Annemarie Forchmann, Rebecca Ruland, Dr. Bastian Malzkorn und Dr. Jörg Felsberg für die tatkräftige Unterstützung im Labor.

Mein herzlicher Dank an meine liebe Chefin Oda Şanel darf hier nicht fehlen. Die Geschäftsführerin der Alzheimer Forschung Initiative e.V. hat es mir ermöglicht, meine Arbeitszeiten so flexibel zu gestalten, wodurch die Arbeit an meiner Dissertation zum Ende hin erst möglich wurde.

Meiner ganzen Familie möchte ich für die emotionale Unterstützung während der langen Zeit herzlich danken, auch für ihre motivierenden Worte und Gedanken. Meinem Mann Kashi und meiner Tochter Mira danke ich für ihre Geduld und die entbehrte Zeit, die sie aufbringen mussten, damit diese Arbeit erfolgreich beendet werden konnte.

10 Ehrenwörtliche Erklärung

Hiermit erkläre ich, dass ich die vorliegende Dissertation eigenständig und ohne unerlaubte Hilfe angefertigt und diese in der vorgelegten oder in ähnlicher Form noch bei keiner anderen Institution eingereicht habe.

Ort, Datum Unterschrift